

NUREG/CR-1808
R1, R2, R4

Countercurrent Air/Water and Steam/Water Flow above a Perforated Plate

Manuscript Completed: October 1979
Date Published: November 1980

Prepared by
C. Hsieh, S. G. Bankoff, R. S. Tankin, M. C. Yuen

Department of Chemical Engineering
Northwestern University
Evanston, IL 60201

Prepared for
Division of Reactor Safety Research
Office of Nuclear Regulatory Research
U.S. Nuclear Regulatory Commission
Washington, D.C. 20555
NRC FIN No. B6188

8012220609

ABSTRACT

The perforated plate weeping phenomena have been studied in both air/water and steam/cold water systems. The air/water experiment is designed to investigate the effect of geometric factors of the perforated plate on the rate of weeping. A new dimensionless flow rate in the form of H^* is suggested. The data obtained are successfully correlated by this H^* scaling in the conventional flooding equation.

The steam/cold water experiment is concentrated on locating the boundary between weeping and no weeping. The effects of water subcooling, water inlet flow rate, and position of water spray are investigated. Depending on the combination of these factors, several types of weeping were observed. The data obtained at high water spray position can be related to the air/water flooding correlation by replacing the steam flow rate to an effective steam flow rate, which is determined by the mixing efficiency above the plate.

TABLE OF CONTENTS

	PAGE
Abstract.....	iii
Table of Contents.....	v
List of Figures.....	vii
List of Tables.....	xi
Nomenclature.....	xiii
Acknowledgements.....	xvii
1. Introduction.....	1
2. Air/Water Experiment.....	3
2.1 Technical Background.....	3
2.2 Experimental Apparatus.....	20
2.2.1 Test Channel.....	20
2.2.2 Water Line.....	20
2.2.3 Air Line.....	24
2.2.4 Instrumentation.....	25
2.2.5 Computer Program.....	26
2.3 Experimental Procedure.....	28
3 Air/Water Experiment Data Analysis.....	30
3.1 Visual Observations.....	30
3.2 Correlation for Coefficient m	32
3.3 Correlation for Coefficient C	34
3.4 Effect of Liquid Inlet Rate.....	40
3.5 Effect of Head of Liquid Pool above the Plate.....	42
3.6 Effect of Liquid Inlet Position and Soft Volume....	42
4 Steam/Cold Water Experiment.....	44
4.1 Technical Background.....	44
4.2 Previous Works.....	48
4.3 Experimental Apparatus.....	51
4.3.1 Test Channel.....	51
4.3.2 Water Line.....	51

4.3.3 Steam Line.....	52
4.3.4 Instrumentation.....	53
4.3.5 Computer Program.....	56
4.4 Experimental Procedure.....	58
5. Results and Discussion for Steam/Water Experiment...	60
5.1 Water Inlet Spray Above The Pool.....	60
5.1.1 15 Hole Data.....	61
5.1.2 Comparison between 15 Hole and 9 Hole Data.....	65
5.1.3 Data Correlation.....	71
5.1.4 5(5A) Hole and 3(3A) Hole Data.....	72
5.2 Water Inlet Spray at the Plate.....	78
5.3 Effect of Liquid Inlet Spray Position.....	91
6. Conclusions and Suggestions.....	94
7. Reference.....	96

Appendix I Computer Program List and Air/Water Reduced Data	104
--	-----

Appendix II Computer Program List and Steam/Water Reduced Data.....	115
--	-----

Figure

1. Geometries of the Test Perforated Plate.....	4
2. Perforated Plate Diagram.....	5
3. Perforated Plate Weep Point Correlation.....	7
4. Oscillation Behavior of Perforated Plate.....	9
5. Perforated Plate Weeping Models.....	11
6. Schematic Diagram of Experimental Apparatus.....	21
7. Isometric Diagram of the Test Channel.....	22
8. Piping of Pressure Measurement Device.....	27
9. Data Correlation with Equation (12), $w = D_h$	33
10. Data Correlation with Equation (23).....	35
11. The α Function Given by Equation (52).....	38
12. Coefficient C in Equation (55) as a Function of L^*	39
13. Data Correlation with Equation (55).....	41
14. Effect of Head of Liquid Pool on the Rate of Weeping.....	43
15. Block's "Universal Flow Regime Map for Direct Contact Condensation.....	45
16. The Flow Regime Map of Direct Contact Con- densation for the PWR Annular Downcomer Geometries.....	47
17. The Flow Regime Map of Direct Contact Con- densation for Perforated Plate Geometries.....	49
18. The Standard Piping Arrangement for steam venturi.	55
19. Effect of Liquid Subcooling to the Weep Point, $h_{in} = 305$ mm, 15 hole data.....	62
20. Some Pictures of Continuous Weeping, $h_{in} = 305$ mm.	63
21. Some Pictures of Oscillatory Weeping, $h_{in} = 305$ mm.....	66

22. Thermocouple T11 Readings at Weep Point.....	67
23. Total Enthalpy Flux at Weep Point, 15 Hole and 9 Hole Data, $h_{in} = 305$ mm.....	68
24. Superficial Steam Velocity through the Holes, 15 Hole and 9 Hole Data.....	70
25. Dimensionless Steam and Water Inlet Flow Rate at Weep Point, 15 Hole and 9 Hole Data, $h_{in} = 305$ mm.....	73
26. Condensation Effect on Weep Point Correlation, 15 Hole and 9 Hole Data, $h_{in} = 305$ mm.....	74
27. Comparison of the Weep Point Data of 5 Hole, 5A Hole, 3 Hole, and 3A Hole Experiment Result...	75
28. Comparison of Superficial Steam Velocity through Holes for 5 Hole, 5A Hole, 3 Hole, and 3A Hole Data.....	77
29. Dimensionless Steam and Water Inlet Flow Rate at Weep Point, 5 Hole, 5A Hole, 3 Hole, and 3A Hole Data, $h_{in} = 305$ mm.....	79
30. Condensation Effect on Weep Point Correlation, 5 Hole, 5A Hole, 3 Hole, and 3A Hole Data, $h_{in} = 305$ mm.....	80
31. 15 Hole Weep Point Data Obtained at Low Water Inlet Position.....	81
32. Some Pictures of Oscillatory Weeping, $h_{in} = 5$ mm.....	82
33. Some Pictures of Stable No Weeping.....	84
34. Some Pictures of Total Dumping.....	86
35. A Picture after the Total Dumping.....	87
36. Weep Point Data Taken at $T_{in} = 12$ °C and $h_{in} = 5$ mm.....	89

37. Effect of Liquid Inlet Spray Nozzle Position on Weep Point, 15 Hole Data.....	92
38. Effect of Liquid Inlet Spray Nozzle Position on Weep Point, 9 Hole Data.....	93

List of Tables

Page

Table

1. Data Matrix of Air/Water Experiment.....	31
2. The Value of α for Each Perforated Plate.....	37
3. Function of Thermocouples.....	54

NOMENCLATURE

A	area
C	coefficient in the conventional flooding equation.
C_o	orifice coefficient in equation (1).
D	diameter.
D^*	Bond Number defined in equation (27).
f	friction factor
F_p	correlation constant in equation (41).
h	height(or head) of liquid.
h'	heat transfer coefficient.
H^*	dimensionless velocity defined in equation (55).
I^*	dimensionless velocity defined in equation (28).
j	superficial velocity through holes.
J^*	dimensionless velocity defined in equation (9).
k	wave number (= $t_p/2$).
k'	constant in Fair's weep point correlation.
L^*	Bond Number defined in equation (53).
m	coefficient in the conventional flooding equation.
$N_{Eö}$	Eotvos Number defined in equation (47).
p	pressure
R_T	thermodynamic boundary.
t_p	Thickness of the perforated plate.
U_{cr}	critical velocity.
w	characteristic length.
W	mass flow rate.
σ	surface tension
τ	shear stress
ρ	density

Subscripts

f	liquid phase
L	liquid phase
g	gas or vapor phase
h	hole
i	inside or interface
in	inlet
o	outside
s	steam
sat	saturated condition
w	wall

ACKNOWLEDGEMENTS

The Mechanical Engineering Staff is humbly thanked for all their marvellous skill in processing the purchasing and construction work. The secretaries: Lillian Kurtz, Brenda Wilson, Pat Dyess, and Larry Rockoff were particularly helpful and tolerant. The shop foreman and personnel: Robert Klaub, Mike Luczak, T. F. Felton, and J. Torluemke proficiently constructed the apparatus used in this experiment.

The contributions from co-investigators can not be thanked too much. They are: Robert Jensen, David Cook, Fae Wang, and Sang Lim.

1. Introduction

The flooding phenomena of vertical counter-current two phase flow have been studied in various types of flow channels. Packed columns were the first to receive a systematic investigation. After forty years, the basic model proposed by Sherwood(1) and Lobo(2) is still widely accepted by chemical engineers in packed tower design(3, 4). Flooding inside circular tubes, which may be encountered in several types of process equipment(e.g., cyclone, liquid film evaporator, updraft condenser, etc.), has probably been given the most extensive studies in this field. Much basic research related to the flooding phenomenon is carried in this type of geometry(5). The understanding accumulated here also serve as a basic guide for the study on other shapes of flow channels.

Recently, due to concern about the refilling and reflooding process in the event of a loss-of-coolant-accident(LOCA) in nuclear reactor safety analysis, flooding phenomena in annuli(6) or outside the fuel rod bundles(7) have drawn attention. Owing to similar concerns the restrictive effect of ascending steam on water flowing downward through a perforated support plate is currently being studied.

Throughout this thesis, the term "dumping" is used to describe the condition where essentially all the inlet liquid falls down through the perforated plate, once the instability starts. Should there be only part of the inlet liquid falling through, it is called "weeping", and the starting point of weeping is called the weep point. Weeping is further divided into two categories: continuous weeping and oscillatory or intermittent weeping.

The objective of the present research is to investigate

weeping in perforated plates with different hole size and geometries with both air/water and steam/cold water system. Study of the air/water system, where the condensation-driven fluid motions have been totally eliminated, can lead to some insight into the hydrodynamic aspects of the weeping phenomenon. The effect of plate geometry, along with several other factors, has been studied. Next, the experiments on the steam/cold water are to determine the effect of condensation on the initiation of weeping. The experimental parameters studied include: number of holes in the test plate, inlet steam mass flow rate, degree of steam superheat, effect of soft volume, inlet water mass flow rate, degree of subcooling of the inlet water, position of water injection, and liquid head above the perforated plate.

2. Air/Water Experiment

Basically, the weeping phenomenon, like any other counter-current flow limiting (CCFL) phenomenon, is a hydrodynamic process where the momentum and frictional drag of the ascending gas/vapor and descending liquid interact with each other.

The air/water experiments were performed in the same test channel with the same perforated plates (Figure 1) designed for the steam/cold water experiment. The following factors may be expected to be important: superficial gas velocity through the perforations j_{gh} , head of liquid pool above the perforated plate h_L , height of liquid inlet point above plate h_{in} , diameter of holes D_h , slot volume V_s , and perforation ratio A_h/A_T .

2.1 Technical Background

Since the early 50's, weeping has been studied by investigators interested in the performance of perforated plate in distillation towers or packed-bed chemical reactors. Operating with the air/water system, Mayfield(9), Arnold(10), and Zene(11) separately reported that the weep point is a function of j_{gh} and h_L (Figure 2). According to their observations, a higher j_{gh} is required to keep the plate from weeping as the head of liquid pool is increased

Supported by data from Hunt(12) and Van Winkle(13), Leibson (14) indicated that superficial gas velocity through the holes j_{gh} can be related to the pressure drop across the plate in the following way:

$$h_p \equiv \Delta p_{12} / (g \rho_f) = \rho_g j_{gh}^2 / (g C_o^2 \rho_f) \quad (1)$$

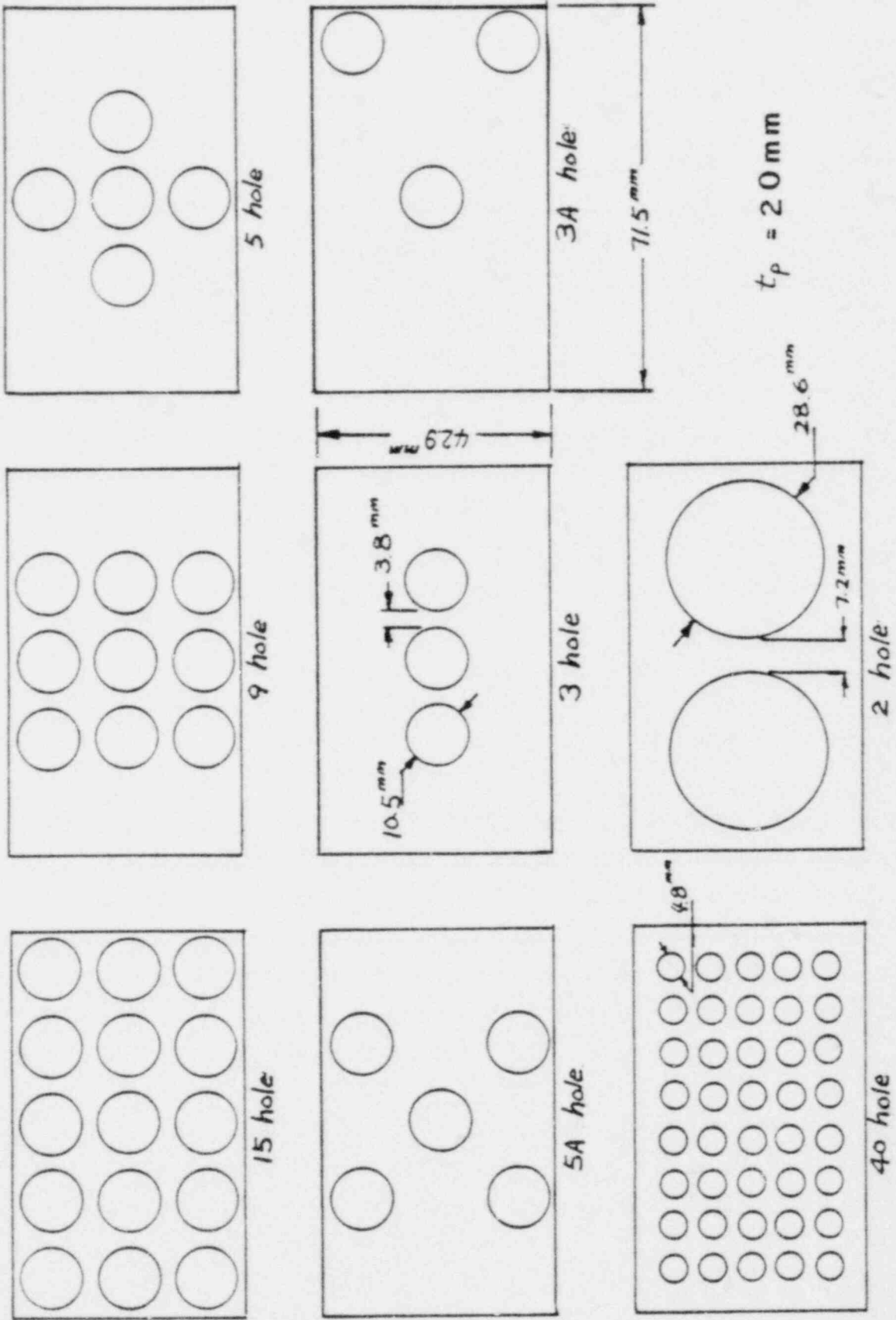


FIGURE 1. Geometries of the test perforated plate.

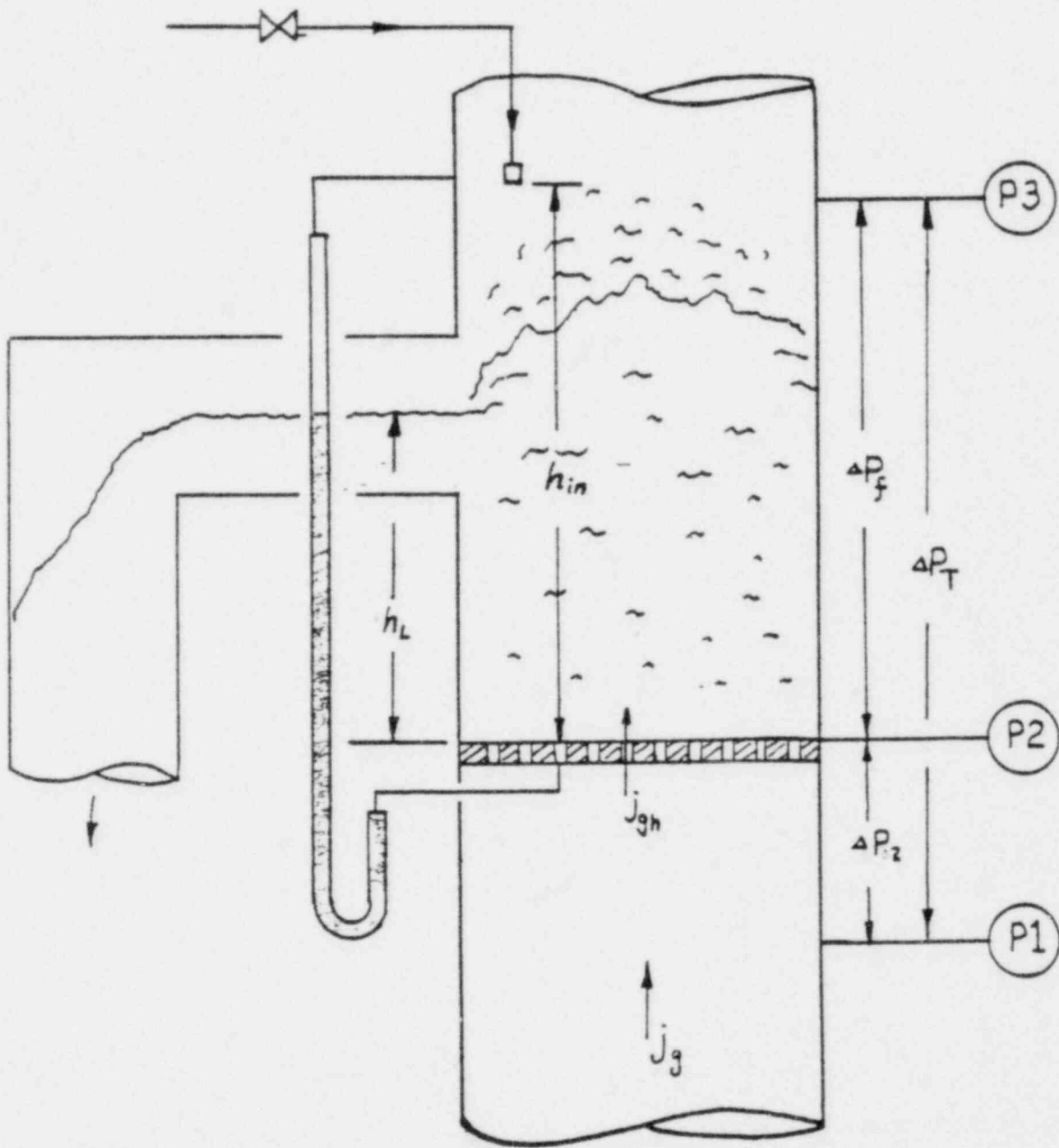


Figure 2. Perforated Plate Diagram

where C_o , the orifice coefficient, is a function of perforation ratio A_h/A_T , ratio of plate thickness to hole diameter t_p/D_h , and hole layout. Though this approach oversimplified the real physical situation where gas/liquid interaction effects are present, it has been convenient for design purposes. He further suggested that the weep point can then be correlated as a relation between h_L and h_p (Figure 3).

Essentially, based on a steady-state force balance across a particular hole in the perforated plate, weeping will occur if and only if the following relation is satisfied (Figure 2):

$$p_2 > p_1 + p_{e1} \quad (2)$$

where p_{e1} is the excess pressure required to overcome the resistance to liquid flow through the holes. It is assumed here that p_1 , p_2 , and p_{e1} are all time independent variables.

By subtracting p_3 from both side of equation (2), this criterion of weep point becomes

$$\Delta p_f > \Delta p_T + p_{e1} \quad (3)$$

Further defining

$$\Delta p_f = \overline{\Delta p_f} + p_{fv} \quad (4)$$

$$\overline{\Delta p_{12}} = \Delta p_T - \overline{\Delta p_f} \quad (5)$$

where $\overline{\Delta p_f}$ means the time average value of Δp_f , etc., equation (3) can then be expressed as

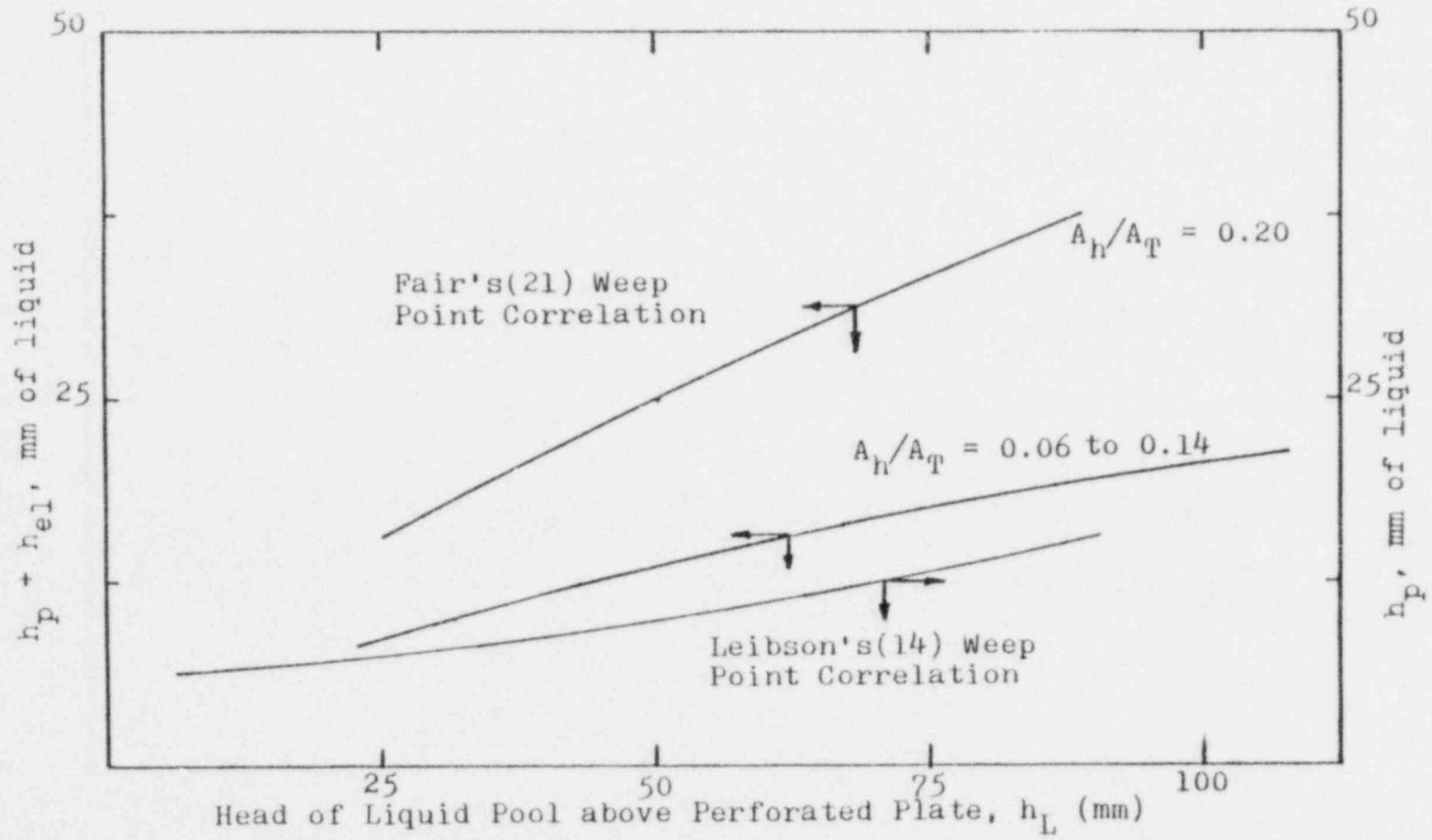


Figure 3. Perforated Plate Weep Point Correlations

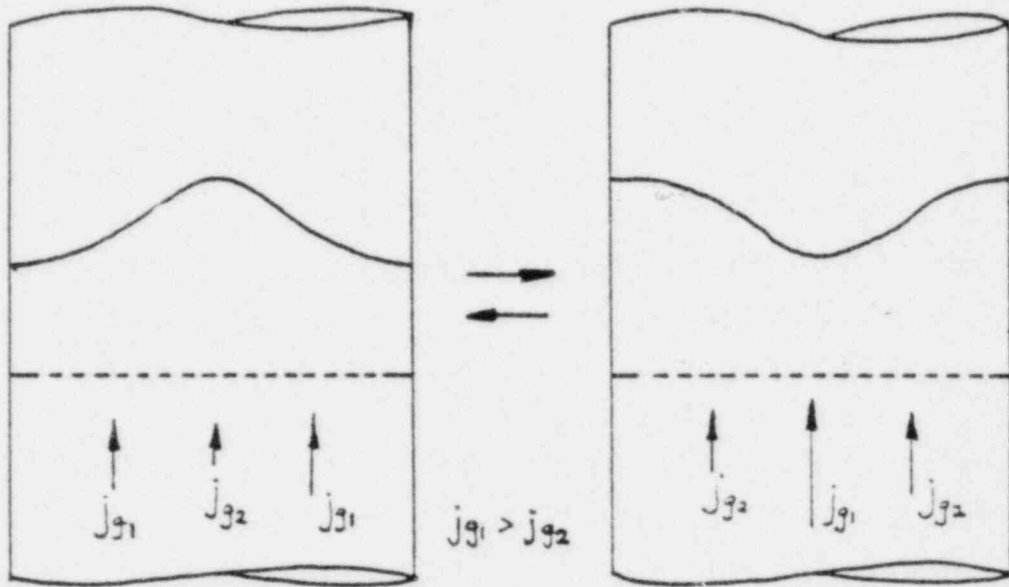
$$P_{fv} > 4p_{12} + P_{e1}$$

(6)

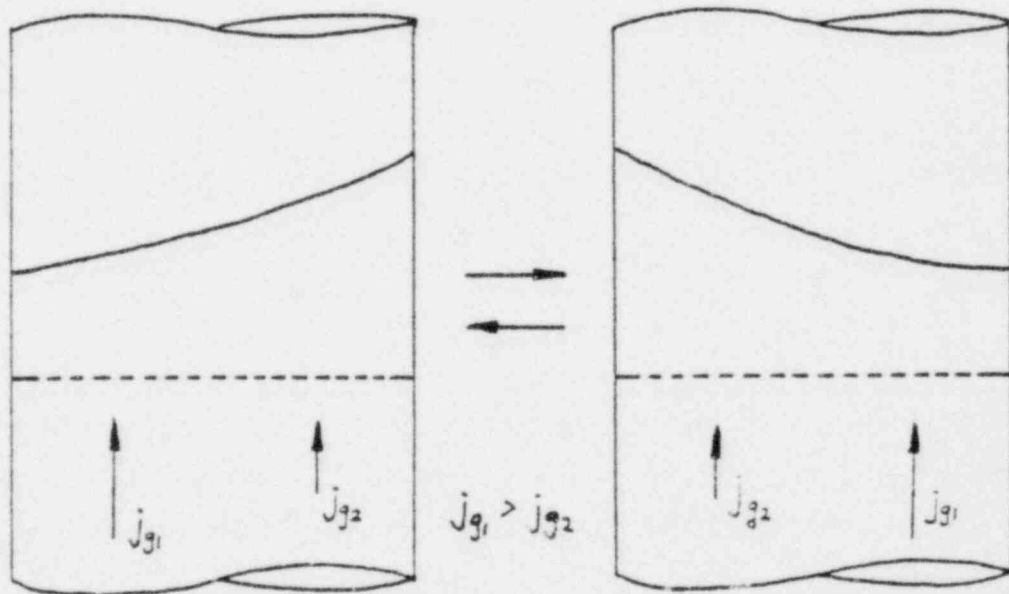
where p_{fv} is the fluctuating component of p_v . Causes of this fluctuation are many. Should the liquid above the plate be sub-cooled, condensation(15) can cause the pressure fluctuation. Two types of oscillation have also been observed when the system is operating at pressures below atmospheric(16). In the first type, full-wave oscillation, a standing wave is generated in the gas/liquid free surface, with the nodes at the walls(Figure 4-I). With further increase in the vapor velocity to a critical point half-wave oscillation is reached where there is a violent slashing from side to side across the direction of liquid flow(Figure 4-II). If there is no condensation or oscillation, Zanelli and Bianco(17) showed that p_{fv} is a function of head of liquid pool h_L only. This may explain why Leibson successfully correlated his weep point data in a h_L vs. h_p curve.

This simple model for weep point prediction has been followed by most of the perforated plate designers(17-20). Up to now, the weep point correlation curves suggested by Fair(21), where P_{e1} is equal to $k'(\delta/D_n)$, is still recommended by Chemical Engineers' Handbook(22) as the standard weep point prediction method.

However, since almost all of these experiments are simulating the operating conditions of the distillation tower, the highest liquid head h_L studied is less than 105 mm, perforation ratio never exceeds 25%, and plate thickness t_p is usually less than 5 mm. Of course, the condensation-driven fluid motion has never been mentioned. Therefore, their results would not be applicable for the weep point prediction on the geometries and operating condition similar to the tie plate of a nuclear fuel assembly in the LOCA condition.



I. Full-Wave Oscillation



II. Half-Wave Oscillation

Figure 4. Oscillation Behavior of Perforated Plate

McCann and Prince(23) initiated theoretical investigations on the rate of weeping. By using potential flow analysis, the rate of weeping in a single orifice was studied. According to their report, weeping of liquid happens after every bubble detachment in a cyclic way as a result of the pressure behind the rising bubble becoming greater than the chamber pressure(Figure 5A). The agreement between their experimental and predicted values is fairly good; nonetheless, this model does not fit the observation of those experiments on a perforated plate where many holes operate all together. Instead, the model suggested by Shoukry and Kolar is closer to the real situation for a perforated plate(24).

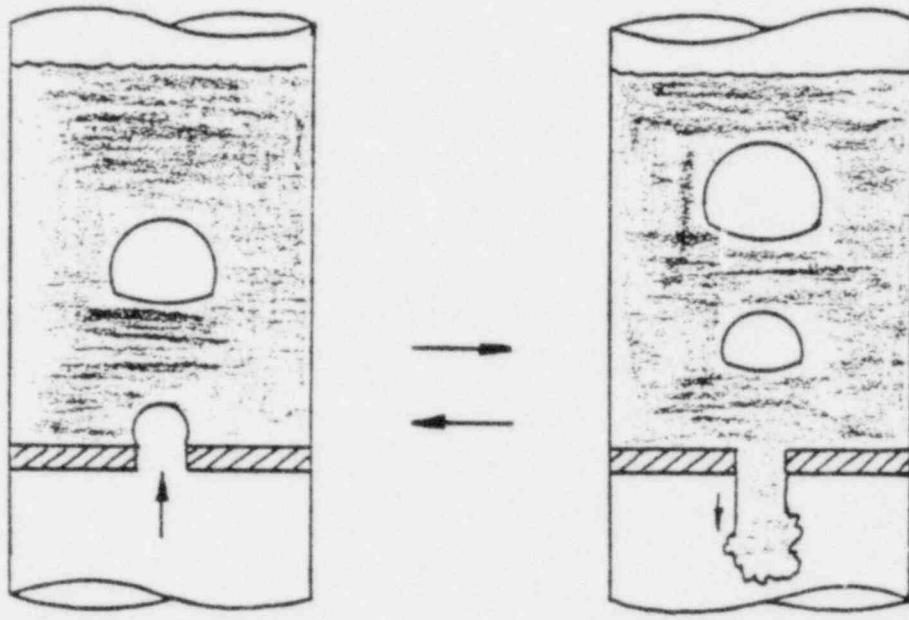
In this model(Figure 5B), the total cross-section area of the plate can be divided into three areas which are instantaneously changing value and position such that:

$$A_T = A_g + A_f + A_b \quad (7)$$

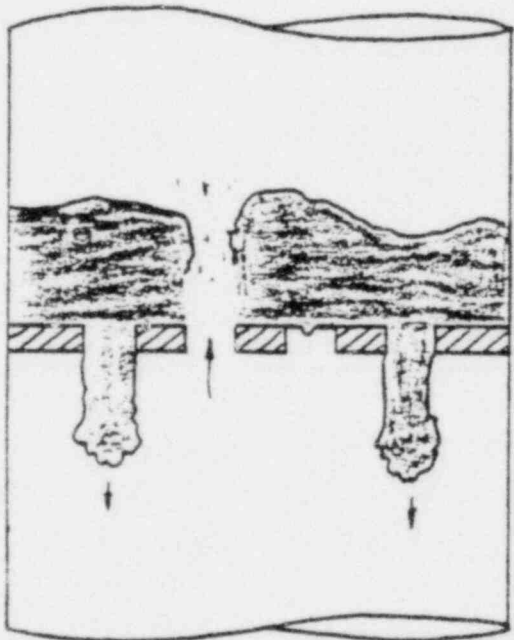
As the liquid flows down in the weeping area A_f , and gas flows up in the gas area A_g , there is no fluid flow in the blocked area A_b . However, no data on the rate of weeping were reported in their research.

Wallis'(25) flooding equation and/or its modifications(26), which has long been used to correlate the flooding data in vertical tubes and annuli, has been again adapted here by many investigators to correlate the data on weeping rate from perforated plates(8, 27).

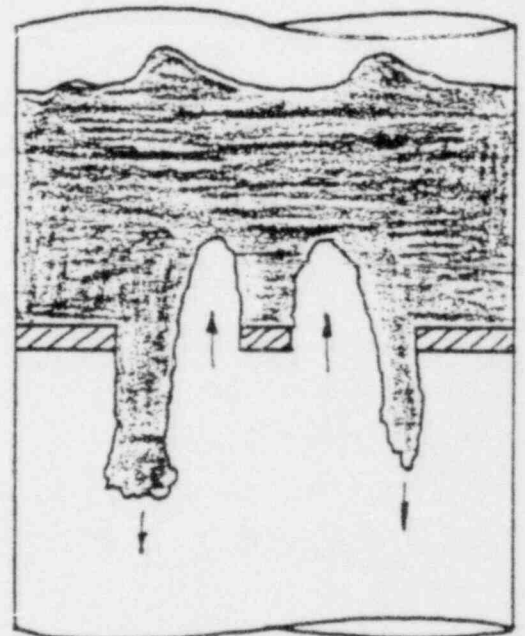
Using a separated cylinder model with the assumption of a constant mixing length in each cylinder, Wallis proved that, in the absence of viscous and surface tension effects, the flooding equation in a vertical two-phase counter-current flow system is



A. Intermittent Weeping



B. Alternative Weeping



C. Counter-current Weeping

Figure 5. Perforated Plate Weeping Models

of the form:

$$J_g^{*2/(n+1)} + J_f^{*2/(n+1)} = 1 \quad (8)$$

$$\text{where } J_{g,f}^* = [\rho_{g,f}/\rho_w(\rho_f - \rho_g)]^{1/2} j_{g,f} \quad (9)$$

and w is a characteristic dimension of the duct cross section. The value of n is equal to 3.5 or 2.5, depending upon whether the mixing length l_f and l_g are scaled by the dimensions of each cylinder or by the overall pipe diameter. Let n take on the intermediate value of 3, equation (8) then becomes

$$J_g^{*1/2} + J_f^{*1/2} = 1 \quad (10)$$

This equation is empirically further modified to:

$$J_g^{*1/2} + m J_f^{*1/2} = C \quad (11)$$

For flooding inside a single vertical tubes, the characteristic dimension w , as suggested by Wallis, is equal to the diameter of the tube.

Based on the survey held by Tien and Liu(5), the value of C depends mainly on the tube inlet and exit geometries, ranges from 0.7 to 1.0, while m has a value of 0.8 to 1.0. For fully turbulent flow the value of m is equal to 1. The curves of both Lobo(2) and Sherwood(1) for flooding in a packed column can also be fitted by this equation as:

$$J_g^{*1/2} + J_f^{*1/2} = 0.775 \quad (12)$$

The Wallis equation has also been adapted to correlate the flooding data in annular geometries. Shires and Pickering(30)

suggested four different types of characteristic dimensions for this type of flow channel:

$$w_1 = D_o \quad (13)$$

$$w_2 = (D_o - D_i)/2 \quad (14)$$

$$w_3 = D_i \quad (15)$$

$$\text{or } w_4 = (D_o^2 - D_i^2)/D_i \quad (16)$$

Though their experiments did not provide enough information to decide the appropriate dimension, the mean hydraulic diameter calculated by equation (16) best brought their annulus data together. Using w_4 as the characteristic length, their air/water flooding data were correlated as:

$$J_g^{*1/2} + J_f^{*1/2} = 0.71 \quad (17)$$

Ueda and Suzuki(7) used as their form of characteristic dimension for the annular geometry:

$$w_5 = (D_o^2 - D_i^2)/(D_o + D_i) = 2 w_2 \quad (18)$$

Using this characteristic dimension, their data can be expressed as

$$J_g^{*1/2} + J_f^{*1/2} = 0.80 \quad (19)$$

while using w_4 , the same data can be correlated as

$$J_g^{*1/2} + J_f^{*1/2} = 0.64 \quad (20)$$

Flooding phenomena in annular geometries with gap size of

the annulus(w_2) between 6.4 mm and 50.8 mm have been investigated by Creare Incorporated and Battelle Coumbus Laboratories(31, 32 33, 34). The data obtained can not be correlated by the use of gap size w_2 as the characteristic length. Since scale effects and L/D effects have not been sufficiently studied, a definitive choice of a characteristic length for the annulus is not possible at present. The average circumference of annulus has been conditionally accepted by Creare Incorporated(6, 35), Battelle Columbus Laboratories(36) and Dartmouth College(37) in their data correlations. This characteristic length can be formulated as

$$w_6 = \pi(D_i + D_o)/2 = \pi(D_i + w_2) \quad (21)$$

$$(D_i \quad \text{if } D_i \gg w_2)$$

Rothe(35) gave a thorough review of the data obtained from these laboratories. By using w_6 as the characteristic length, all the data can be correlated by equation (11) with m ranging between 0.7 and 0.8, and C between 0.34 and 0.42. Since D_i is five to ten times larger than w_2 in the annuli studied, correlating the data with w_6 as the characteristic length essentially means that the flooding condition is relatively independent of the gap size. Further investigation in larger annulus is necessary to verify the proper characteristic length for equation (11).

Pushkina and Sorokin(26) suggested another form of characteristic length:

$$w_7 = [d/(g(\rho_f - \rho_g))]^{1/2} \quad (22)$$

This characteristic length is similar to the horizontal wave length used in Taylor instability. Introducing this wave length into equation (11) will result in:

$$K_g^{*1/2} + m K_f^{*1/2} = C \quad (23)$$

where K^* , the Kutateladze number, is

$$K_{f, g}^* = \rho_{f, g}^{1/2} j_{f, g} / [g \sigma (\rho_f - \rho_g)]^{1/4} \quad (24)$$

Their experiments shows that the breakdown of liquid film downflow(the zero liquid penetration point) can be expressed as

$$K_g^* = 3.2 \quad (25)$$

Essentially, K^* can be rewritten in the following form:

$$K^* = J^* D^{*1/2} \quad (26)$$

where D^* is a dimensionless characteristic length

$$D^* = D [g(\rho_f - \rho_g)/\sigma]^{1/2} \quad (27)$$

D^* is the square root of the Eötvös number, or equivalently one half of the square root of the Bond number(38), and is a ratio of buoyancy and surface tension force. Wallis and Makkenchery(39) found that J^* correlated the data over a limited range of D^* from 3 to 20, while the criterion $K^* = 3.2$ was more appropriate for D^* larger than 30. Recent work by both Battelle Columbus Laboratories(36) and Dartmouth College(37) indicated that neither parameter K^* nor parameter J^* with circumference as the characteristic length can satisfactorily correlate the data over a wide range of scale.

Based on the Helmholtz instability concept for annular geometries, a new dimensionless flow rate scaling I^* is now under development(40, 48). This I^* scaling is expressed as

$$J_g^{*1/2} + (\rho_g/\rho_f)^{1/2} J_f^{*1/2} = [\sigma k B(k, R_o, R_i) / (g(\rho_f - \rho_g)D)]^{1/4} \quad (28)$$

$$\text{where } B(k, R_o, R_i) = \frac{[I_1(kR_o)K_1(kR_i) - K_1(kR_o)I_1(kR_i)]}{[I_1(kR_o)K_0(kR_i) - K_1(kR_o)I_0(kR_i)]} \quad (29)$$

I, K are the modified Bessel functions, and k is a critical wavelength. The characteristic length is suggested to be either w_3 or w_6 . However, one sees that in the limit as $R_o \rightarrow \infty$, $R_i \rightarrow \infty$, with $R_o - R_i$ fixed, $B \rightarrow 0$, which does not agree with equation (11) (as it should). In order to generalize equation (28), they suggested that $B(k, R_i, R_o)$ be replaced by D^α , leading to

$$J_g^{*1/2} + J_f^{*1/2} = [\sigma k D^{\alpha-1} / (g(\rho_f - \rho_g))]^{1/4} \quad (30)$$

It is suggested that when $\alpha=1$, equation (30) is reduced to J^* scaling, for $\alpha=0$, it goes to K^* scaling, and for $0 < \alpha < 1$, equation (30) represents an intermediate I^* scaling. However, one should notice that while all the terms in the left hand side of equation (30) are dimensionless, the right hand side of this equation is not a dimensionless term, which may cause some problems in the data analysis.

By the use of the momentum equation, Wallis(29) obtained another form of the flooding equation:

Ignoring compressibility effects and variations of liquid film thickness, a momentum balance on the gas core of an annular two-phase flows yields:

$$(dp/dz) + \rho_g g + 4\tau_i/D\sqrt{\alpha} = 0 \quad (31)$$

where τ_i is the interfacial shear stress, which may be related to the interfacial friction factor f_i as

$$f_i = 2\tau_i \alpha^2 / \rho_g j_g^2 \quad (32)$$

By considering the force balance for the entire cross-section of the tube, one can have

$$(dp/dz) + \rho_g g + (1-\alpha)(\rho_f - \rho_g) = 4\tau_w/D \quad (33)$$

And the relation between the wall shear stress τ_w and the wall friction factor f_w is given as

$$f_w = 2\tau_w (1-\alpha)^2 / \rho_f j_f^2 \quad (34)$$

By combining equations (31) and (33), the gas and liquid flow rate can be related as

$$2f_i J_g^{*2} / \alpha^{5/2} + 2f_w J_f^{*2} / (1-\alpha)^2 = (1-\alpha) \quad (35)$$

Provided the friction factors f_i and f_w are known, the limiting J_f^* and J_g^* can be obtained as an envelope of curves generated with $(1-\alpha)$ as a parameter. This envelope will lie above the flooding curve given by equation (12) in the J_g^* vs J_f^* plane.

Sun(49) suggested that in addition to equation (35), the equation of continuity should also be considered:

$$(1/\alpha)J_g^* + (\rho_f/\rho_g)^{1/2} J_f^*/(1-\alpha) = U_{cr} (\rho_f/gD(\rho_f-\rho_g))^{1/2} \quad (36)$$

where U_{cr} is the critical relative velocity between the phases.

The flooding limitation is, then, to find the intersection

of equation (35) and equation (36), along with the proper expressions for f_i and f_w , at various values of the void fraction α . The flooding curve obtained is a convex line in the $J_g^{*1/2}$ vs $J_f^{*1/2}$ plane. Therefore, the suitability of these flooding models for any particular channel geometry can easily be verified by the data distribution in a $J_g^{*1/2}$ vs $J_f^{*1/2}$ plane.

Tobin's steam/water flooding data on a 7x7 BWR fuel bundle sleeves(41) shows a straight line in the $K_g^{*1/2}$ vs $K_f^{*1/2}$ plane, which means the conventional flooding relation expressed as equation (12) or (23) is more suitable for this case. These data are correlated as

$$K_g^{*1/2} + K_f^{*1/2} = 1.79 \pm 2\% \quad (37)$$

Jones' data(8) for 8x8 BWR fuel bundle upper tie plate is correlated as:

$$K_g^{*1/2} + K_f^{*1/2} = 2.07 \pm 8\% \quad (38)$$

Naitoh's data(42) for BWR 8x8 upper tie plate is

$$K_g^{*1/2} + K_f^{*1/2} = 2.06 \pm 6\% \quad (39)$$

Mohr and Jacoby(43) reported their air/water flooding data obtained with a full size model of the upper core and upper regions corresponding to a single pressurized water reactor(PWR) fuel bundle of both Westinghouse Electric Corporation and German Kraftwerk Union(KWU) designs. Their data can also be correlated by straight lines in the form of

$$K_g^{*1/2} + m K_f^{*1/2} = c \quad (40)$$

Depending on the particular geometry studied, the value of m varied between 0.7 and 2.2, and C between 1.31 and 2.04. Therefore, one can conclude that the flooding phenomena for this case are heavily geometry dependent.

2.2 Experimental Apparatus

2.2.1 Test Channel

Figure 6 shows the schematic diagram of the experimental apparatus. A detail drawing of the test channel is shown in Figure 7. The channel frame, which includes the side, top and bottom plates, is made of 12.7 mm thick brass. In order to provide visual observation during the experiment, the front and back wall of the channel are made of transparent Lexan. After covering the contact surfaces between Lexan and brass with silicone adhesive, the Lexan plates are clamped to the brass frame by tie rods. This method effectively prevented any leakage from the Lexan-brass contact surfaces.

The plate geometries that have been tested in air/water system have been labeled (Figure 1): 15 hole, 9 hole, 5 hole, 5A hole, 3 hole, 3A hole, 40 hole and 2 hole. The hole diameter (D_h) in the 2 hole plate is 28.6 mm, and in the 40 hole plate is 4.8 mm. D_h in all other test plates is fixed at 10.5 mm, which is same as the lower tie plate of the German KWU PWR fuel assembly. The dimension of all the plates is 72 mm x 43 mm. The thickness of the plates, which is also simulating the KWU geometry, is 20 mm.

The perforation ratio, the ratio of total hole area to channel cross-section area, has been varied between 42.3% and 8.5%. The 15 hole plate, with the perforation ratio of 42.3%, has a geometry similar to that of the KWU lower tie plate.

2.2.2 Water Line

Tap water from building 1-1/4 inch water supply line is

POOR ORIGINAL

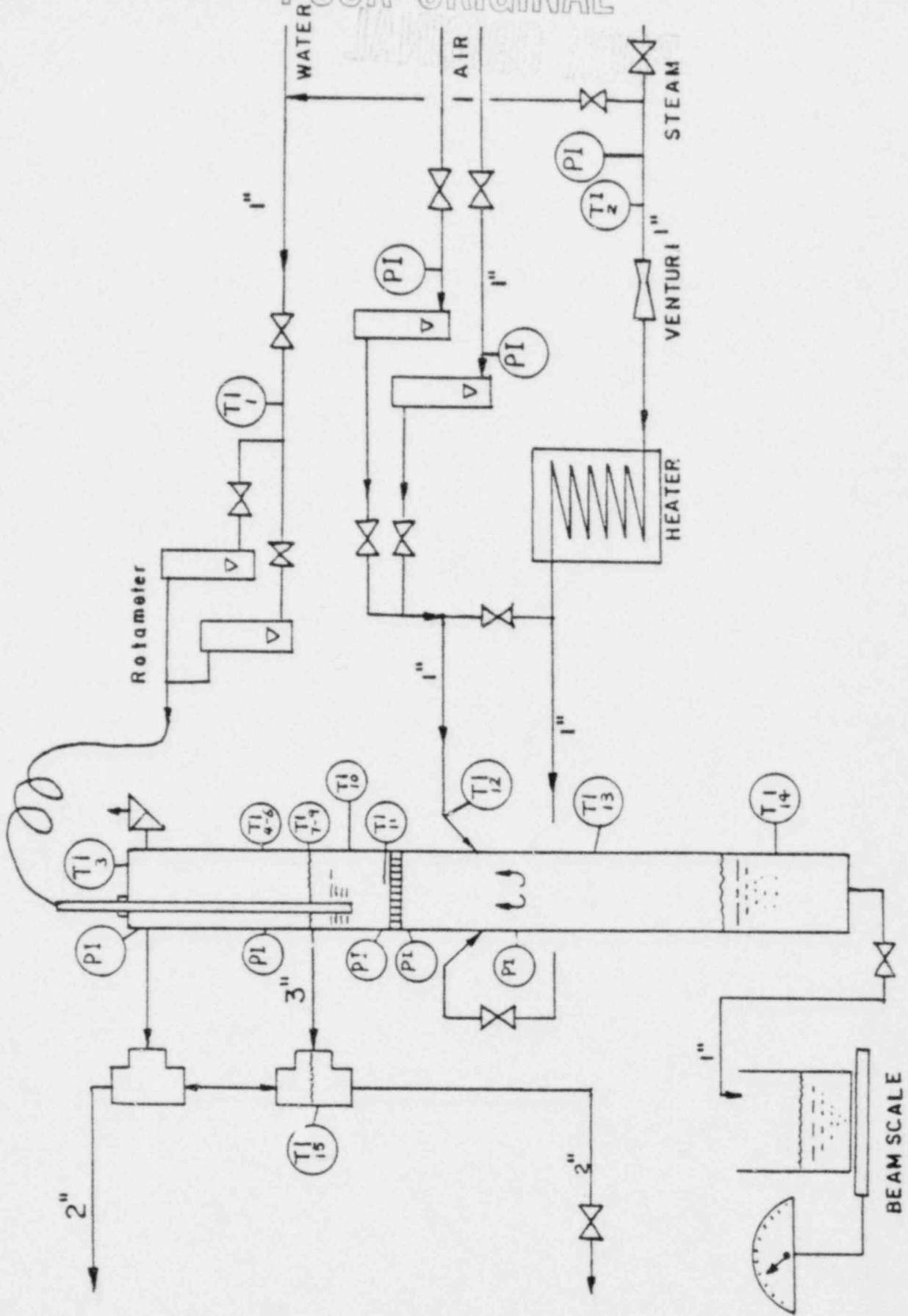


FIGURE 6. Schematic diagram of experimental apparatus.

POOR ORIGINAL

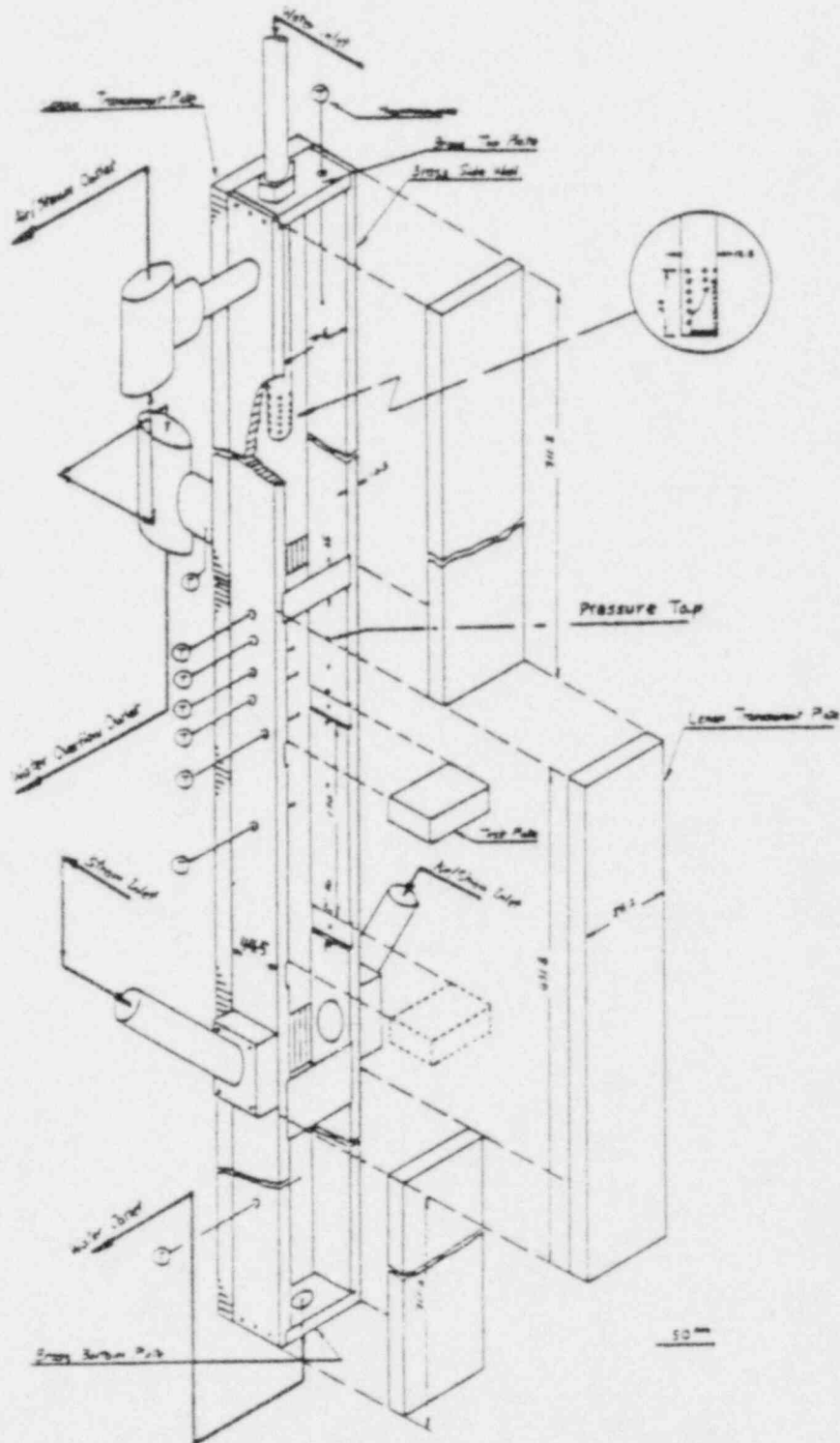


Figure 7. Isometric Diagram of the Test Channel

brought to the test channel by a 1 inch brass pipe line. During the whole period of experiment, the tap water temperature varied from 276 K(winter) to 288 K(summer). Water is fed into the channel through a 1/2 inch flexible hose connected from the water line to a water inlet spray device. This device is made of a 1.5 m long 1/2 inch O. D. brass tube. At the bottom end of this tube, the whole cross-section area is sealed by welding, while 5 rows of 3 mm diameter holes, 6 holes in each row, are drilled along the wall of the tube.

Water to the channel flows out horizontally through these holes, so that the downward direction momentum flux of the feed water can then be minimized. The distance between the test plate and the bottom tip of the spray tube, h_{in} , can be adjusted. After h_{in} is adjusted, the spray tube is fixed to the top plate of the channel by tightening a swagelock fitting at the top of the channel.

A 50 mm I.D. water overflow port is attached on the Lexan back wall of the channel. By changing the position of the test perforated plate, the distance between the centerline of the port and the top of the plate can be adjusted to either 267 mm or 445 mm. It is assumed that this distance is equal to the head of clear liquid above the plate, h_L (Figure 3). Excess water that can not weep downward will flow out the channel through this port, passing a 50 mm I.D. pyrex glass tee, and then flowing down to the water sump. This pyrex glass tee, with its main function as a gas-liquid separator, facilitates a visual observation of the onset of water overflowing.

Water weeping down through the perforated plate will flow out through a 1 inch nozzle at the bottom plate of the channel. A 1-1/4 inch I.D. flexible hose connected to this nozzle can lead the water either to the water sump or to the beam scale measurement to determine the rate of weeping. By adjusting the high point

of the hose the liquid level in the lower section of the channel, and hence the soft volume, can be altered.

2.2.3 Air Lines

Two independent air supply lines have been connected to the test channel. A 1 inch brass line can supply air from the departmental air compressor at 800 kPa with a maximum flow rate of $1.18 \times 10^{-2} \text{ m}^3/\text{s}$. Another 3/8 inch air line connected from building air supply facility can supply air at 300 kPa with its maximum flow rate equal to $1.17 \times 10^{-3} \text{ m}^3/\text{s}$.

Air and/or steam will flow into the channel through two 1 inch nozzles built into the side wall of the channel. Pointing downward, these nozzles make a 45 degree angle to the side wall of the channel, in order to minimize the entrance effect of the inlet gas momentum.

After passing through the perforated plate, air/steam can flow out either with water through the water overflow port mentioned above or through a 1 inch nozzle on the side wall right beneath the top plate of the channel. Both of these gas streams then combine into a 3 inch flexible hose and flow out of the window. Pressure drop along along this gas outlet pipe line is very small; hence, operating pressure of the channel in all test runs is very near to atmospheric pressure.

2.2.4 Instrumentation

The water flow rate is measured by two rotameters installed in parallel along the water line, with range: 0.0227 kg/s to 0.273 kg/s and 0.0379 kg/s to 0.417 kg/s. The maximum water flow rate, scaled to the KWU experiment, exceeds 0.038 kg/s/hole for the test plates with 10.5 mm diameter holes. Therefore, the water flow rate must be greater than 0.57 kg/s to run the 15 hole test plate. The flow rate through these rotameters can be controlled separately by adjusting two 1 inch brass globe valves. The rate of weeping is measured by a beam scale and a watch. Detailed measurement procedures are described in section 2.2.6 of this thesis. No measurement was made of the rate of water overflow.

The air flow rate is measured by two rotameters connected to the two air lines mentioned in section 2.2.3. The scales on these rotameters are 2 to 25 SCFM and 0.15 to 2.47 SCFM. Both the rotameter readings and the pressure at the rotameter inlet are required to calculate the air mass flow rate. A pressure gauge is, therefore, installed at the entrance of each rotameter. The air flow rate can be controlled by adjusting the globe valves both up and down stream of the rotameter. Opening the upstream globe valve will increase both the rotameter reading and pressure gauge reading, while opening the downstream valve will increase the rotameter reading but decrease the pressure gauge reading.

The temperature of the inlet water is measured by thermocouple T1 (Figure 6), installed upstream of the water rotameters. The temperature of the inlet air is measured by thermocouples T4 and T5. These measurements show that the water temperature was 285 ± 3 K. Readings of the remaining thermocouples were not recorded.

Two Validyne DP103 Extra Low Range Differential Pressure

Transducers were installed for pressure measurement. The range of these transducers is from 0.15 kPa to 3.6 kPa. Figure 8 shows the piping of these transducers. Along the sidewall of the channel, pressure taps have been installed. The pressure drop between any two of them can be measured by connecting them to the pressure transducer via a Swagelock quick-connect assembly. The absolute pressure at any pressure tap point can also be measured by connecting the positive end of the pressure transducer to the tap while leaving the negative end open to the atmosphere.

2.2.5 Computer Program

A computer program has written in FORTRAN IV to carry out the calculation and data plotting tasks. All the important variable names in the Program is given in Appendix I. Input of the Program includes rate of liquid weeping W_f (lbs/s), air rotameter reading W_g (SCFM), and pressure gauge reading P_g (psig). Superficial gas and liquid velocity through the holes are calculated by:

$$F_p = \exp(-0.05088459721 + 0.02841336269 \times \ln(P_g) - 0.05218174597 \times \ln(P_g)^2) \quad (41)$$

$$j_{gh} = W_g / (60.0 \times F_p \times A_h), \text{ ft/s} \quad (42)$$

These equations are obtained from Fischer&Porter Catalog 10A1022. Superficial liquid velocity is calculated by equation (43):

$$j_{fh} = W_f / (P_f \times A_h) \quad (43)$$

The conventional flooding equation in the form of equation (12) or equation (23) with several types of characteristic length were

POOR ORIGINAL

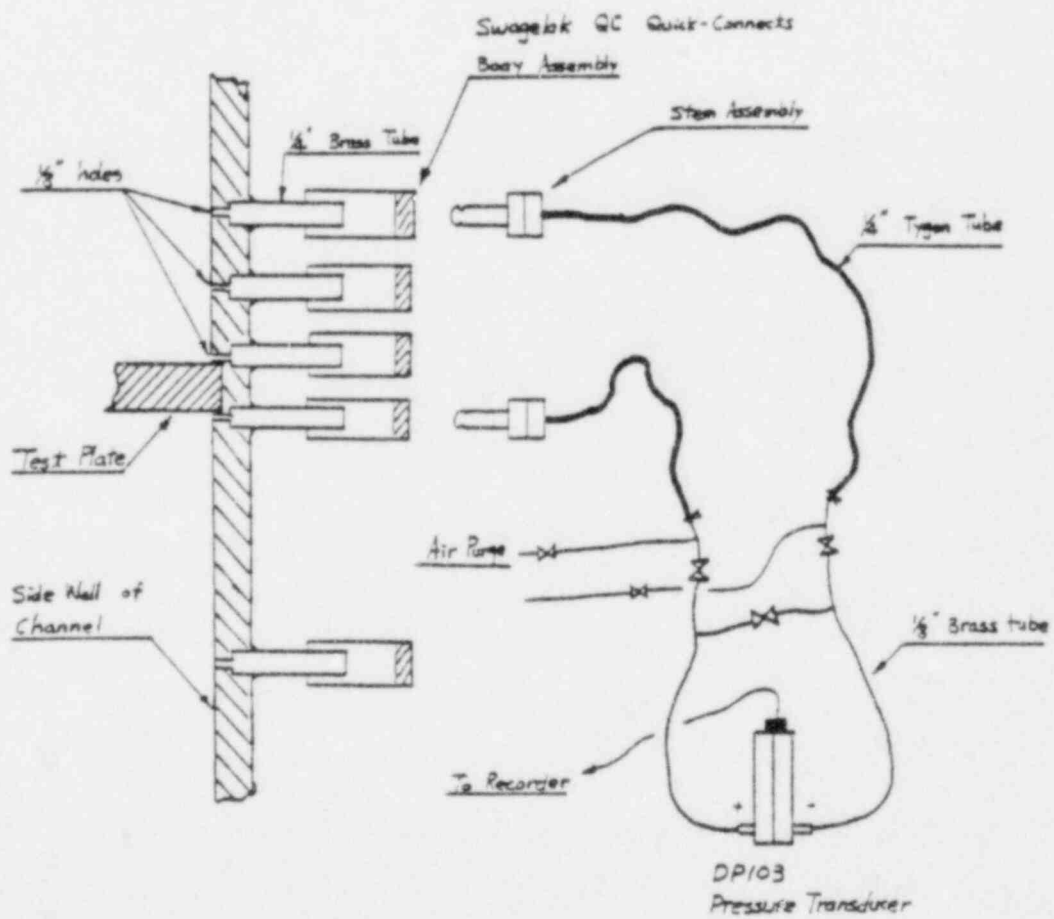


Figure 8. Piping of Pressure Measurement Device

tried to correlate the data. Physical properties of the fluid, which includes density of air and water, and surface tension of water, are all assumed constant. Results of these correlations are discussed in Chapter 3.

2.3 Experimental Procedure

The standard experimental procedure can be listed as follows:

1. Select a test perforated plate. Fix it into its position in the channel.
2. Fix the height of water inlet nozzle.
3. Fix the water inlet flow rate at the pre-selected rotameter reading.
4. Measure the rate of weeping by beam scale and stop watch through the following steps:
 - 4.1 Leave the empty water container on the beam scale. Balance the scale with a weight.
 - 4.2 Measure the time(sec.) required for a pre-set amount of water(lbs.) to flow into the container. Calculate the water flow rate in lbs/sec.
 - 4.3 Repeat step 4.2 at least twice for different amount of water accumulated.
 - 4.4 Take the average value obtained in step 4.2 to 4.3 as the

rate of weeping. Without water overflowing, this value should be equal to the rotameter reading obtained in step 3.

5. Turn on the air inlet control valves. Record the rotameter reading and pressure gauge reading.
6. Measure the rate of weeping at this air flow rate by following steps 4.1 to 4.4.
7. Increase the air flow rate to a new reading. Record the air rotameter reading and the pressure gauge reading.
8. Repeat step 6 to 7 at a different air flow rates, and measure the rate of water weeping.
8. After enough data points have been collected through step 6 to 8, further increase the air flow rate to the weep point, which is determined by visual observation. Record the air flow at the weep point.
10. Repeat step 3 to 9 at different water flow rates to verify the influence of inlet water rate, if any, on the rate of weeping.
11. (Option) Repeat step 2 to 10 at different heights of water inlet, h_{in} , to study the influence of water inlet position on the rate of weeping.
12. (Option) Repeat step 1 to 10 at different heads of water above the plate, h_L , to study its influence on the rate of weeping.

3. Air/Water Experiment Data Analysis

Altogether, the data of 195 test runs have been collected in the air/water experiments. The parameters studied in these experiments include: height of liquid pool above the plate h_L , liquid inlet position h_{in} , liquid inlet flow rate, and soft volume. The data matrix is given in Table 1.

The flooding model in the form of equation (12) or equation (23) is adopted for analysis of the data obtained. This analysis will involve the selection of a proper characteristic length w for the flooding equation, and the correlation of coefficient m and C in the equation.

3.1 Visual Observations

In the 40 hole, 15 hole and 9 hole experiments, the ascending air and descending water flowed separately through different holes. Most of the holes near the channel wall were occupied by the descending water, while the air usually flowed through the holes near the middle of the plate, and there was essentially no counter-current flow at any particular hole. As the air flow rate increased, the number of holes which were filled with descending water was decreased. The weep point is then defined as the operating condition where no further weeping occurred, as in Shoukry and Kolář's model(24). (Figure 5B)

For the 5(5A) hole, and especially the 3 hole experiments, the mode of liquid delivery changed to intermittent weeping(Figure 5A). We can see bubble detachment in the pool, followed by a falling stream of liquid.

Table 1. Data Matrix of Air/Water Experiment

	h_L (mm)	h_{in} (mm)	W_{Lin} (Kg/s)	No. of Data Point
15 Holes	267	305	0.165	6
	267	5	0.165	18
	267	305	0.243	6
	267	305	0.474	5
	445	305	0.248	11
	445	100	0.475	10
9 Holes	267	305	0.182	12
	267	305	0.282	10
5 Holes	267	5	0.318	6
	267	305	0.318	6
	267	5	0.248	6
	267	305	0.248	9
5A Holes	267	305	0.147	11
	267	305	0.118	10
3 Holes	267	305	0.292	6
	267	305	0.099	9
	267	305	0.168	7
40 Holes	267	305	0.248	18
2 Holes	267	305	0.273	11
	267	305	0.335	11
	267	305	0.216	7

As for the 2 hole experiment, counter-current weeping occurred in each hole. Though 3 different types of weeping have been observed, they will all be analyzed by the flooding equation in the form of equation (12) or equation (23).

3.2 Correlation for Coefficient m

As a first trial, the data were plotted with $J_g^{*1/2}$ against $J_f^{*1/2}$ in Figure 9. The data of each plate can be fitted by a straight line which means the relation of

$$J_g^{*1/2} + m J_f^{*1/2} = C \quad (44)$$

holds here. The negative value of the slope of these lines is equal to m. As shown, all the lines, except the one for 40 hole data, can be correlated to $m = 1$. Data obtained in BWR or PWR tie plate geometries by Jones(8), Naitoh(42) and Mohr(52) also confirmed that $m = 1$.

The data of the 40 hole experiment can be correlated as

$$J_g^{*1/2} + 1.44 J_f^{*1/2} = 1.9 \quad (45)$$

with the coefficient of determination equal to

$$r^2 = 0.9958 \quad (46)$$

This higher value of m is possibly caused by the surface tension effect. As mentioned by Wallis(38), surface tension will dominate in the two-phase flow system when the following equation is satisfied:

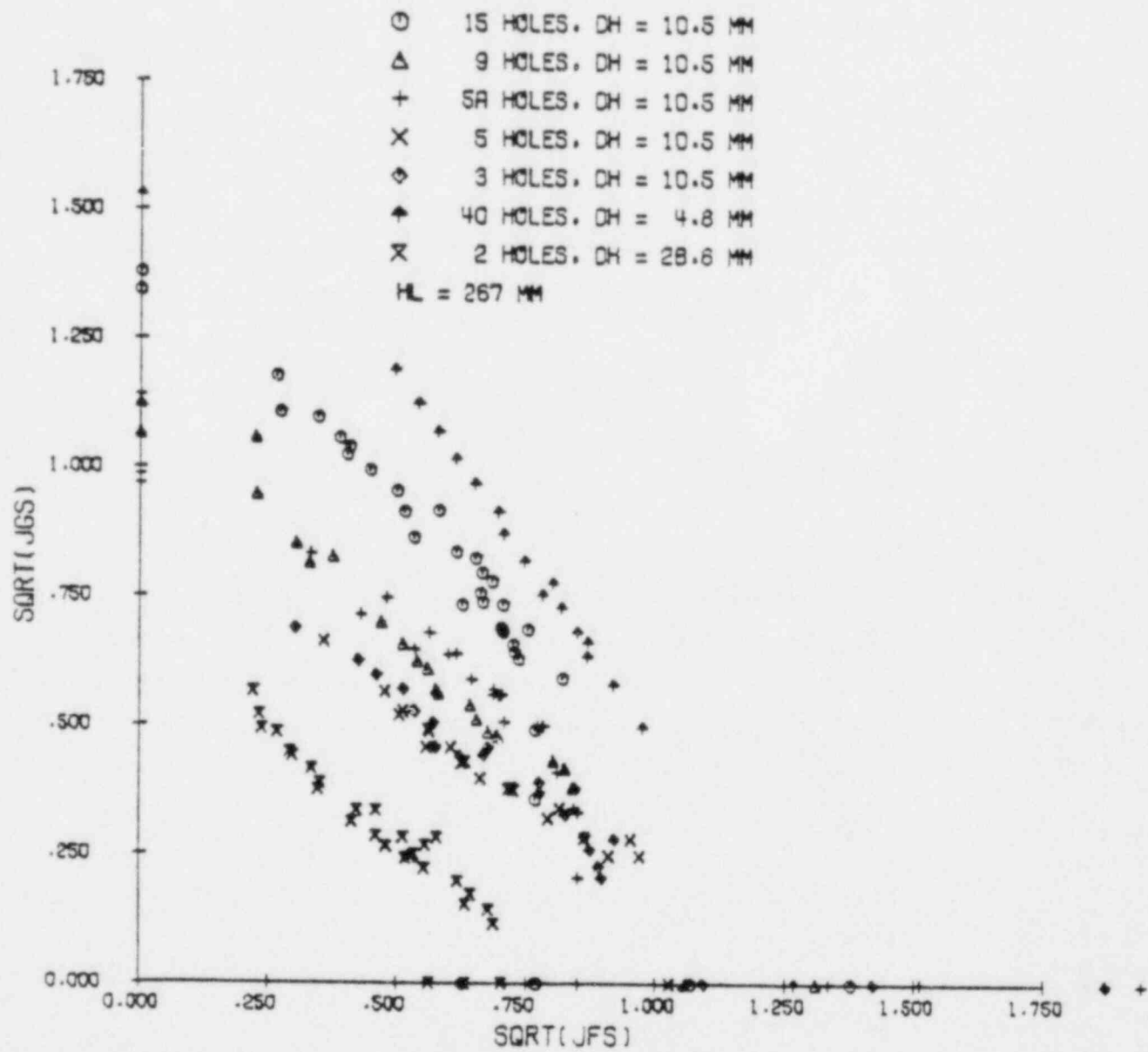


Figure 9. Data Correlation with Equation (12), $w = D_h$.

$$N_{E\ddot{o}} = [gD^2(\rho_f - \rho_g)/\sigma] < 3.37 \quad (47)$$

For 40 hole plate, $D_h = 4.76$ mm, and its Eötvös number is

$$N_{E\ddot{o}} = 3.03 < 3.37 \quad (48)$$

Therefore, in the low air flow rate region, surface tension could reduce the rate of water delivery, resulting a higher value of m .

3.3 Correlation of Coefficient C

As shown on Figure 9, the dependence of coefficient C on the geometry of the perforated plate can not be properly eliminated by using diameter of hole as the characteristic dimension. In other words, the coefficient C obtained in this way in a particular perforated plate will not be applicable for other perforated plates. Sun(28) has made the same conclusion in his flooding correlation for EWR bundle side-entry orifices.

Equation (23) was then tried in order to correlate the data. The result is plotted as $K_g^{*1/2}$ vs. $K_f^{*1/2}$ in Figure 10. It shows that the coefficient C is still influenced by some geometric factors of the perforated plate.

Based on a hanging film model, Wallis(36, 37) indicated that the Kutateladze number, i.e., equation (23), is more suitable for the flooding correlation of large tubes ($D^* > 30$), while equation (12) can be used in the range of $3 < D^* < 20$. Hence, a new dimensionless flow rate is suggested as:

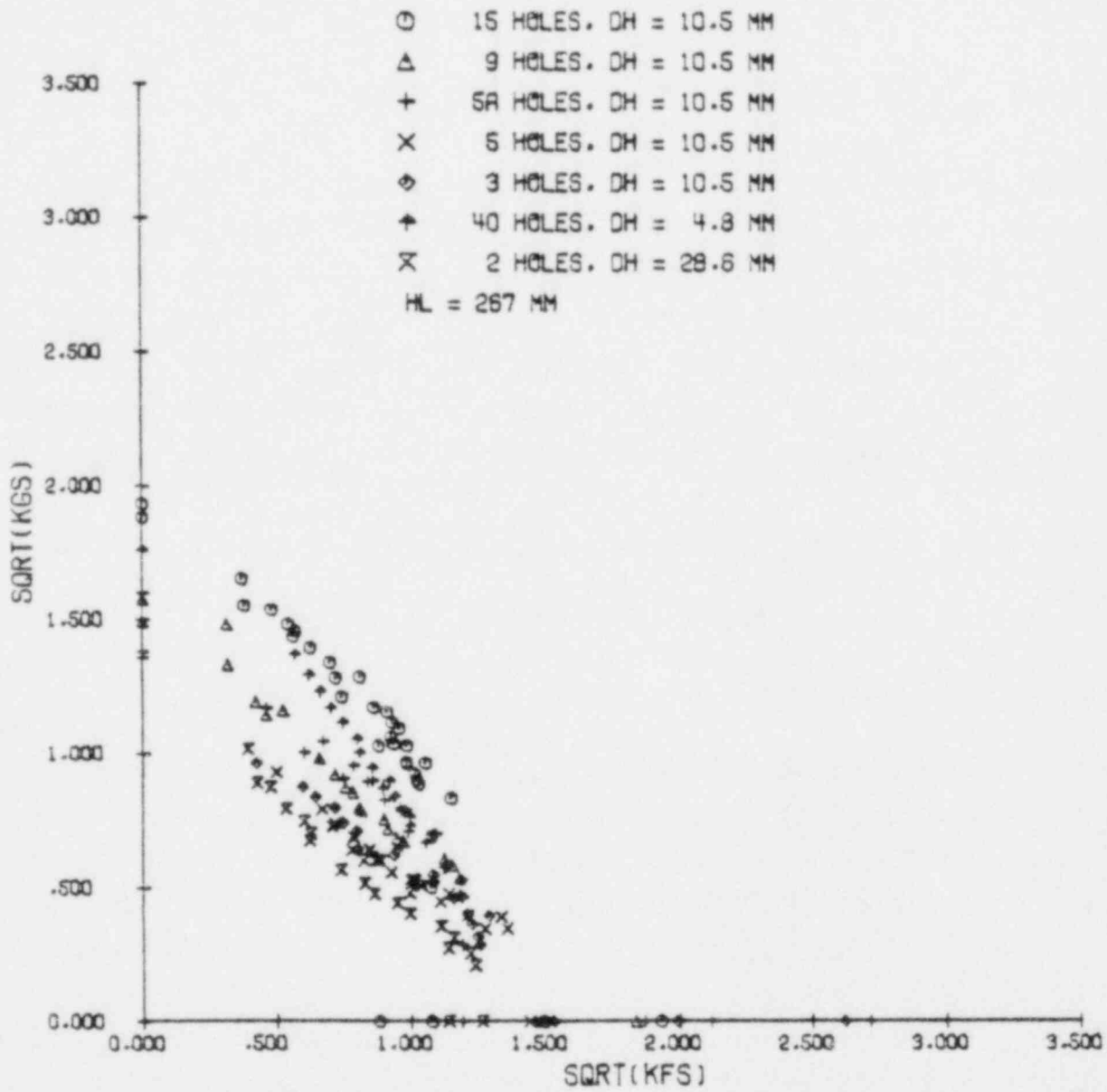


Figure 10. Data Correlation with Equation (23).

$$H_g^{*1/2} + H_f^{*1/2} = C \quad (49)$$

where $H_{f,g}^* = [\rho_{f,g}/g w_8 (\rho_f - \rho_g)]^{1/2} j_{f,g}$ (50)

$$w_8 = D_h^{(1-\alpha)} [\sigma/g (\rho_f - \rho_g)]^{\alpha/2} \quad (51)$$

The value of α lies in the interval between zero and one. when α is equal to zero, w_8 is just equal to D_h and equation (49) reduces to the form of equation (12) with J^* as the appropriate scaling form. For α equal to one, $w_8 = w_7 (= [\sigma/g (\rho_f - \rho_g)]^{1/2})$, and thus K^* scaling results. For α between zero and one, equation (49) represents the H^* scaling. Therefore, H^* scaling is essentially a smooth transitional scaling between J^* and K^* scaling.

The α is defined as a hyperbolic tangential function of kD_h and perforation ratio A_n/A_T .

$$\alpha = \tanh[(kD_h)(A_n/A_T)] \quad (52)$$

This function is plotted in Figure 11. Table 2 gives the value of α for each perforated plate tested in this experiment. By the use of this α function in equation (51), it is found that the value of C in equation (49) can be correlated as a function of L^* ($= n\pi D_h [g(\rho_f - \rho_g)/\sigma]^{1/2}$) only. The plot of C for each plate against the Bond number L^* , as illustrated in Figure 12, shows that the relation between C and L^* can be represented by a simple linear function. By method of linear regression, this line is fitted as:

$$C = 1.07 + 4.33 \times 10^{-3} L^* \quad (53)$$

with coefficient of determination:

Table 2. The Values of α for Each Perforated Plate

Labels of Plates	D_h	D_{hk}	A_h/A_T	α
15 hole	10.5	3.2	.423	0.884
9 hole	10.5	3.2	.254	0.671
5 hole 5A hole	10.5	3.2	.141	0.422
3 hole 3A hole	10.5	3.2	.085	0.264
40 hole	4.8	1.5	.232	0.335
2 hole	28.6	9.0	.418	0.999

$$\alpha = \tanh[(D_{hk})(A_h/A_T)]$$

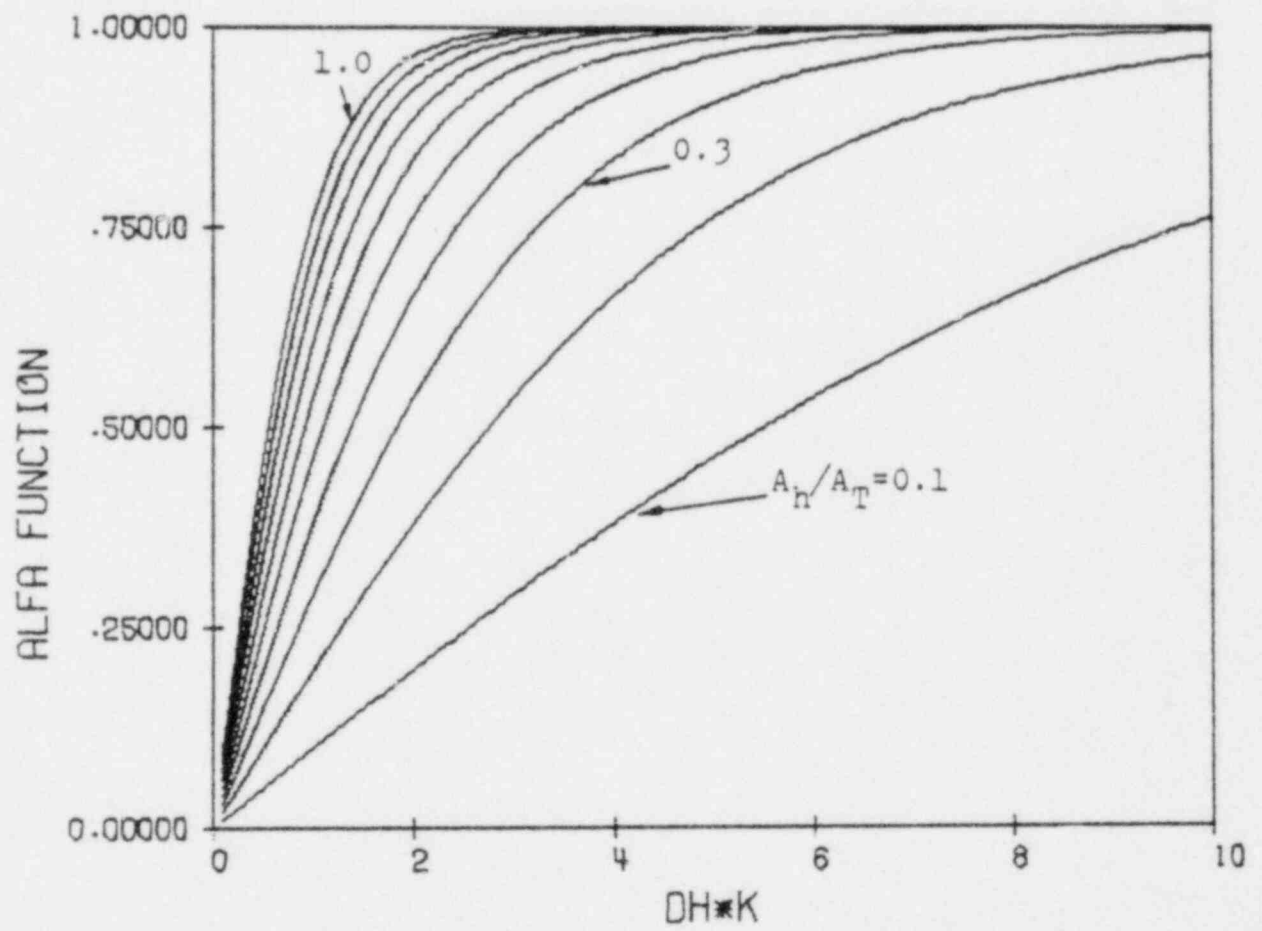


Figure 11. The α function given by equation (52).

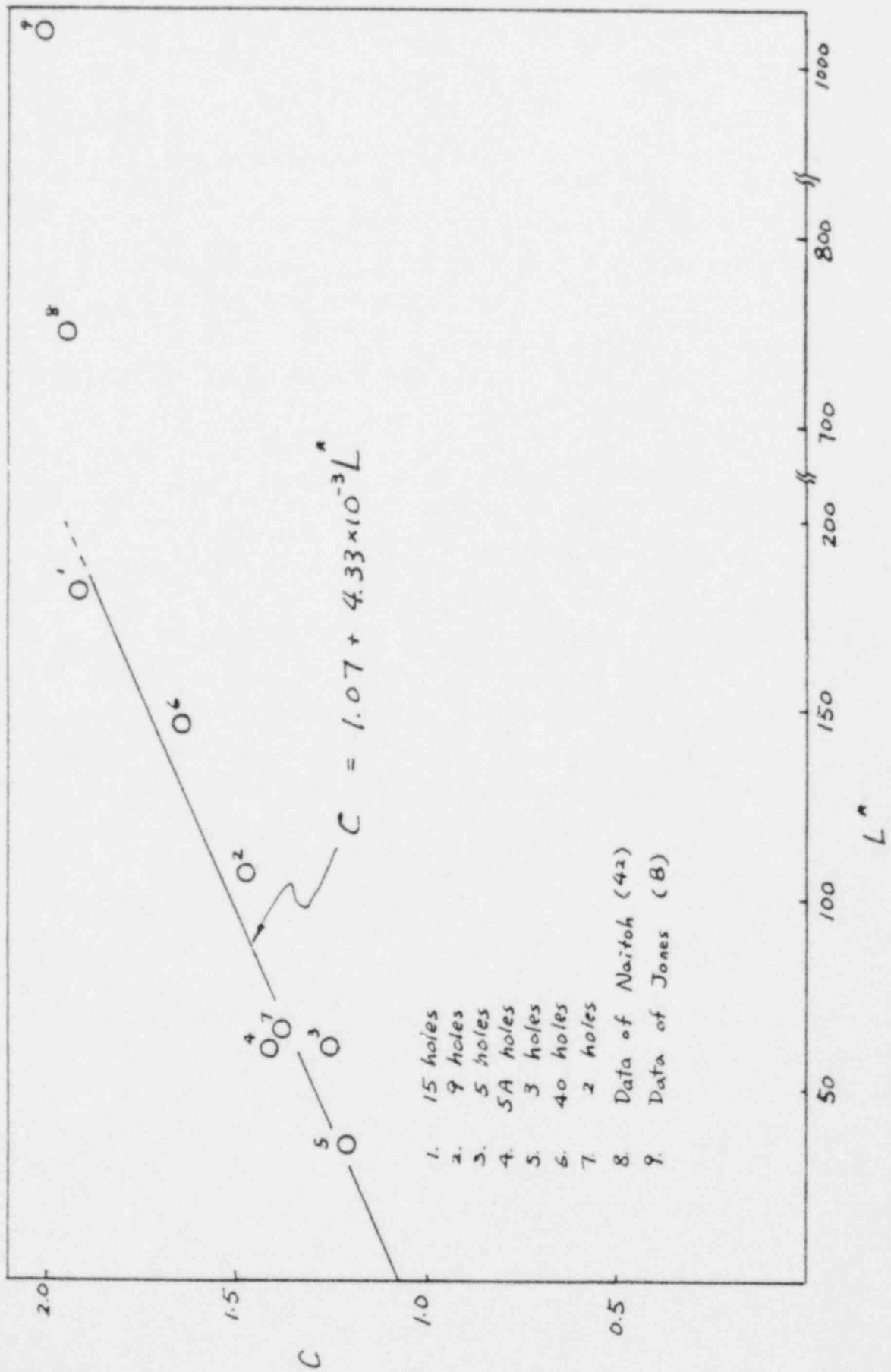


Figure 12. Coefficiency C in equation (55) as a function of L^n .

$$r^2 = 0.93 \quad (54)$$

The applicable range of equation (49) is $30 < L^* < 200$. Data obtained in BWR upper tie plate geometries reveals that as L^* becomes large, the value of C approaches a upper limit of 2.0.

Therefore, a general equation for perforated plate weeping rate prediction is suggested as

$$H_g^{*1/2}/C + H_f^{*1/2}/C = 1 \quad (55)$$

$$\text{where } C = 1.07 + 4.33 \times 10^{-3} L^* < 2.0 \quad (56)$$

Figure 13 shows the data plotted with $H_g^{*1/2}/C$ vs. $H_f^{*1/2}/C$. Based on the data shown, it is reasonable to conclude that equation (55) are an adequate rate of weeping data correlation. This equation, along with equation (56) and (52) will then be used in the correlation of steam/cold water experimental data.

3.4 Effect of Liquid Inlet Rate

The dimensionless liquid inlet rate is plotted on the abscissa of Figure 13 as $H_f^{*1/2}/C$. The data for each perforated plate, though taken at several different liquid inlet rates, fit a single curve with a constant slope, which means the rate of weeping is independent of inlet liquid rate. This conclusion agrees with the results of other investigators(8, 42, 52).

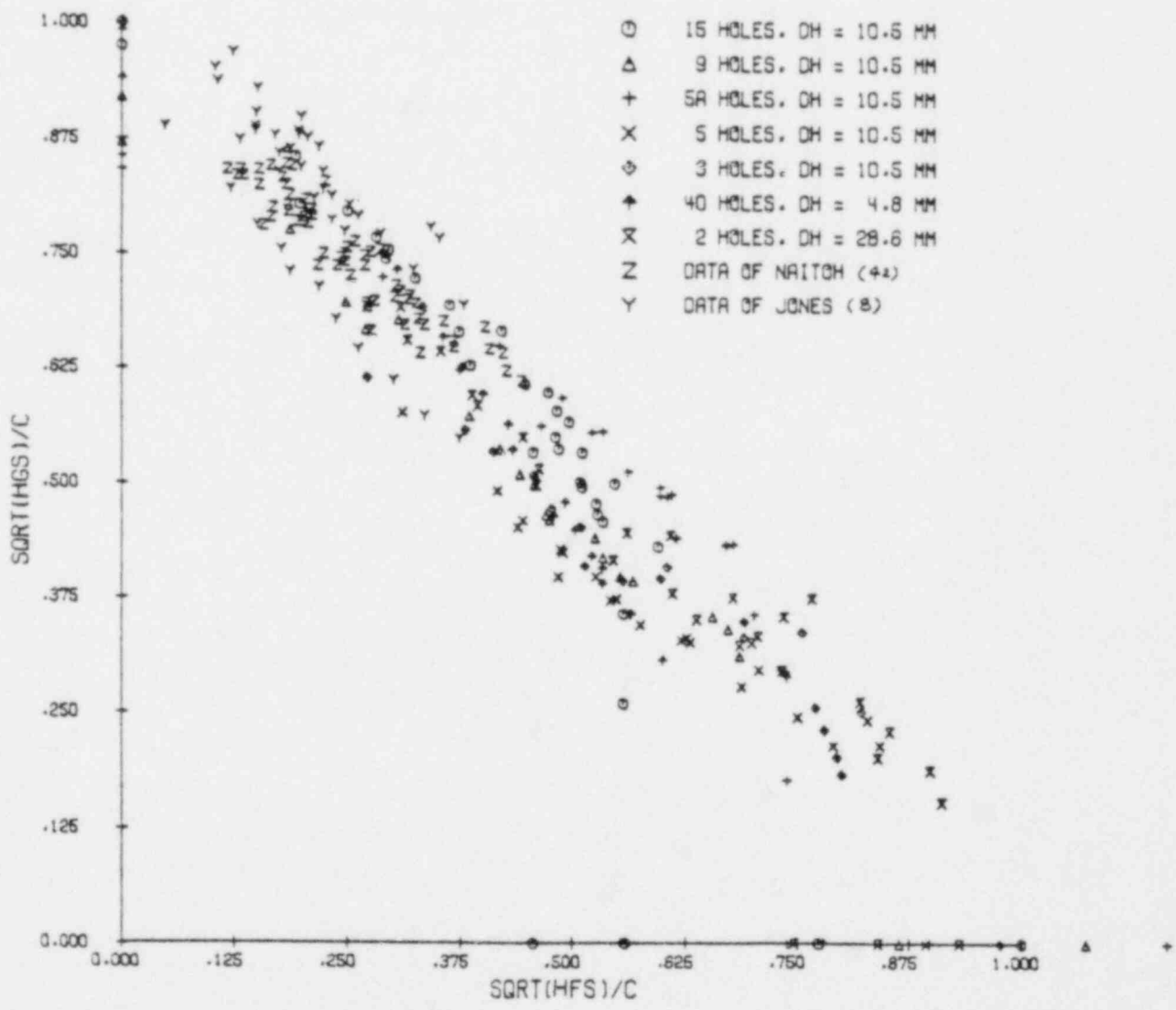


Figure 13. Data Correlation with Equation (55).

3.5 Effect of Head of Liquid Pool above the Plate

The liquid pool head(h_L) has been varied between 1500 mm and 40 mm in Naitoh's BWR 8x8 upper tie plate weeping experiment (42). In this experiment h_L does not have observable effect on the rate of weeping. The effect of h_L on the rate of liquid delivery in annular geometry has also been investigated in Air/Water system at Dartmouth(37). As reported, the rate of liquid delivery is independent of liquid head as soon as the liquid head exceeds 50 mm. However, Mohr(43) proclaimed that increasing the liquid head h_L will cause a higher rate of liquid delivery.

Figure 14 shows the 15 hole test plate data obtained at two values of h_L . The rate of weeping is the same in both cases. Hence, we conclude that the rate of liquid downflow is independent of the liquid head h_L in the geometry studied.

3.6 Effect of Liquid Inlet Position and Soft Volume

The liquid inlet spray position has been varied between 5 mm and 600 mm. Since all the liquid streams are injected horizontally into the channel, the effect of liquid inlet momentum on the rate of weeping has been minimized. The position of liquid inlet spray, as expected, does not produce observable effect on the rate of weeping.

The soft volume range from $6.75 \times 10^{-4} \text{ m}^3$ to $2.86 \times 10^{-3} \text{ m}^3$ has been tested in a few runs on the 15 hole test plate. No effect of this factor on the rate of weeping has been observed.

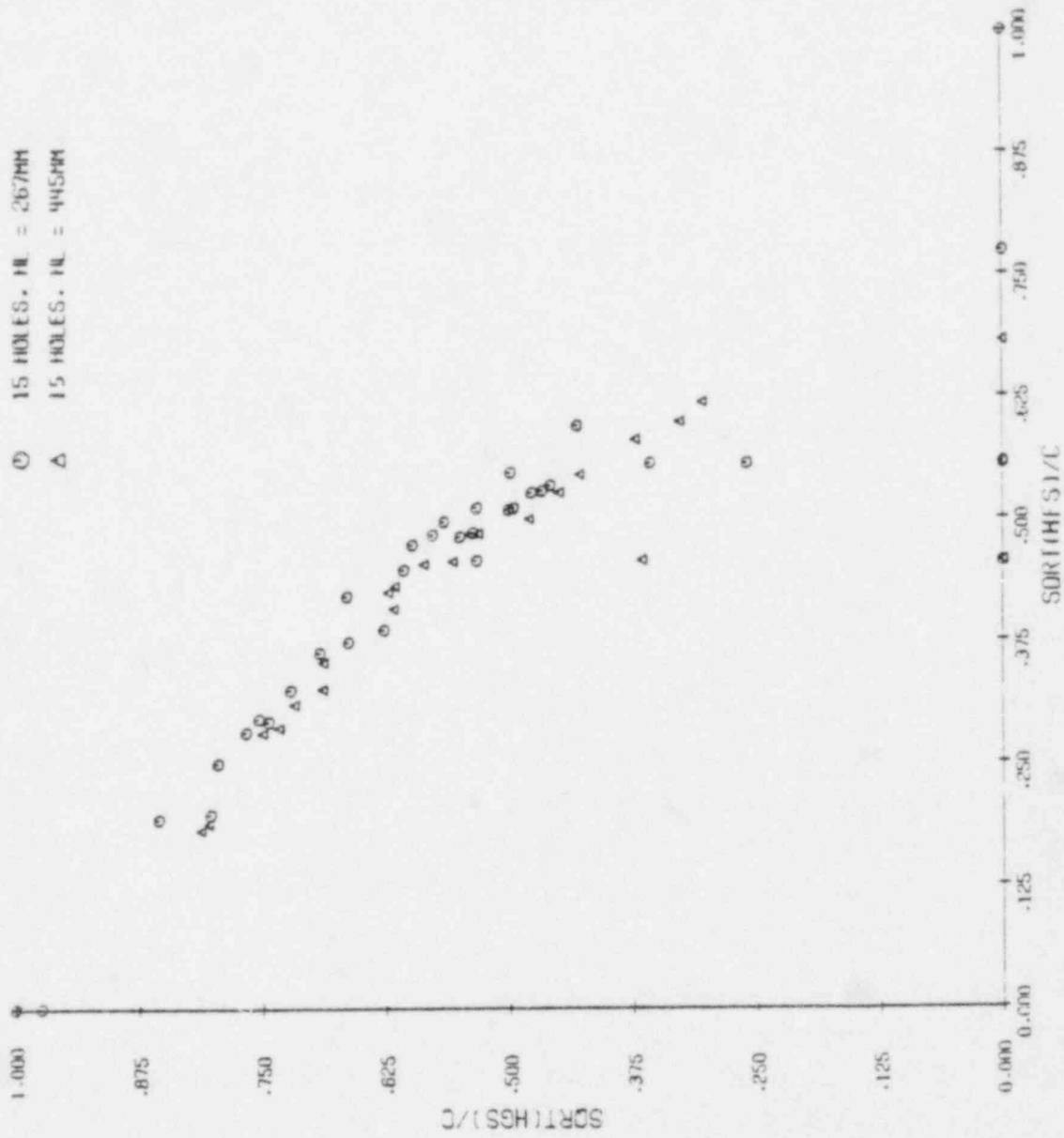


Figure 14. Effect of Head of Liquid Pool (h_L) on the Rate of Weeping

4. Steam/Cold Water Experiment

The objective of the steam/cold water experiment is to study the effect of subcooled water to the onset of weeping. At a fixed value of water flow rate and subcooling, the steam flow rate at which the water above the plate starts to leak through the perforations, along with all the thermocouples and pressure transducer readings at this point, is recorded. Water flow rates up to 0.7 kg/s, water temperature between 285 K and 359 K, and water inlet spray position between 5 mm and 710 mm have been tested. Depending on the combinations of these parameters, several types of weeping and dumping have been observed and studied.

4.1 Technical Background

Various aspects of condensation-driven fluid motions have been examined and discussed by Block(15). The thermodynamic ratio $R_T (= C_f(T_{sat} - T_f)W_f/h_{fg}W_g)$ is adopted as the main parameter in characterizing the performance of condensing two-phase flow systems. The line $R_T = 1$ separates the "universal flow regime map for direct contact condensation" into two major regions (Figure 15). The region $R_T > 1$, where complete condensation of the vapor is possible, is further divided into three sub-regions, but no detailed discussion was made for the performance characteristics of region $R_T < 1$.

The experiments held in annular or perforated plate geometries have revealed some new information to this flow regime map. In addition to the thermodynamic boundary $R_T = 1$, a hydrodynamic boundary is observed in the region $R_T < 1$. This hydrodynamic boundary can be expressed in the form of equation (12)

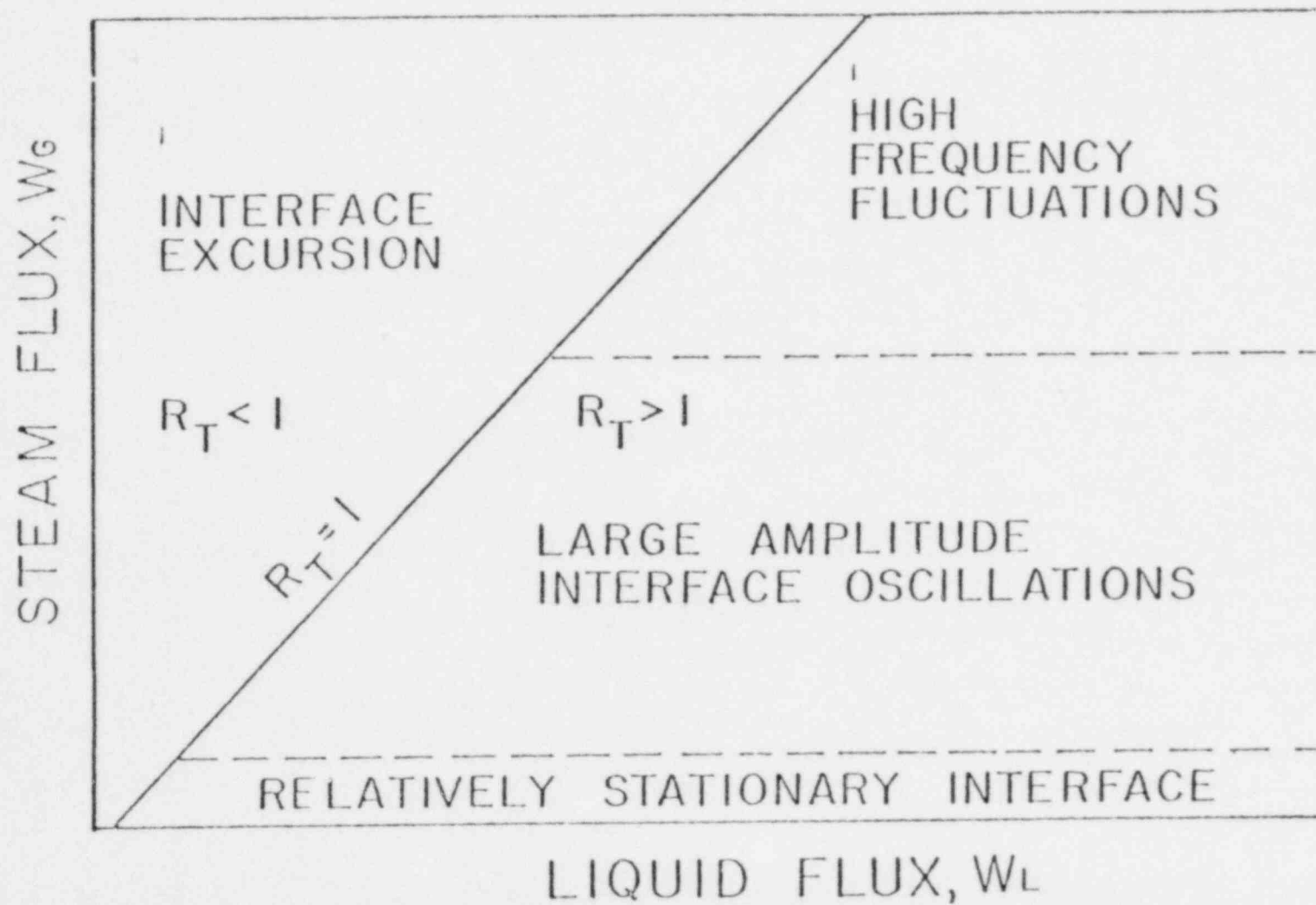


Figure 15. Block's "Universal Flow Regime Map for Direct Contact Condensation".

or equation (55).

Figure 16 is a typical flow regime map for PWR downcomer geometries. In the region (1), where the steam flow rate is so high that both the hydrodynamic and thermodynamic boundary are exceeded, the Emergency Core Coolant(ECC) can not flow down against the ascending steam, and it is called ECC bypass(6). The region (2) represents the operating condition where the end of ECC bypass may occur. The region (3) covers both sides of line $R_T = 1$. The flooding equation in this region can be expressed as(6, 35):

$$(J_{gc}^* - f[(T_{sat} - T_f)C_p/h_{fg}](\rho_f/\rho_g)^{1/2}J_{f,in}^*)^{1/2} + m J_{fd}^{*1/2} = C \quad (57)$$

where f , the condensation ratio, is correlated empirically as a function of operating pressure P and dimensionless liquid inlet flow rate $J_{f,in}^*$.

The boundary between the region (3) and the region (4) is given by

$$J_{gc}^* - f[(T_{sat} - T_f)C_p/h_{fg}](\rho_f/\rho_g)^{1/2}J_{f,in}^* = 0 \quad (58)$$

All the steam will be condensed in the region (4), resulting a total delivery of the ECC water.

For perforated plate, both Jones(8) and Naitoh(42) indicated that once the temperature of downflowing liquid(T_f in equation (58)) is less than the saturated temperature(T_{sat}), some steam will be condensed before it can reach the plate. As a result, more water can flow down, and triggers the total dumping. In

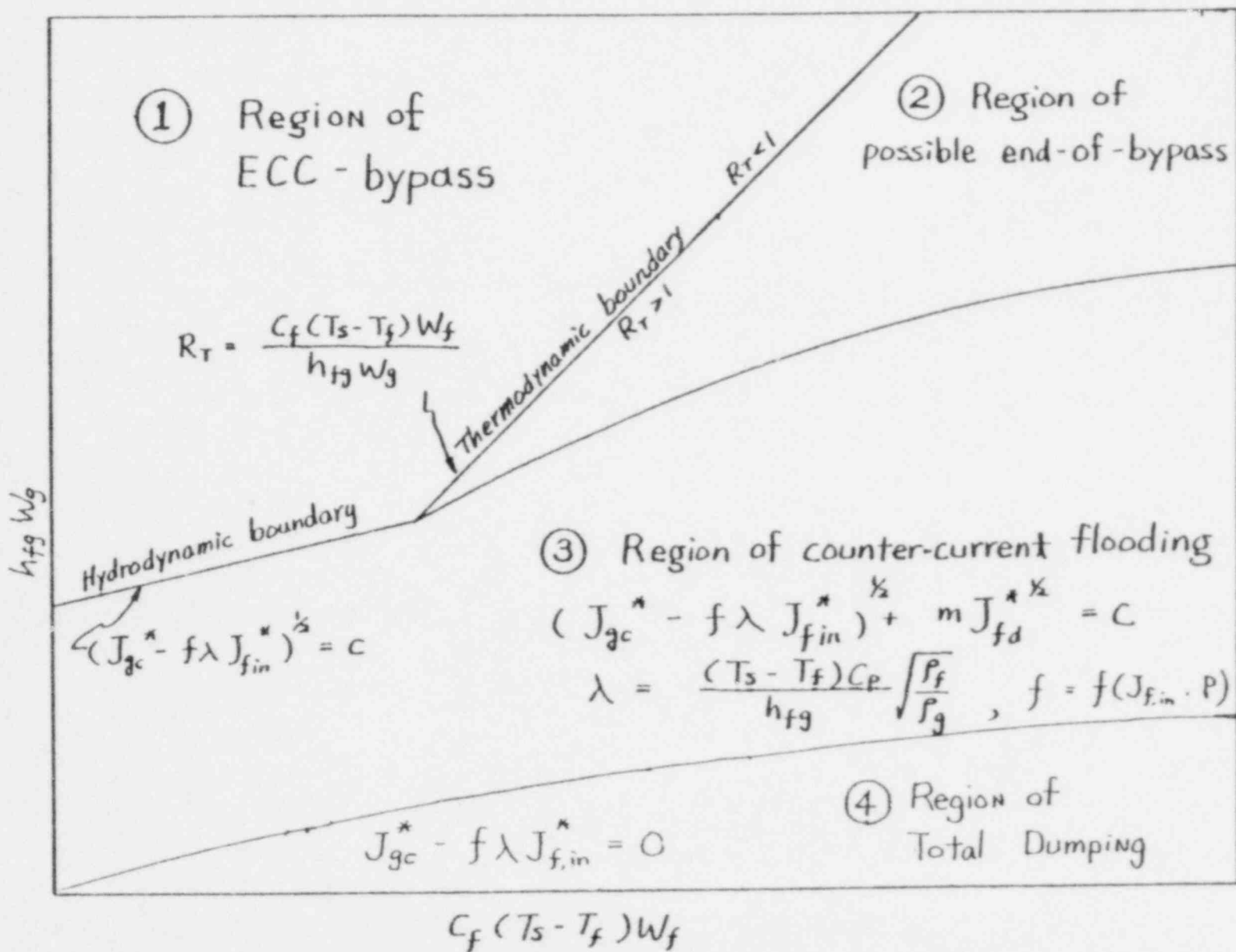


Figure 16. The Flow Regime Map of Direct Contact Condensation for the PWR Annular Downcomer Geometries.

other words, the condensation efficiency (f) is equal to one in this case. Setting $f = 1$ in equation (58), this equation will then reduced to $R_T = 1$. Hence, for perforated plate the boundary between the region (3) and (4) of Figure 16 will coincide with the thermodynamic boundary $R_T = 1$, resulting a flow regime map like Figure 17. Jones(8) and Naitoh(42) held their steam/water weeping experiments in region (2). Both of them indicated that in this region the rate of weeping is independent of the water sub-cooling. Operating in the region (3) and (4), Duffey(50) studied the time elapsed between injection of water and the transition to downflow. The present investigation in steam/cold water system is to locate the boundary between weeping and no weeping regions in this flow region map, and to study the mixing efficiency at this boundary.

4.2 Previous Works

The operating condition at the weep point has been studied by the investigators in Northwestern University(51) in the steam /water system. The test channel is made of a 2 inches I.D. pyrex glass tube. A 6.4 mm thick perforated plate with six holes of 6.4 mm diameter has been studied in this channel. Water is injected out horizontally through a tube which is attached to the center of the perforated plate. Holes in this tube, which admit the water into the channel, are located right above the plate.

In this experiment, water temperature is kept at building tap water temperature, which varied between 280 K and 288 K. The steam inlet temperatures have been varied between 373 K and 518 K to study the effect of steam superheat on the weep point.

67

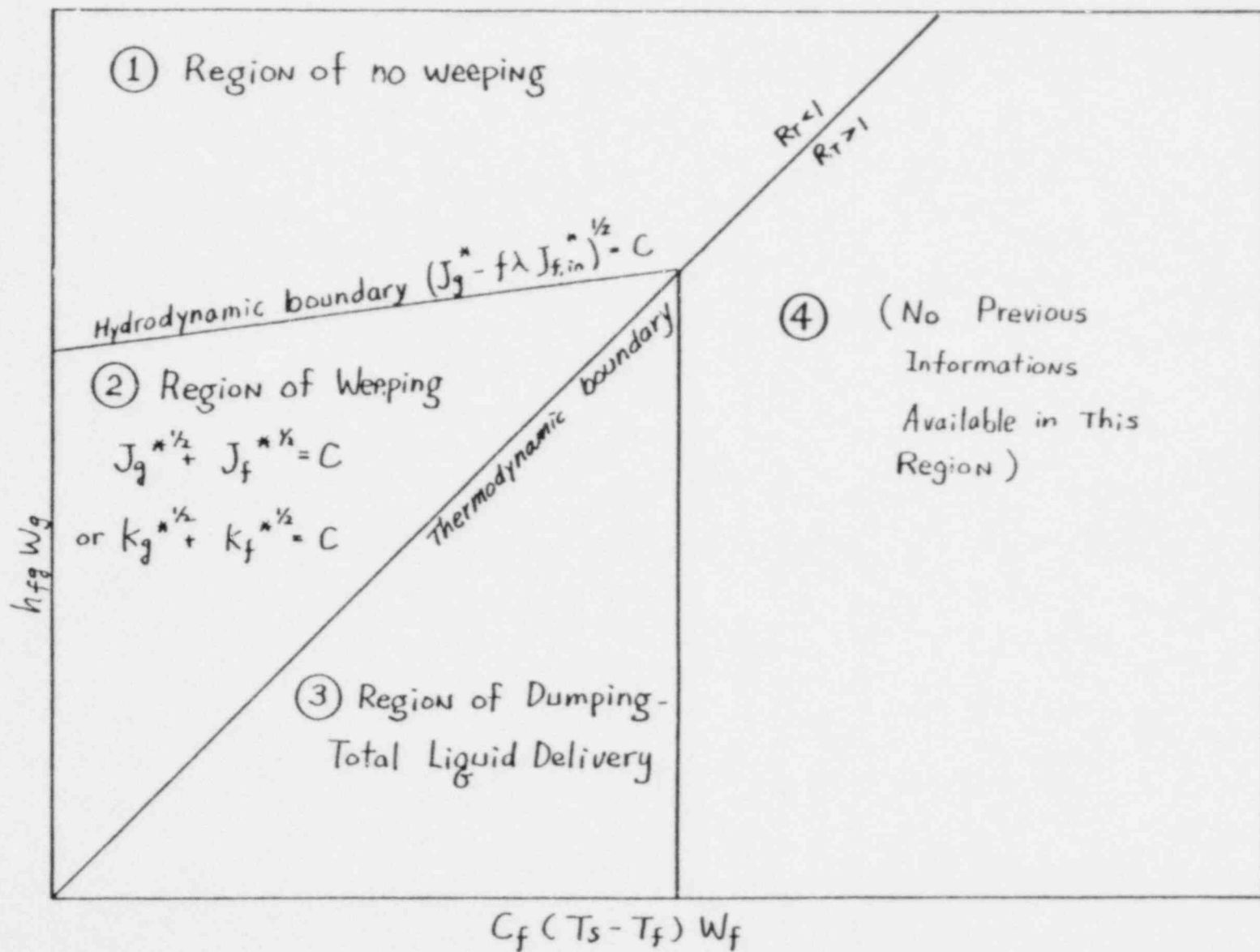


Figure 17. The Flow Regime Map of Direct Contact Condensation For Perforated Plate Plate Geometries.

Several important observations have been obtained in this experiment:

1. The head of liquid pool above the plate (h_L) between 50 mm and 350 mm did not have any discernible effect on the weep point.
2. At high water flow rate (0.151 kg/s) and large h_L (254 and 356 mm) two types of liquid delivery were observed--- "oscillatory weep" and "total dumping". The oscillatory weeping is characterized by its severe oscillation in the water pool above the plate. When the steam flow rate is reduced to a point where all the steam can be condensed right above the plate, the pressure fluctuation in the water pool is eliminated, and a stable no weeping condition is, therefore, maintained. Further decreasing the steam flow rate can trigger the total dumping.
3. The effect of steam superheat ranging between 0 K and 145 K can be correlated by taking into account the sensible heat of superheated steam in the thermal calculation and the change of steam density in the hydrodynamic calculation.

4.3 Experimental Apparatus

4.3.1 Test Channel

The same test facilities for the air/water experiment is used here for the steam/water experiment. The detailed descriptions of the apparatus and the channel are given in section 2.2. The perforated plates tested in this experiment include(Figure 1): 15 hole, 9 hole, 5 hole, 5A hole, 3 hole, and 3A hole.

4.3.2 Water Line

The water line used here is the same one used in air/water experiment. The water inlet temperature ranging between tap water temperature and 358 K can be adjusted by the control of steam purging rate to the water line. Two 3/8 inch steam purging lines are connected from 1 m upstream of the 1 inch steam venturi to 0.8 m upstream of the water rotameter. At any fixed water flow rate, the water temperature can be adjusted to within 0.2 K of the desired value by this device.

The water inlet temperature is measured by thermocouple T1 (Figure 6) located at 0.3 m upstream of the water rotameter. The temperature of the downflow water is measured by thermocouple T14, while the overflowing water is measured by thermocouple T15 located at the overflow port. A overflow weir of 25 mm height is installed in the port to guarantee the tip of T15 is immersed in the water. Detailed descriptions about the temperature measurement of the two phase mixture above the test perforated plate will be given in section 4.3.4.

Since the experiment is concentrated on a weep point study, no measurement on the rate of weeping has been made. The rate of weeping at the weep point is equal to zero. It is, therefore, assumed that the rate of water overflow is equal to the sum of the water inlet rate and the rate of steam condensation. The rate of steam condensation is estimated by the water phase enthalpy balance.

4.3.3 Steam Line

Steam at 800 kPa is obtained from the building main steam line. Passing a water separator, the steam venturi system installed mainly for other experiments held in the same laboratory, and several valves, the dry steam is directed to the test channel via a 1 inch brass pipe. The degree of steam superheat can be controlled by an electrical heater. The steam flow rate is controlled by two 1 inch stainless steel globe valves installed before the 1 inch air and/or steam entrance nozzles of the test channel.

The soft volume upstream of the perforated plate can be adjusted by changing the liquid level in the lower chamber of the channel. Since the water temperature at the steam/water interface in this chamber can be saturated very soon, and the heat loss through the channel wall can be assumed negligible, the rate of steam condensation in this lower chamber is ignored.

After passing the two-phase mixture above the perforated plate, the steam left, if any, flows out of the test channel through a 3 inch hose. The pressure drop through this hose is small enough to keep the operating pressure of the channel

near atmospheric for the whole range of steam flow rate. The steam outlet temperature is measured by thermocouple T3 installed at the top plate of the test channel. A pressure relief valve is also installed on the side wall near the the top plate. Should the operating pressure in the channel exceed 200 kPa, this valve can relieve the pressure by venting the steam to the atmosphere.

4.3.4 Instrumentation

The detailed description of water rotameters is given in section 2.2.4.

The steam flow rate is usually measured by a BARCO 1/2"-402 venturi installed horizontally on the 1 inch steam line between the steam purge outlet nozzles and the electrical heater(Figure 6). Therefore, this venturi reading is independent of the steam purging rate. The standard piping arrangement for the steam venturi is given in Figure 18. Knowing the differential pressure reading of the venturi, along with the absolute pressure and temperature of the steam, the mass flow rate of the steam can be calculated with the aid of the calibration curve of the vanturi. For steam flow rate higher than the maximum measurement capacity of this venturi, a BARCO 3/4"-425 venturi, which belongs to the venturi system of the laboratory, is used.

Table 3 gives the locations and functions of all the thermocouples used in the experiment. All the thermocouples attached to the channel are fixed by Cajon Ultra-Torr Fittings installed on the side wall of the channel. These fittings can be made leak tight by finger-tightening, while traversing the thermocouples can easily be done by loosening the cap of the fitting. Among all the

Table 3. Function of Thermocouples

TI	Position	Phase
1	70 cm upstream of water rotameters	L
2	50 mm up stream of 1 inch steam venture	V
3	Top plate of the test channel	V
4	177 mm above the perforated plate	V-L
5	152 mm above the perforated plate	V-L
6	127 mm above the perforated plate	V-L
7	102 mm above the perforated plate	V-L
8	77 mm above the perforated plate	V-L
9	52 mm above the perforated plate	V-L
10	27 mm above the perforated plate	V-L
11	2 mm above the perforated plate	V-L
12	Steam inlet nozzle	V
13	Lower chamber of the channel	V
14	Lower chamber of the channel	L
15	Liquid overflow nozzle	L

Note: L : Liquid V : Vapor

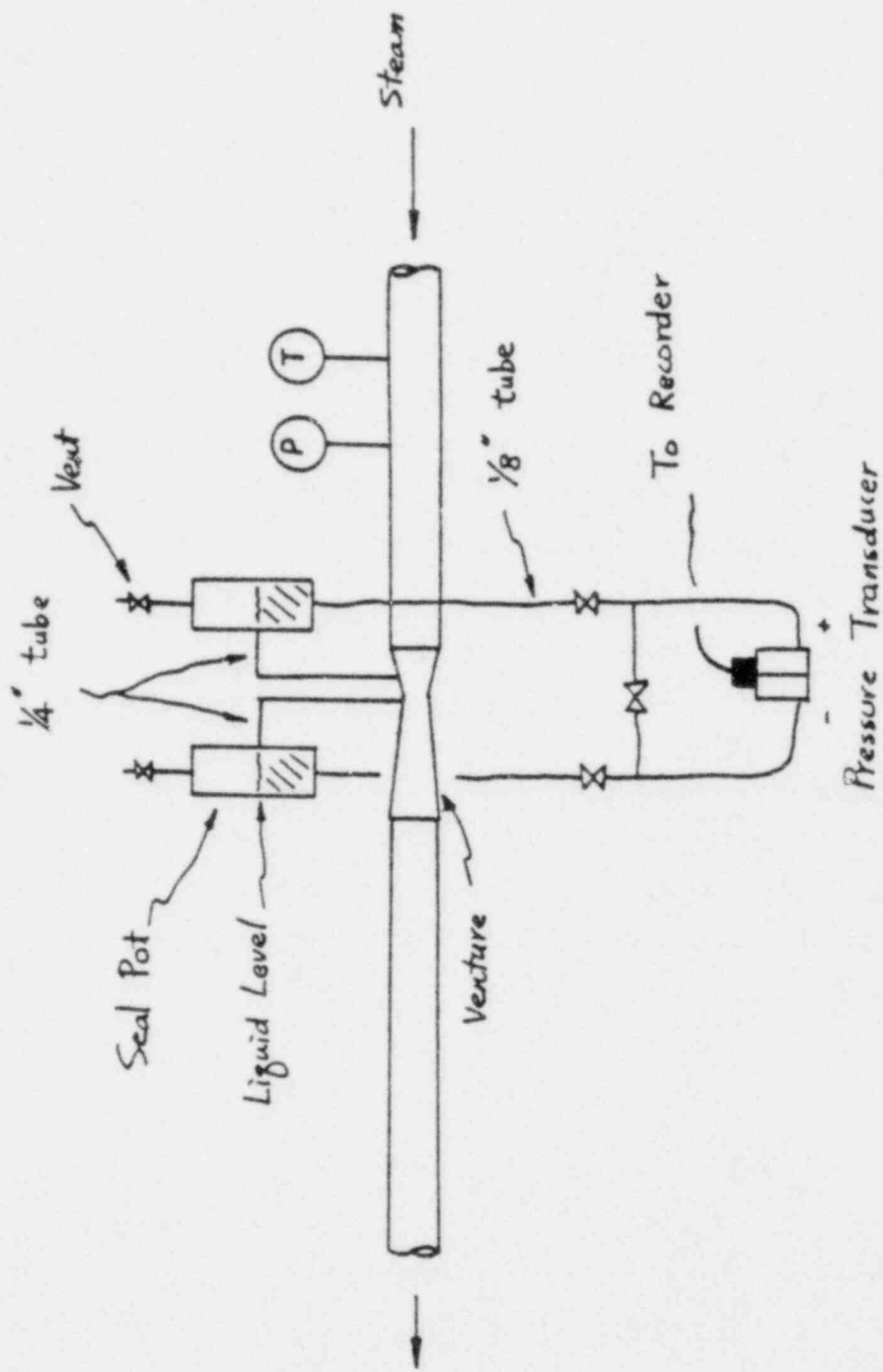


Figure 18. The Standard Piping Arrangement for Steam Venturi

thermocouples, more attention must be given to T12, which was installed to measure the dry steam temperature at the inlet nozzle. It tends to give a false reading of 373 K (saturated steam temperature at 1 atmosphere) if the tip of the thermocouple is wetted by a water droplet.

The temperature of the vapor/liquid mixture above the perforated plate is measured by thermocouples T4 - T11. The tip of T11 is 2 mm above the perforated plate. By properly traversing this thermocouple, the temperature of two thirds of the cross-section area above the plate can be measured. Thermocouples T4 to T10, all lying on the centerline of the side wall of the channel with an equal spacing of 25 mm, can provide some picture about the temperature distribution above the plate.

Detailed description about the channel operating pressure measurement device is given in section 2.2.4 and Figure 8. Since the steam will tend to condense in the pipe line of the pressure transducer, a constant air purge is usually required to maintain a stable pressure reading.

4.3.5 Computer Program

A computer program written in FORTRAN IV language is used for the tasks of data reduction and plotting.

The steam flow rate through the 1/2"-402 venturi is calculated by equation (59):

$$W_s = 0.051 (V/\rho_g) \quad \text{lbs/sec.} \quad (59)$$

where V is the voltage reading from the pressure transducer connected to the venturi. If the 3/4"-425 venturi is used, the steam mass flow rate is calculated by equation (60).

$$W_s = 0.35 (V/\rho_g) \quad \text{lbs/sec.} \quad (60)$$

The physical properties of the steam(enthalpy, entropy and specific volume) can be calculated by the Subroutine PHIS2. The description and the calling sequence of this subroutine are given in Appendix II.

The liquid inlet flow rate is calculated by the following equations:

$$R = 0.4118 + 0.03611 \times W_1 + 0.001042 \times W_1^2 \quad (61)$$

If $W_1 > 0.724$, set $W_1 = 0.724$

$$W_f = (W_1 \times R + W_2)/60 \quad \text{lbs/sec.} \quad (62)$$

where W_1 and W_2 are the readings of water rotameter A and B. These equations are obtained by rotameter flow rate calibration held in the laboratory.

In addition to these flow rates, several temperature readings are also sent into the program; the thermodynamic ratio and the enthalpy flux of the steam and the water can, therefore, be calculated.

The superficial steam and water velocity through the holes and the dimensionless flow rate H_g^* and H_f^* , are also calculated in this program. Finally, the reduced data is plotted by plotter 565 of Northwestern University Computer Center via CalComp Basic

Plotting Package.

A list of this program is given in Appendix II.

4.4 Experimental Procedure

Since visual observation is the only method used in weep point determination, the repeatability of the experiment must be constantly verified. A standard experimental procedure designed for this purpose is listed as follow:

1. Select a test perforated plate. Fix it into the channel.
2. Fix the height of the water inlet spray. Four different water inlet spray positions have been tested: 5 mm, 102 mm, 305 mm, and 710 mm.
3. Open all the valves from the main steam supply pipe to the steam flow rate control valves at the channel steam inlet nozzles. Run the steam for 3 - 5 minutes to clear the steam line from the condensed water and possibly the accumulated air.
4. Zero the voltage readings of pressure transducer of the steam venturi and DP103 differential pressure transducers of the channel pressure measurement.
5. Check the function of all the thermocouples.
6. Turn off the steam.

7. Open the water. Usually, the water flow rate starts at 0.023 kg/s. Gradually increase the steam flow rate to the weep point, which is defined as the point where the water downflow ceases. Record the steam flow rate and pressure, water flow rate and all the relative thermocouples readings. The operating pressure in the channel can also be measured at this point.
8. Further increase the steam flow rate. Then approach the weep point from a high steam flow rate. Record the same informations mentioned in step 7 at this point.
9. Increase the water flow rate, 0.03 kg/s each time. Repeat step 7 to step 8. A complete set of test runs is finished at the maximum water flow rate of 0.65 kg/s.
10. Repeat step 7 to step 9. This time the water flow rate is changed randomly in the range between 0.03 kg/s and 0.65 kg/s. A comparison between the data obtained in step 9 and in step 10 can serve as an indication of the repeatability of the visual weep point determination.
11. Repeat step 2 to 10 at different water inlet height.
12. Repeat step 1 to 11 for different perforated plates.

For the 15 hole perforated plate, steps 2 to 10 have been repeated at 6 different water inlet temperature between 285 K to 359 K in an attempt to study the effect of water subcooling.

5. Results and Discussion for Steam/Water Experiments

The flooding phenomena above a perforated plate are quite different in the steam/cold water system from those in the air/water system. Since the ascending steam contacts the cold water directly above the perforated plate, condensation-driven fluid motions can play a significant role in triggering water breakthrough. This thermal effect may be governed by several factors including : water subcooling, steam superheat, and above all, the position of the water inlet spray nozzle, which determines the mixing efficiency.

In the current steam/water test matrix, steam temperatures ranged from 373 K to 421 K, and water temperatures varied between 285 K and 359 K; the number of holes in the support plate ranged from 3 to 15; and the water inlet position was varied from 5 to 710 mm above the plate. Because of the strong effect of the water inlet position, the data for high and low position are discussed separately below.

5.1 Water Inlet Spray Above The Pool

During those experiments, the distance between the centerline of the water overflow port and the top of the perforated plate(and hence the height of the liquid pool above the plate, h_L) was fixed at 267 mm. A liquid inlet height of 305 or 710 mm, therefore, means the liquid inlet spray was above the pool surface.

Water spraying out from the inlet nozzle fell gravitationally after hitting the side wall of the test channel. Only a portion of this water contacted with the steam, with the remainder bypassing through the overflow port.

5.1.1. 15 Hole Data

Figure 19 shows the 15 hole weep point data obtained at five different temperatures. The effect of water subcooling, as shown, can be correlated in this total enthalpy flux plot. The steam enthalpy flux required to stop the weeping, starting at a value of 40 KW, gradually approaches a maximum limit of 71 KW as the water enthalpy is increased. No relation can be found between this line of weep point and the line of thermodynamic ratio $R_T = 1$.

Two types of weeping were observed during the experiment. Continuous weeping (Figure 20) happened when the liquid enthalpy flux is very low ($W_f C_p (T_{sat} - T_f) < 15$ KW). All the inlet water was well saturated at this condition, and the steam can flow through the two-phase mixture above the plate without much being condensed. The pressure transducer readings showed that except for high frequency noise, operating pressures both upstream and downstream of the perforated plate were fairly constant. If the steam velocity through the holes is lower than a certain value, its frictional drag can no longer hold all the liquid above the plate, resulting in continuous weeping.

When the liquid enthalpy flux was increased, more steam was required to keep the plate from weeping. The amount of this extra steam is determined by the condensation effect in a two-phase mixture layer close to the plate. This condensation effect is proportional to the total liquid enthalpy flux with a proportional constant f of 0.24 for 15 hole data (Figure 19). The proportional constant is named the mixing efficiency, because it represents the degree of mixing between the water inlet and the plate. As shown in Figure 20, the ascending two-phase mixture

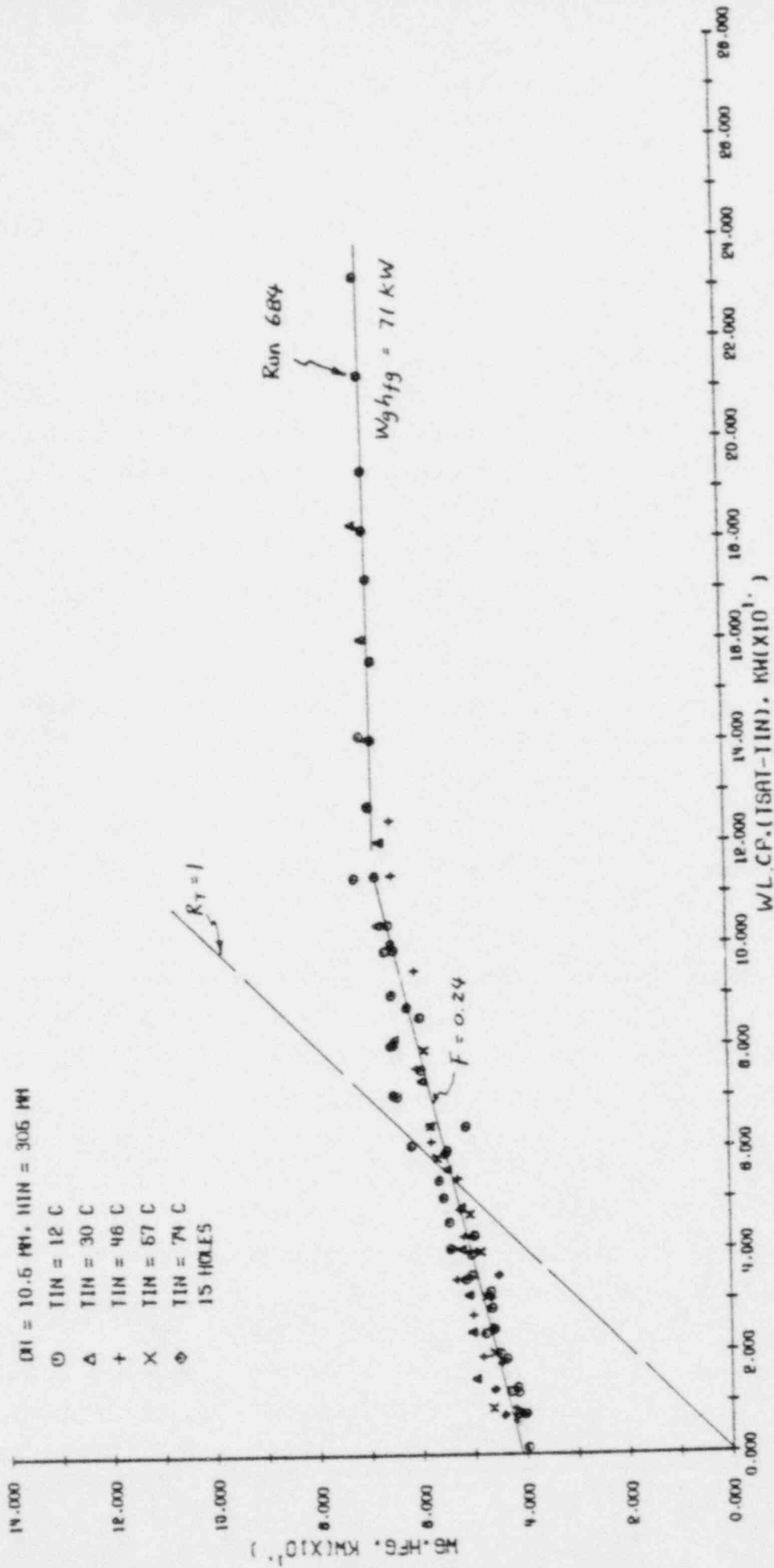
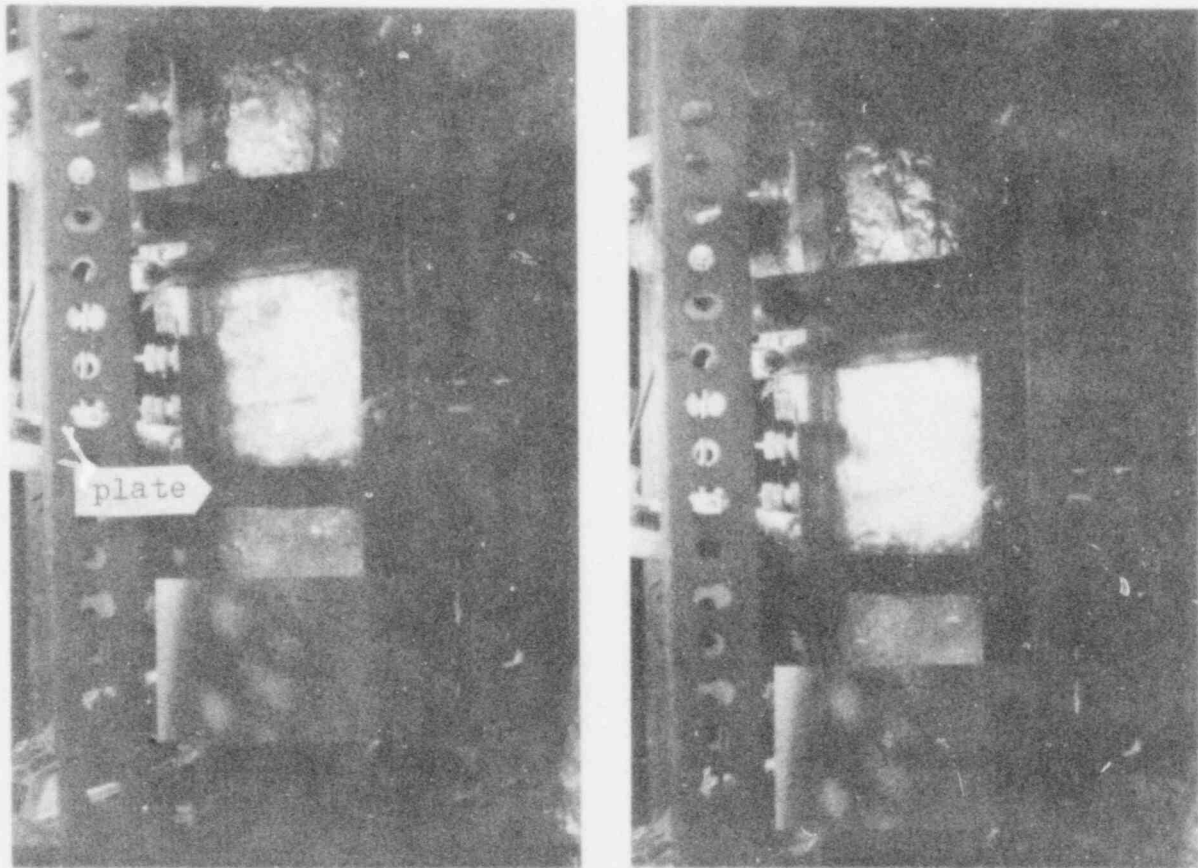


Figure 19. Effect of Liquid Subcooling to the Weep Point, $h_{in} = 305 \text{ mm}$, 15 Hole Data

POOR ORIGINAL



$$W_f = 0.076 \text{ kg/s}$$

$$T_f = 285 \text{ K}$$

$$W_g = 0.018 \text{ kg/s}$$

$$T_g = 413 \text{ K}$$

Figure 20. Some Pictures of Continuous Weeping, $h_{in} = 305 \text{ mm}$

POOR ORIGINAL

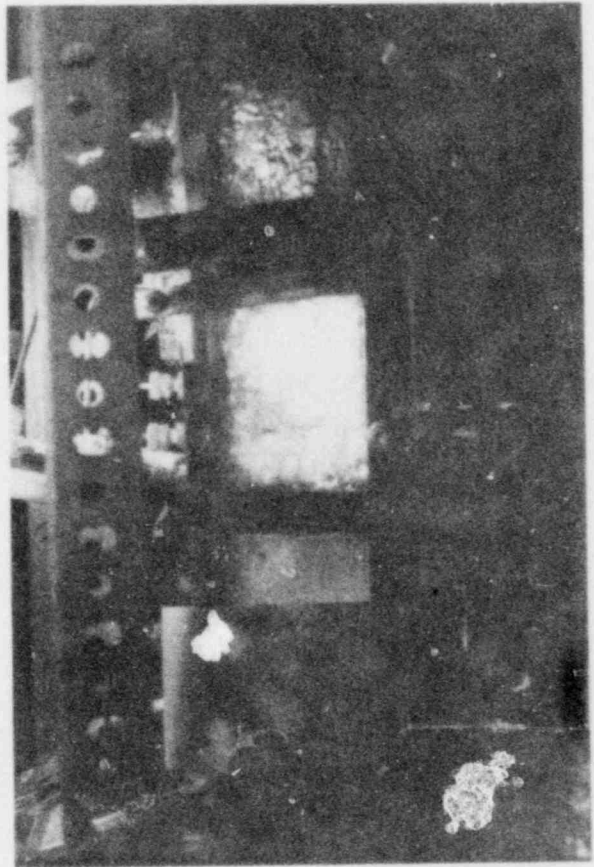
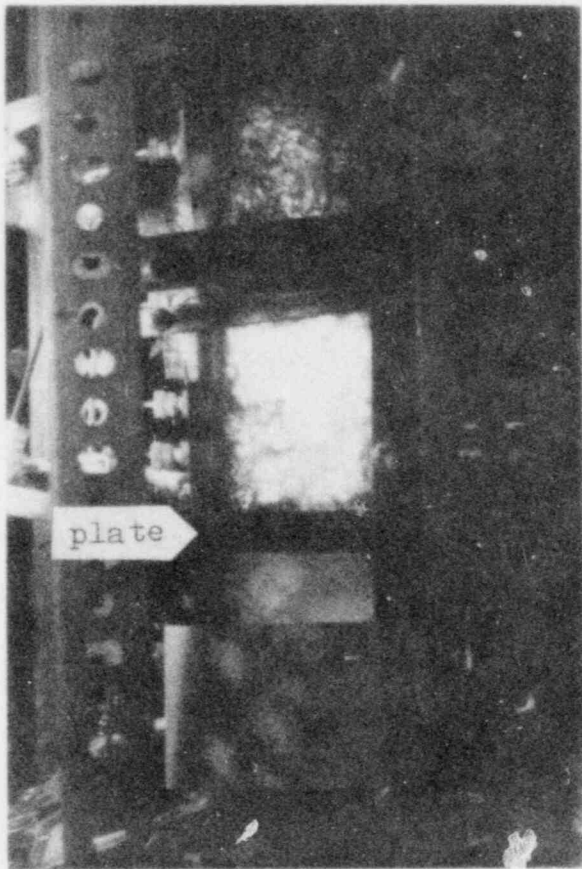
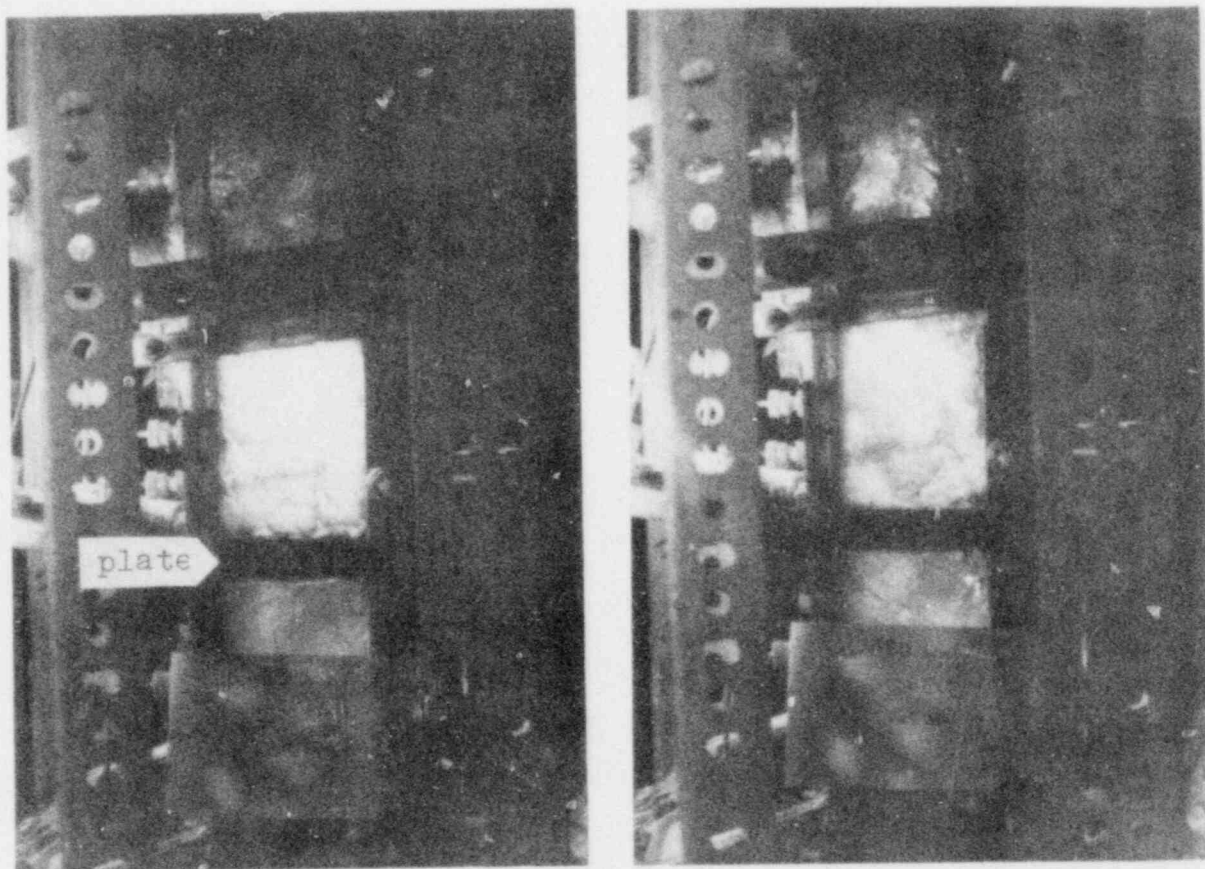


Figure 20. (Continued)

POOR ORIGINAL



$$W_f = 0.68 \text{ kg/s}$$

$$T_f = 285 \text{ K}$$

$$W_g = 0.056 \text{ kg/s}$$

$$T_g = 413 \text{ K}$$

Figure 21. Some Pictures of Oscillatory Weeping,
 $h_{in} = 305 \text{ mm}$.

essentially covered the whole cross-section of the channel, water from above had no means of bypassing down to the plate, resulting in a poor mixing efficiency(0.24) in this case.

Once the liquid enthalpy flux exceeded 50 KW, the steam could all be condensed before it reached the top of the pool. A layer of water was then formed above the two-phase mixture above the plate. Along with the increasing of liquid enthalpy flux, this water layer become thicker, and its buffer effect become larger. Eventually, the degree of mixing reaches a maximum. Further increasing the water enthalpy flux can only resulting in a larger portion of cold water overflow without much influence on the two-phase mixture above the plate. This phenomenon can clearly be identified in Figure 19 when the liquid enthalpy flux is greater than 120 KW.

When liquid enthalpy flux was increased, the type of weeping at the weep point also changed from continuous to oscillatory(Figure 21). Oscillatory weeping is characterized by the intermittent downflow of cold water along with the fluctuation of the operating pressure. Figure 22 shows a typical thermocouple reading obtained at Run 684 operating in high liquid enthalpy flux region. As shown by the reading of this thermocouple, which is located 2 mm above the plate, cold water penetrated all the way down to the plate, and then passed through the holes of the plate. The oscillatory weeping of this run has a frequency around 1 cps.

5.1.2 Comparison between 15 Hole and 9 Hole Data

Figure 23 shows both the data of 15 hole and 9 hole experi-

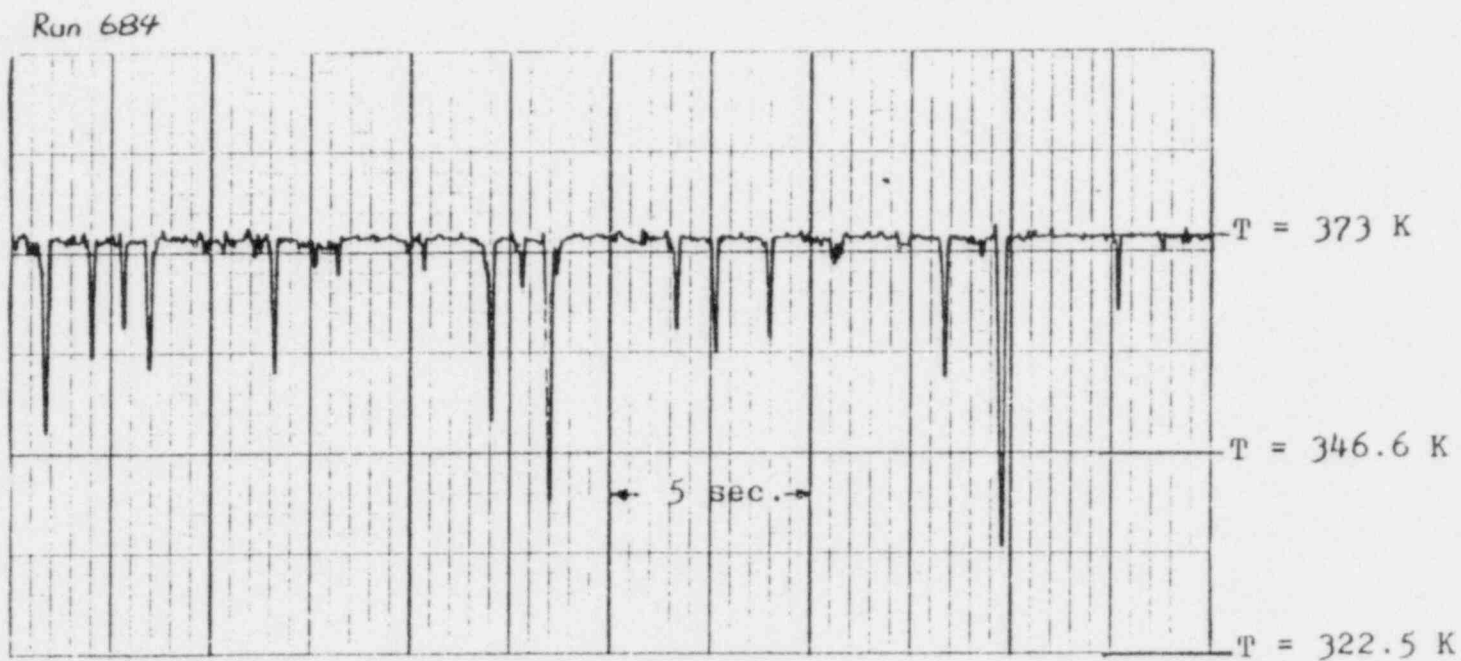


Figure 22. Thermocouple T11 Readings at Weep Point.

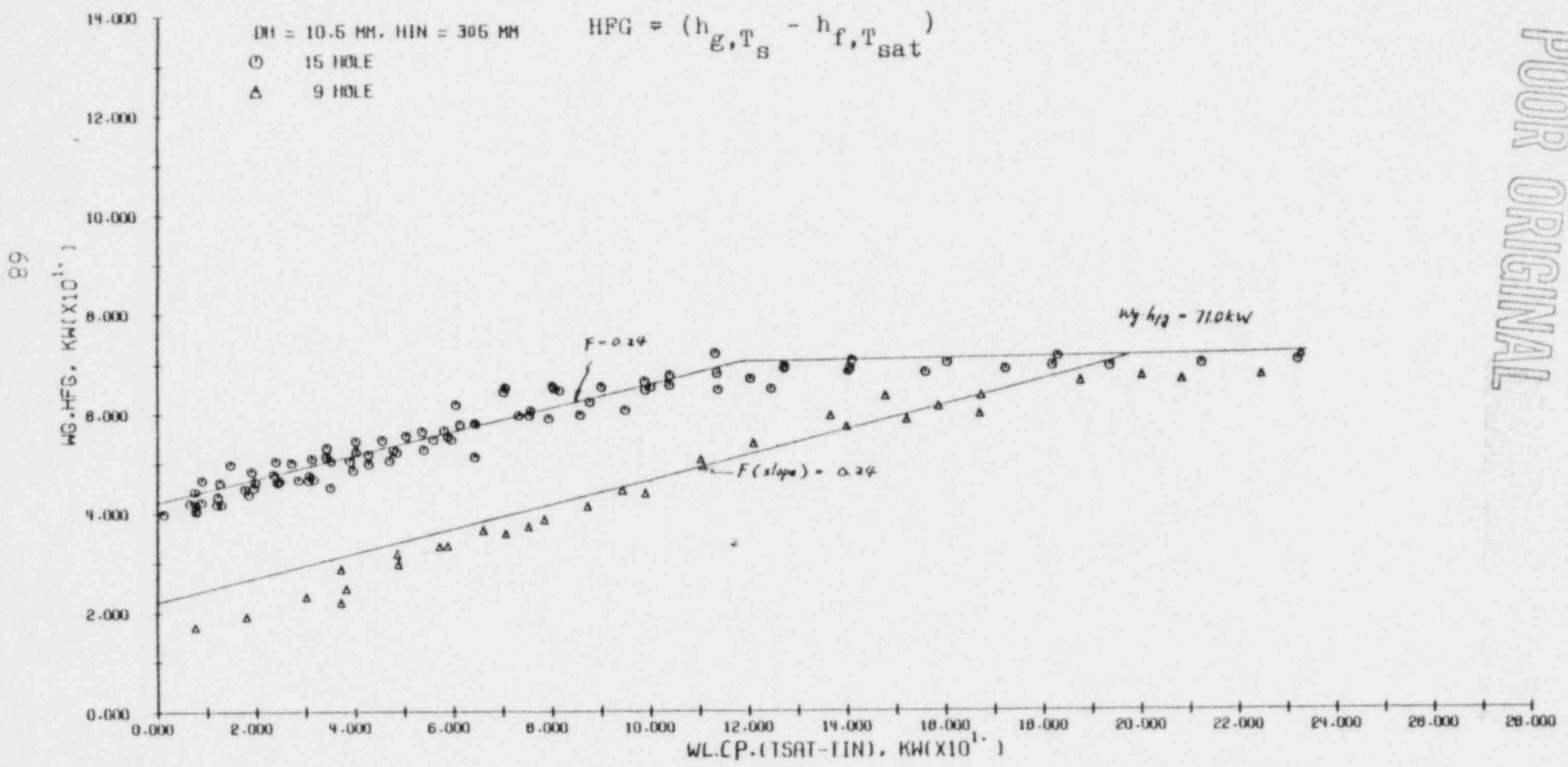


Figure 23. Total Enthalpy Flux at Weep Point, 15 Holes and 9 Holes Data, $h_{in} = 305$ mm.

ment. Two common features can be discerned easily from this Figure:

1. The mixing efficiency of both experiments are equal to 0.24.
2. Both experiments show the same maximum required total steam enthalpy flux at 71 KW.

Visual observation confirmed that the two-phase mixture zone above the plate in 9 hole experiment still covered the whole cross-section area of the channel; therefore, cold water can not find any bypass to reach the vicinity of the plate. As a result, the 9 hole experiment shows a mixing efficiency of 0.24, the same as 15 hole data.

A same maximum steam enthalpy flux for both 15 hole and 9 hole data suggested that these two plates not only have the same mixing efficiency, but also have the same upper limit of the degree of mixing, which can not be exceeded by further increasing the water enthalpy flux. Since Figure 23 is a total enthalpy plot, the same maximum total steam enthalpy flux means that the weep point at this high enthalpy flux condition depends on the mixing condition of the channel as a whole, and not on the flow condition at each hole.

Figure 24 is the same data plotted with the superficial steam velocity through the holes vs. the total water enthalpy flux. A comparison between this Figure and Figure 23 shows that:

1. At low water enthalpy flux, though the total amount of steam enthalpy required to stop the weeping is different, the steam velocity through the holes is the same, which means the hydrodynamic effect is the dominant factor of the onset of weep-

POOR ORIGINAL

DI = 10.5 MM, HIN = 305 MM
○ 15 HOLE
△ 9 HOLE

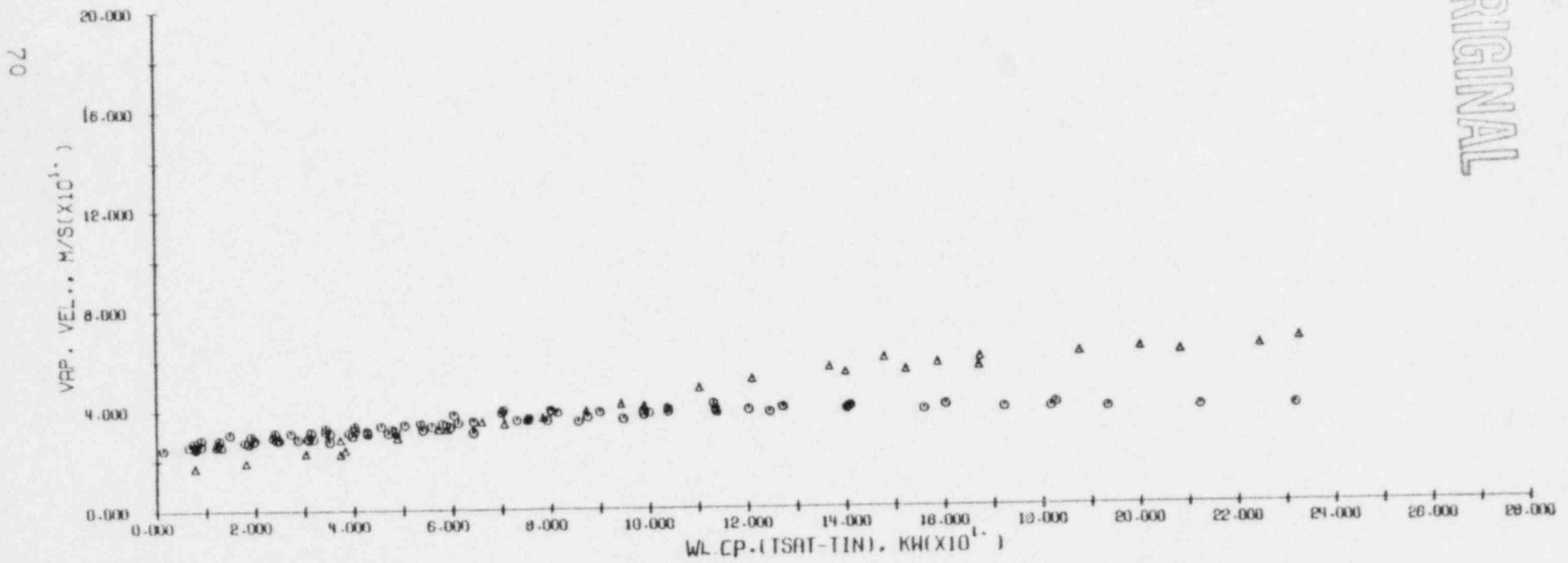


Figure 24. Superficial Steam Velocity through the Holes, 15 Holes and 9 Holes Data,

$h_{in} = 305 \text{ mm.}$

ing.

2. At high water enthalpy flux, the total steam enthalpy flux is the same, but the superficial steam velocity through the holes of 9 hole experiment is 1.7 times larger than that of 15 hole data. It is suggested that at high water enthalpy flux the condensation effect governed by the degree of mixing of the channel as a whole is the controlling factor of the onset of weeping.

In order to combine these two effects into one equation, the ideal of the effective steam flow rate (5, 6, 33) is considered for the data correlation.

5.1.3 Data Correlation

The dimensionless effective steam flow rate in the form of H^* scaling is defined as

$$H_{g,e}^* = H_g^* - f[C_p(T_{sat} - T_f)/h_{fg}](P_f/P_g)^{1/2}H_{f,in}^* \quad (63)$$

where H^* scaling is suggested from the air/water data correlation, and f is the mixing efficiency obtained from Figure 23.

By the use of this effective steam flow rate, the flooding equation obtained in air/water experiment, i.e., equation (55), becomes:

$$H_{g,e}^{*1/2}/C + H_f^{*1/2}/C = 1 \quad (64)$$

At the weep point no water will fall through the holes:

hence, H_f^* is equal to zero, and equation (64) is reduced to

$$H_{g,e}^{*1/2}/C = 1 \quad (65)$$

where the coefficient C is given in equation (56).

Equation (65) is then used to correlate the 15 hole and 9 hole steam/cold water weep point data by setting $f = 0.24$ with an upper limit of steam enthalpy flux of 71 KW.

Figure 25 is the dimensionless steam and water inlet flow rate plotted in the form of $H_g^{*1/2}/C$. It shows the value of $H_g^{*1/2}/C$ is very close to one at low water inlet flow rate. This means that the steam/water data agree fairly well with the air/water data when the condensation effect is insignificant.

Once the liquid enthalpy flux, and hence the condensation effect is increased, the dimensionless steam inlet flow rate is replaced by the effective steam flow rate. Figure 26 is the same data plotted with the left hand side of equation (65) against the dimensionless liquid inlet flow rate. It shows the concept of effective steam flow rate has successfully related the steam/cold water data obtained at high water inlet position to the air/water correlation.

5.1.4 5(5A) Hole and 3(3A) Hole Data

Figure 27 shows the results of 5, 5A, 3, and 3A hole experiments. Comparing with the data shown in Figure 23, one can find that:

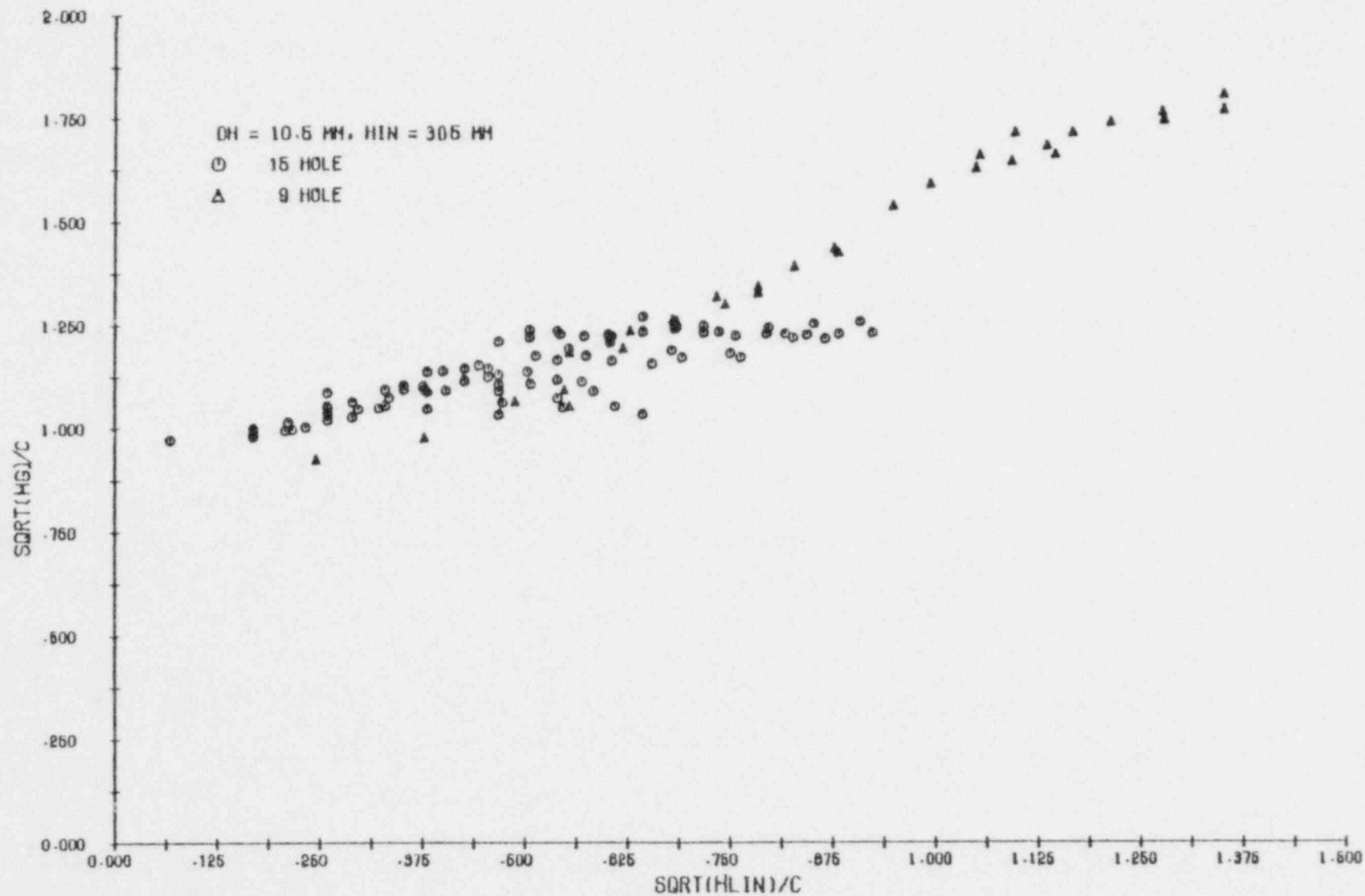


Figure 25. Dimensionless Steam and Water Inlet Flow Rate at Weep Point, 15 Holes and 9 Holes Data, $h_{in} = 305 \text{ mm}$.

72

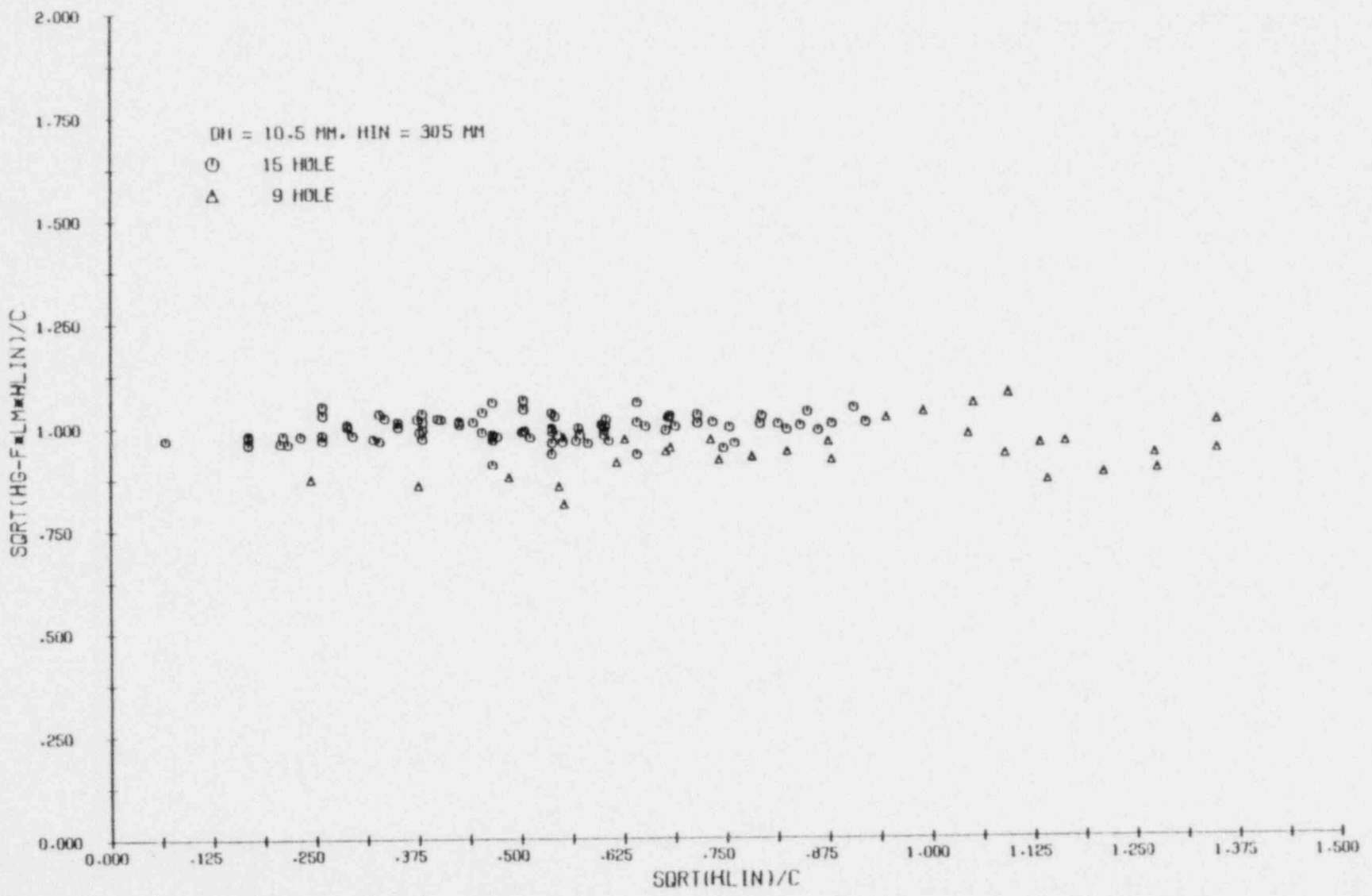


Figure 26. Condensation Effect on Weep Point Correlation, 15 Holes and 9 Holes Data, $h_{in} = 305 \text{ mm}$.

POOR ORIGINAL

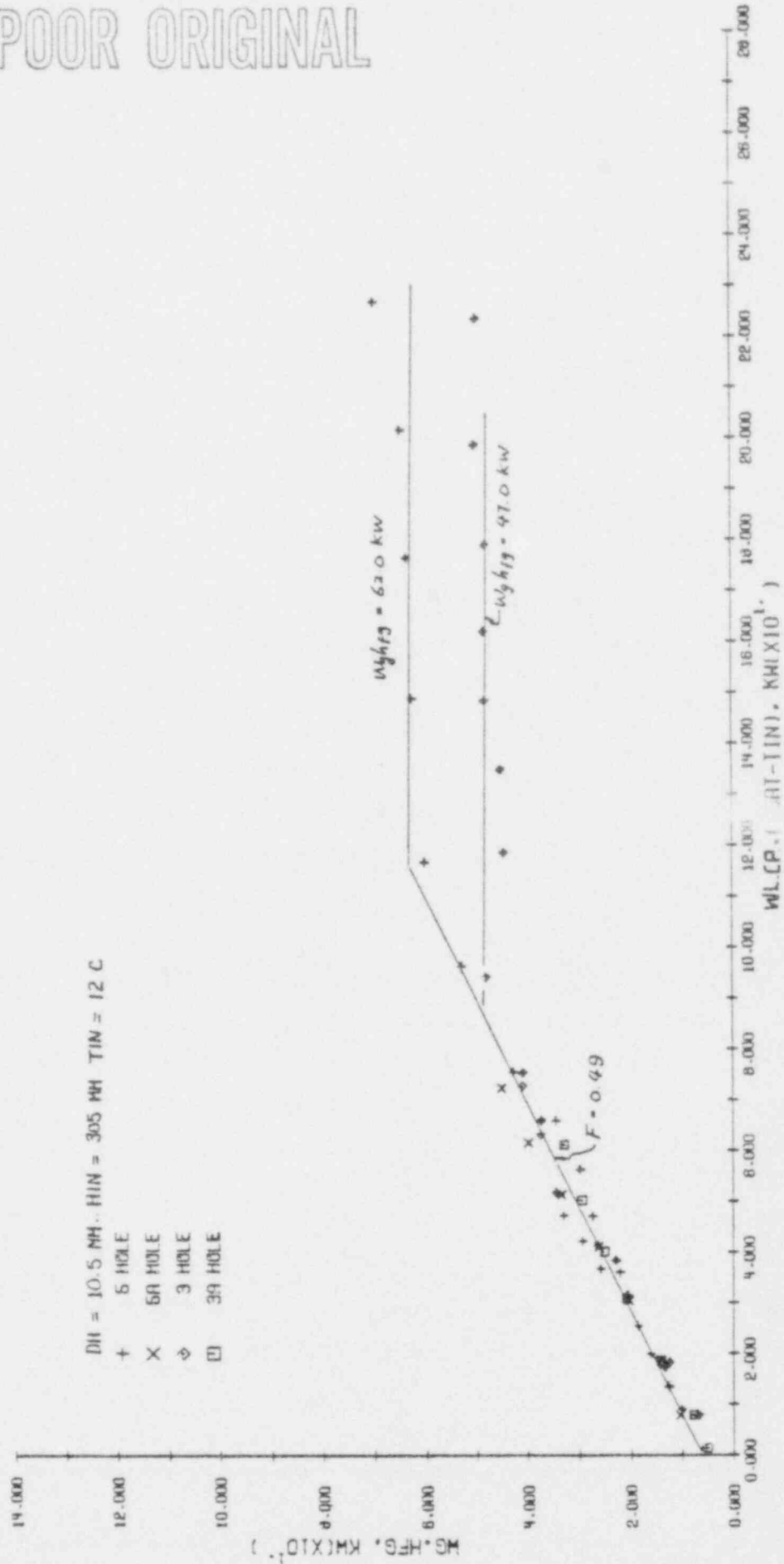


Figure 27. Comparison of the Weep Point Data of 5 Holes, 5A Holes, 3 Holes, and 3A Holes Experiment Result.

1. The mixing efficiency here ($f = 0.49$) is almost two times larger than that of 15 hole and 9 hole experiment.
2. The maximum steam enthalpy flux required to stop the weeping is lower than that of 15 hole and 9 hole experiment.

With the number of holes equals to or less than 5, the total hole area is less than 15% of the whole cross-section area of the channel. It can be observed that the two-phase mixture will now cover only the middle portion of the channel cross-section area, leaving the rest of the area filling by water. Water can easily reach the vicinity of the perforated plate, resulting a higher mixing efficiency of 0.49.

Since more steam will be condensed in the vicinity of the plate, the height of the two-phase mixture zone will then be decreased. This means a thicker water layer with a higher buffer effect will be built up between the top of this zone and the overflow port. As a result, the upper limit of the degree of mixing, and hence the maximum steam enthalpy flux required to stop the weeping will be decreased. Figure 27 shows that this maximum steam enthalpy flux has a value of 62 KW for the 5 hole experiment data and a value of 47 KW for the 3 hole experiment data.

Figure 28 is the superficial steam velocity through the holes for these runs. At low water enthalpy fluxes, where the condensation effect is not dominant, the velocity through the holes is almost the same for all these plates. Once the condensation effect starts playing a role in triggering the weeping, the steam velocity of the 3 hole experiment is higher than that of the 5 hole experiment in order to maintain the same amount of total steam enthalpy flux.

POOR ORIGINAL

DI = 10.5 MM. HIN = 305 MM

- + 5 HOLE
- x 5A HOLE
- ◇ 3 HOLE
- 3A HOLE

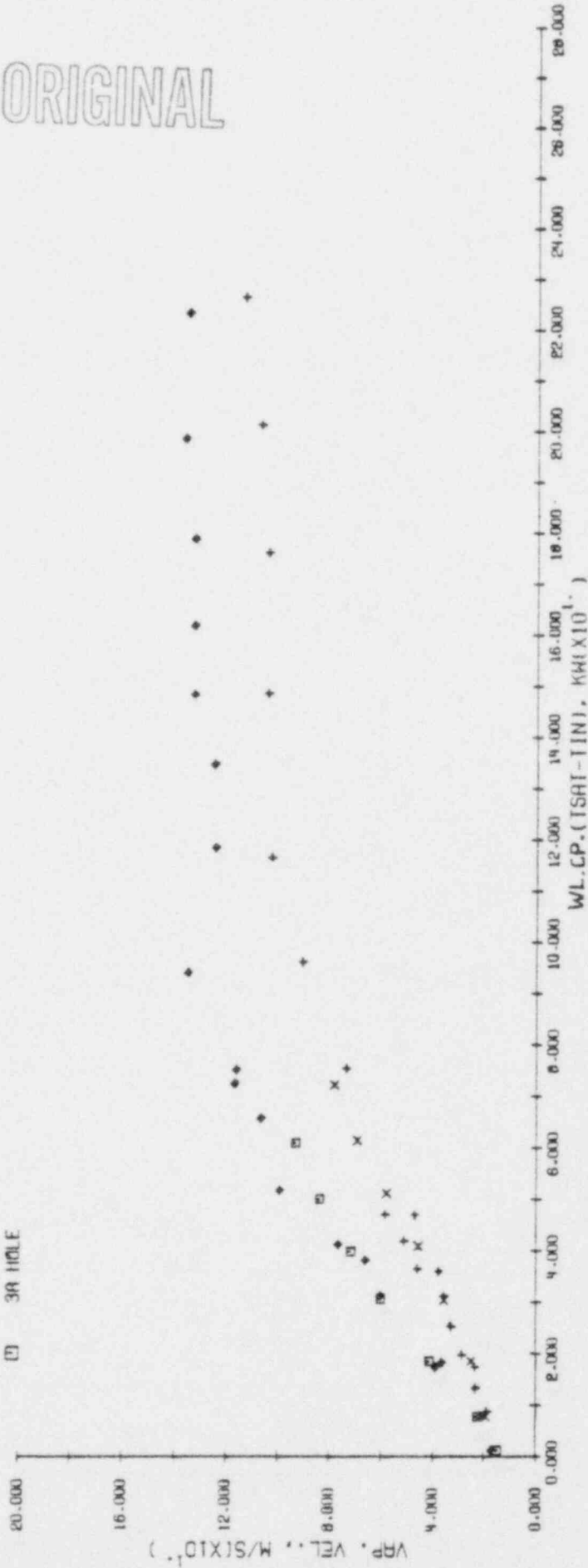


Figure 28. Comparison of Superficial Steam Velocity through Holes for 5 Holes, 5A Holes, 3 Holes, and 3A Holes Data.

Figure 29 is the same data plotted as $H_g^{*1/2}$ vs. $H_f^{*1/2}$. Again, it shows at low water flow rate the data agrees with the air/water correlation very well ($H_g^{*1/2}/C = 1$).

Figure 30 then replaced the steam flow rate with the effective steam flow rate defined in equation (63). It shows that the data are still in close agreement with the air/water correlation. Therefore, one can conclude that so long as the mixing efficiency f can be determined for the particular geometry of the channel and plate, equation (55) and (56) are suitable for both steam/water and air/water weeping data correlation.

5.2 Water Inlet Spray at the Plate

As the water inlet spray been positioned right above the plate, essentially all the inlet water will have the chance to contact with the steam before leaving the channel, and huge condensation rate will occur in the vicinity of the plate. As a result, the weeping phenomenon at this operating condition can be significantly different from that of a high liquid inlet position experiment.

With the water inlet spray height kept at 5 mm, Figure 31 shows the 15 hole weep point data obtained at six different water inlet temperatures. Comparing with the data obtained at high water spray experiment, two distinct phenomena are shown by the data point of 12 °C (285 K) experiment:

1. In the region $R_T > 1$, the oscillatory weep point boundary is close to the thermodynamic boundary $R_T = 1$.

POOR ORIGINAL

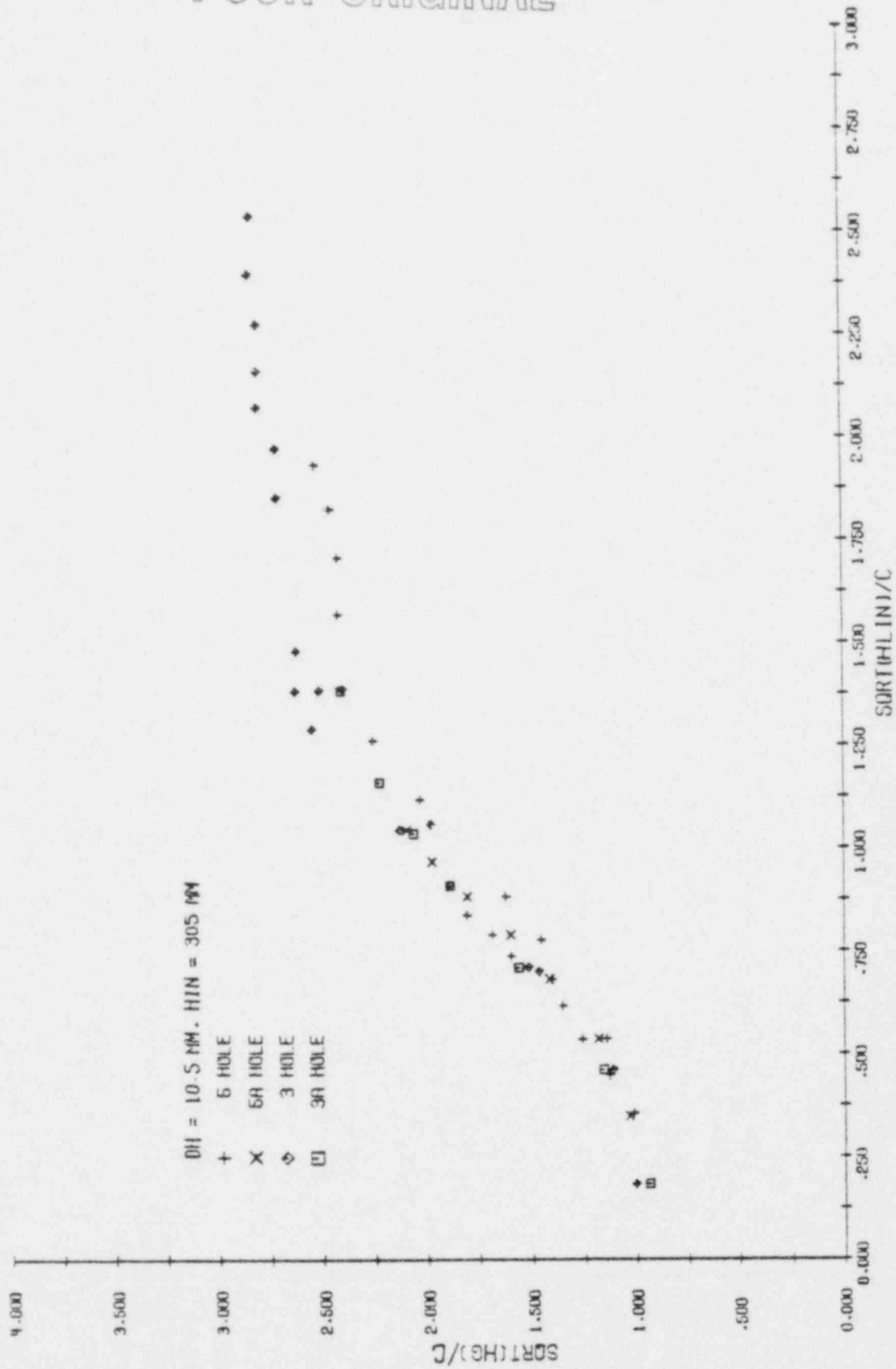


Figure 29. Dimensionless Steam and Water Inlet Flow Rate at Weep Point, 5 Holes, 5A Holes, 3 Holes, and 3A Holes Data, $h_{in} = 305$ mm.

POOR ORIGINAL

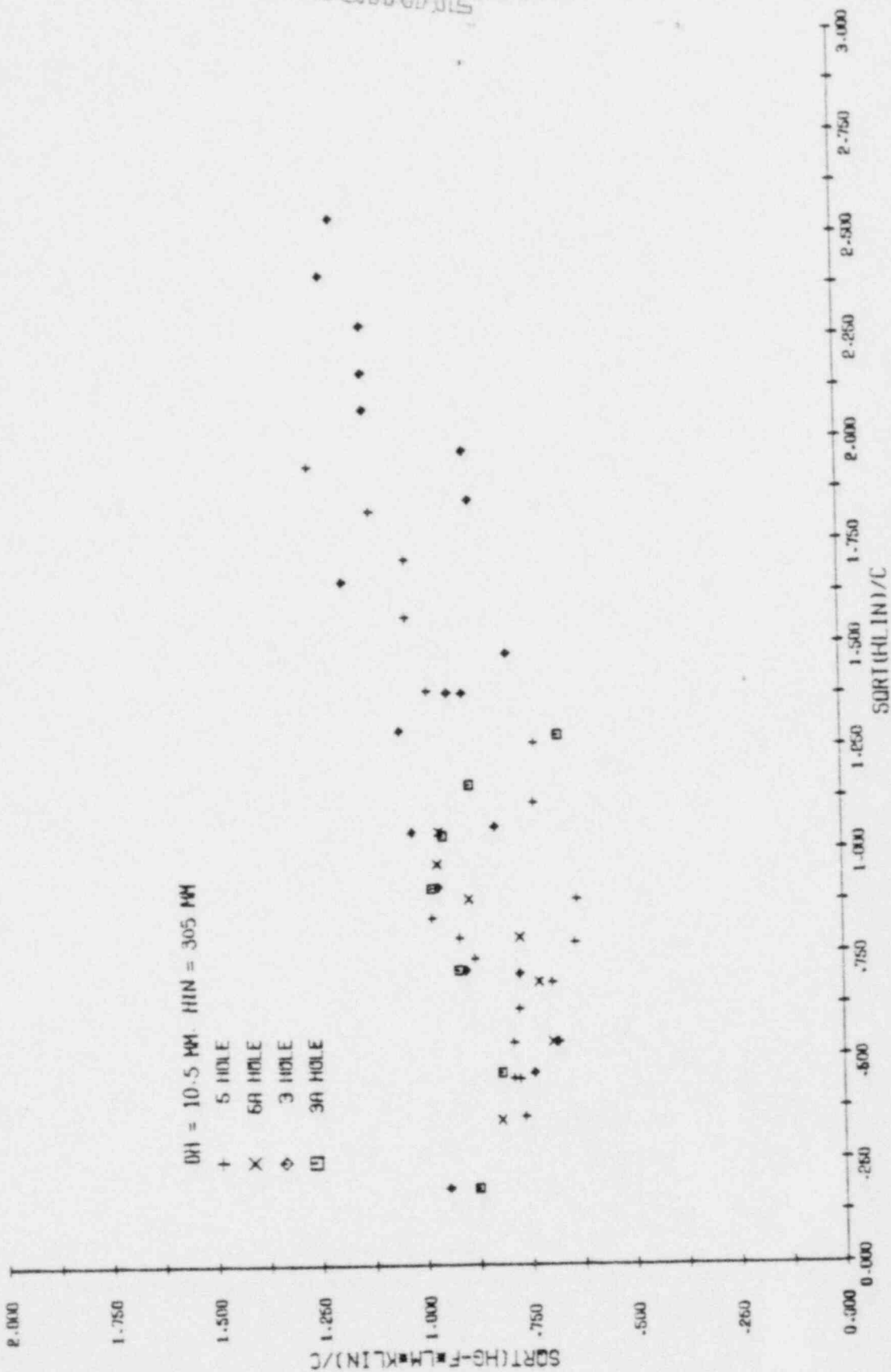
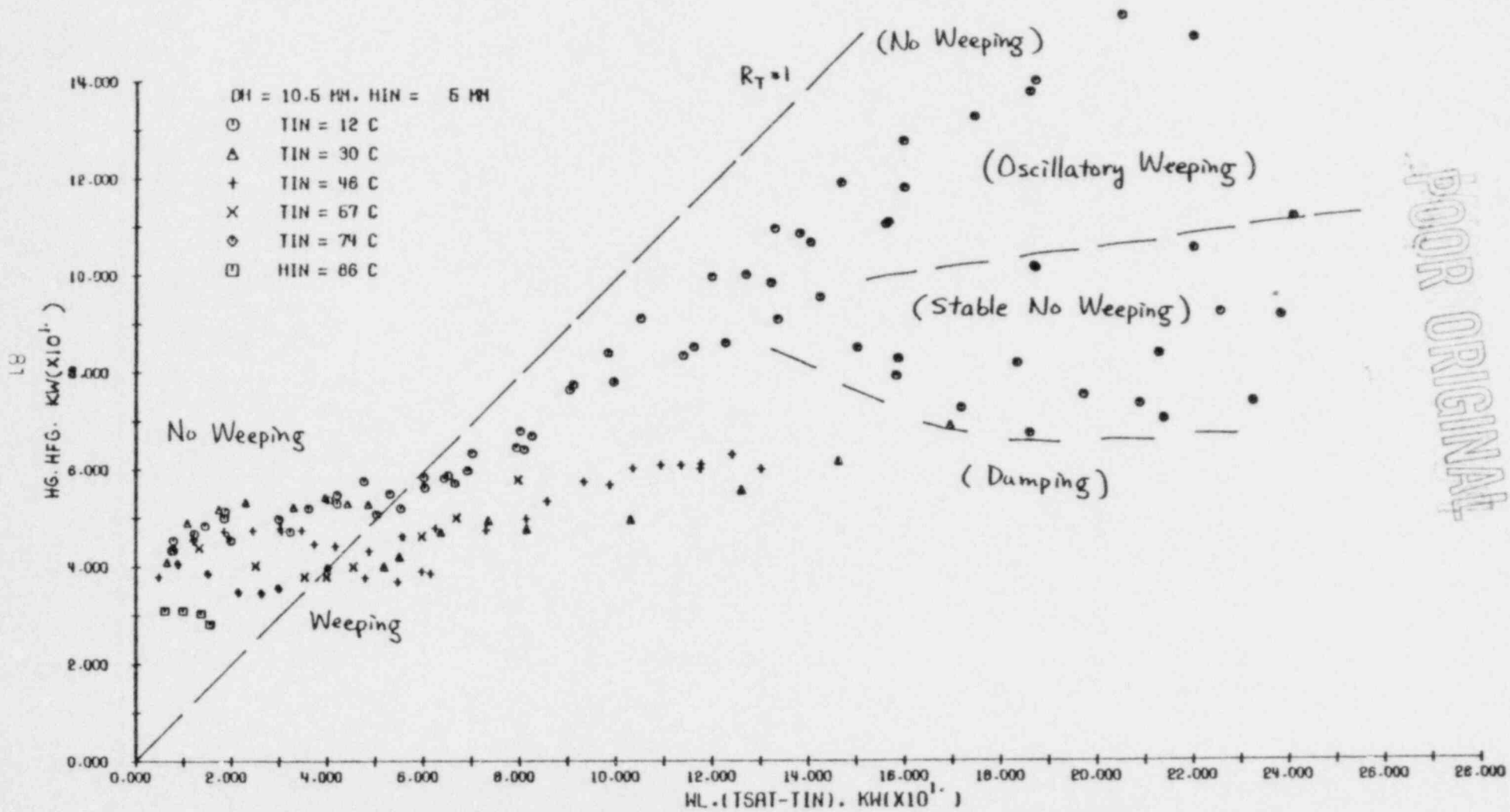


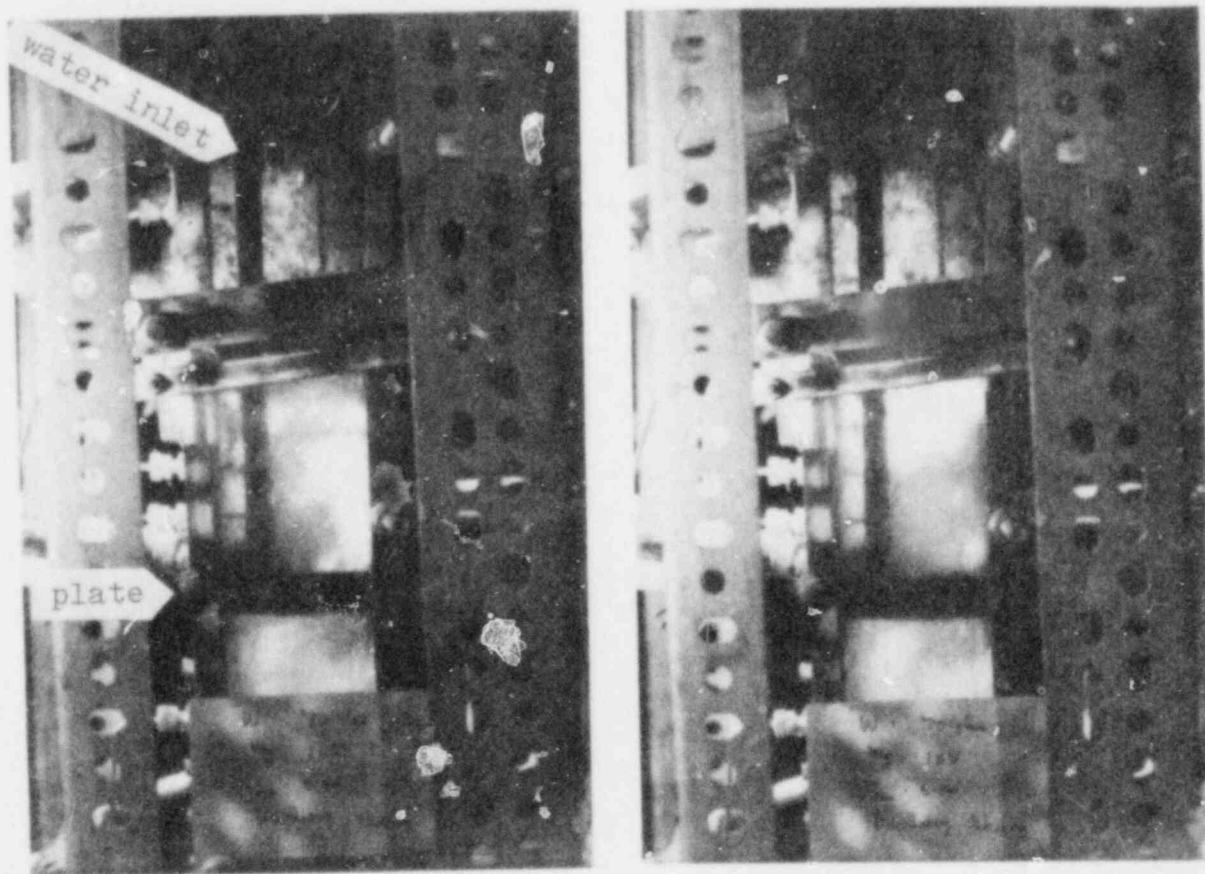
Figure 30. Condensation Effect on Weep Point Correlation, 5 Holes, 5A Holes, 3 Holes, and 3A Holes Data, $h_{in} = 305 \text{ mm}$.



POOR ORIGINAL

Figure 31. 15 Hole Weep Point Data Obtained at Low Water Inlet Position

POOR ORIGINAL



$$W_f = 0.53 \text{ kg/s} \quad T_f = 285 \text{ K}$$

$$W_g = 0.12 \text{ kg/s} \quad T_f = 413 \text{ K}$$

Figure 32. Some Pictures of Oscillatory Weeping.

POOR ORIGINAL

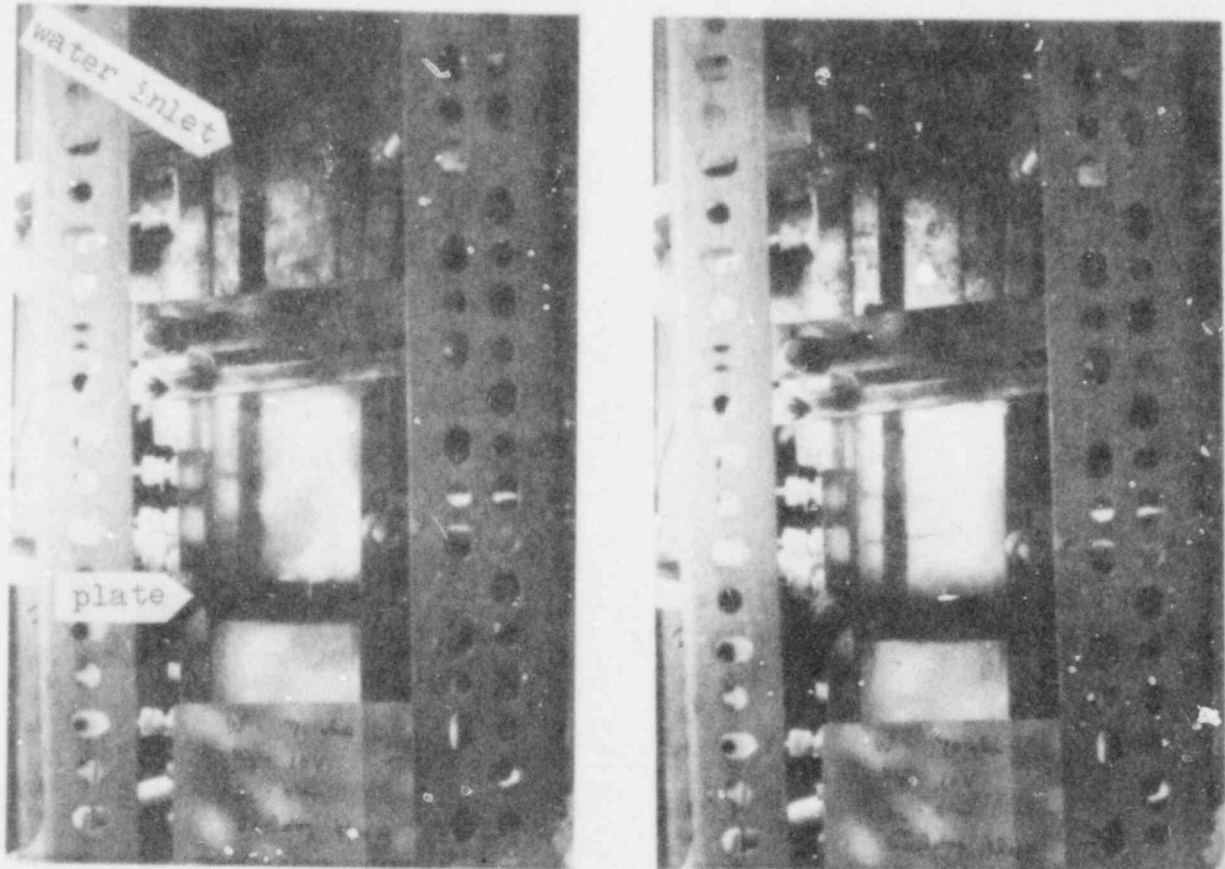
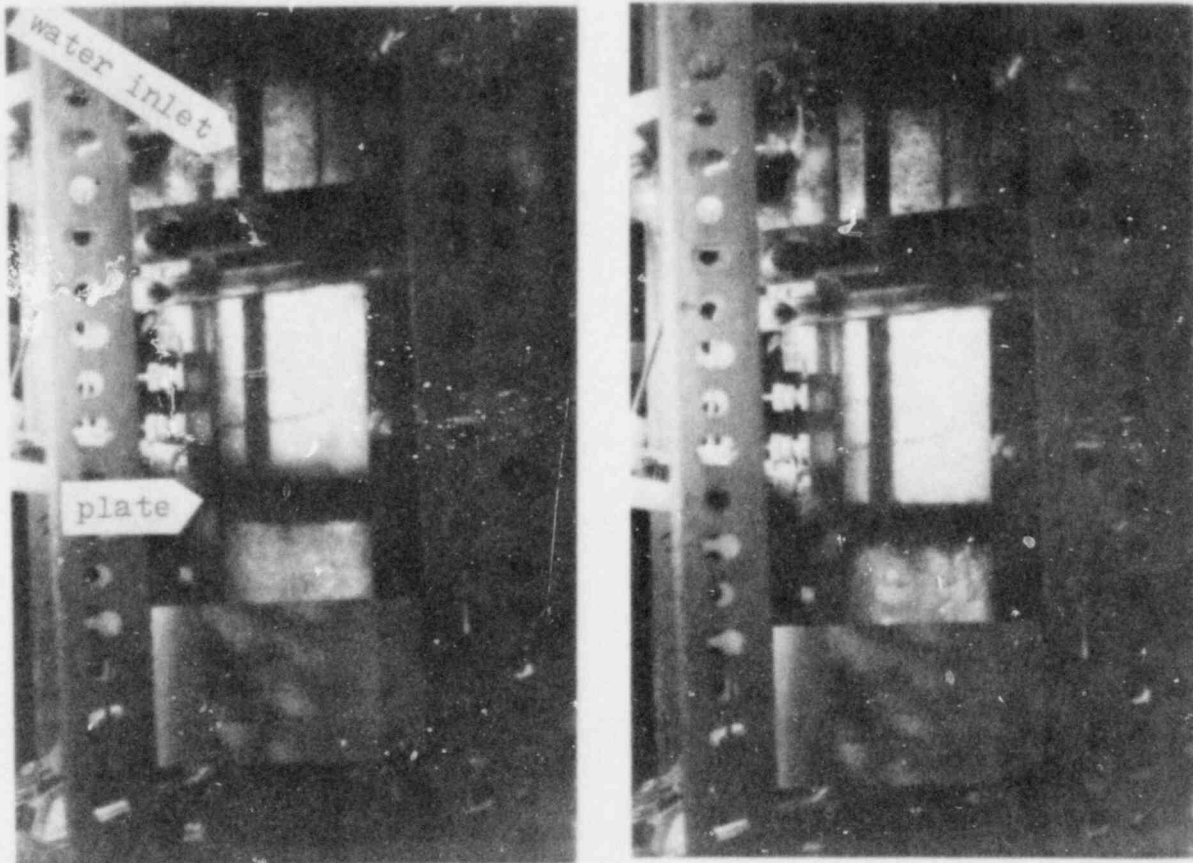


Figure 32. (Continued)

POOR ORIGINAL



$$W_f = 0.53 \text{ kg/s} \quad T_f = 285 \text{ K}$$

$$W_g = 0.072 \text{ kg/s} \quad T_g = 413 \text{ K}$$

Figure 33. Some Pictures of Stable No Weeping.

POOR ORIGINAL

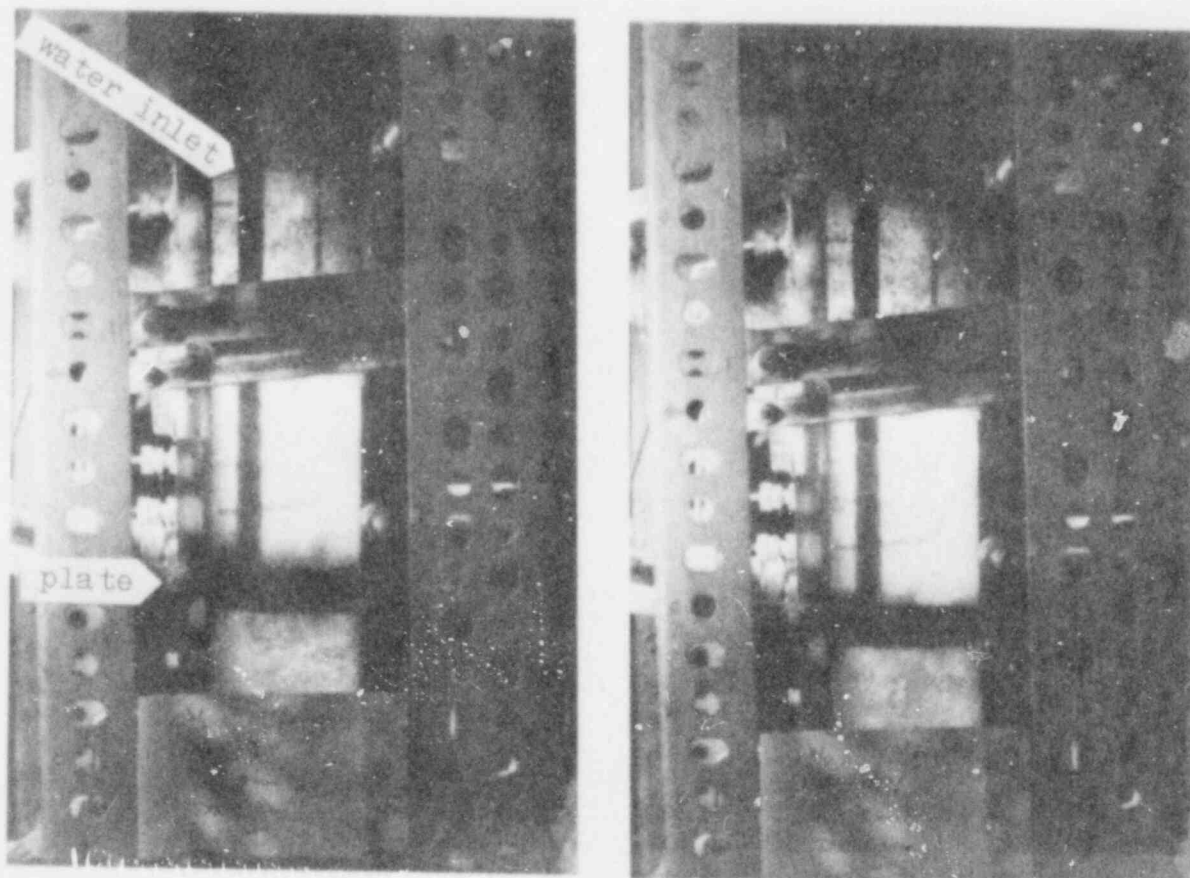
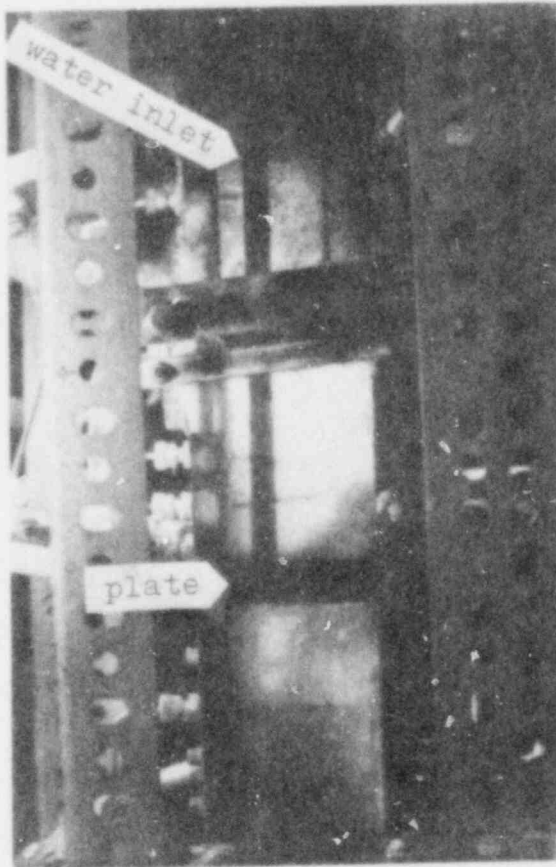
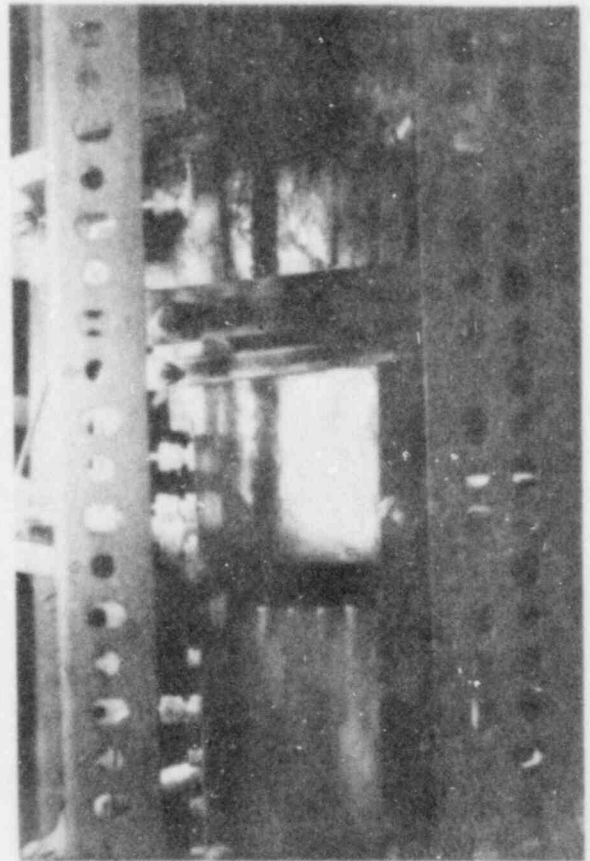


Figure 33. (continued)

POOR ORIGINAL



before the
Dumping



at the
Dumping

Figure 34. Some pictures of Total Dumping

POOR ORIGINAL

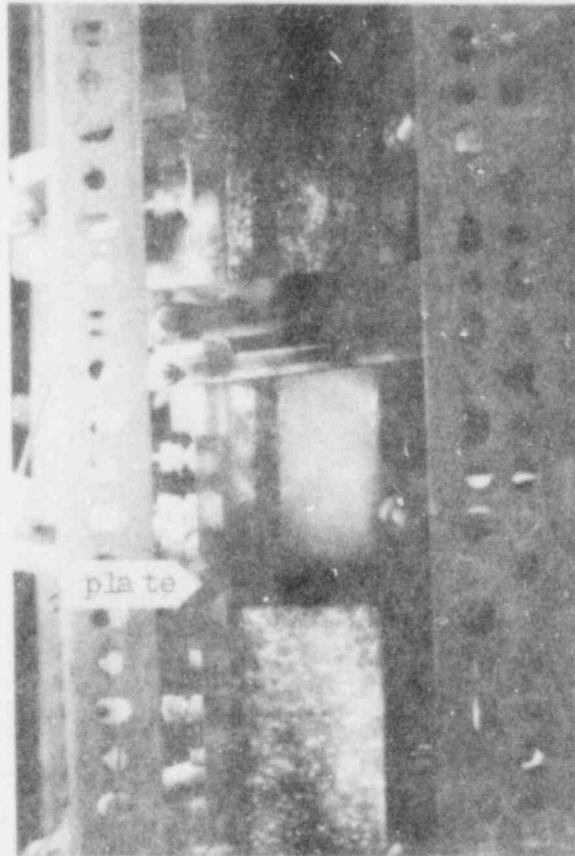


Figure 35. A Picture after the Total Dumping

2. A stable no weeping region is observed when the steam enthalpy flux is decreased from the oscillatory weeping. Further decreasing the steam flow rate from the stable no weeping region will cause total water dumping.

Figure 32 shows some pictures taken at the oscillatory weeping condition. Severe pressure fluctuation is observed. As shown in these pictures, the steam/water interface is quite unstable, and the weeping is accompanied with the collapse of the steam region above the plate.

Figure 33 shows some pictures taken at the stable no weeping condition. All the steam is condensed at the vicinity of the plate, leaving a clear layer of liquid between the plate and the overflow port. Except for high frequency noise, no pressure fluctuation was observed in this region.

Further decreasing the steam flow rate will cause total dumping, which is shown by some pictures taken before, at, and after the dumping. The clear water pool accumulated in the stable no weeping condition now all dumped through the plate(Figure 34,35).

The other data in Figure 31 are obtained at some higher temperatures. The whole phenomenon discussed above disappeared, and the hydrodynamic effect seems to be the dominant factor in this operating condition. Presently, no correlation has been obtained for the subcooling effect in this case.

Figure 36 shows the weep point data collected for different plates with the water inlet temperature at 12 °C and water inlet height of 5 mm. Two common features are observed among these data:

1. Starting from the $R_T < 1$ region(the hydrodynamic control

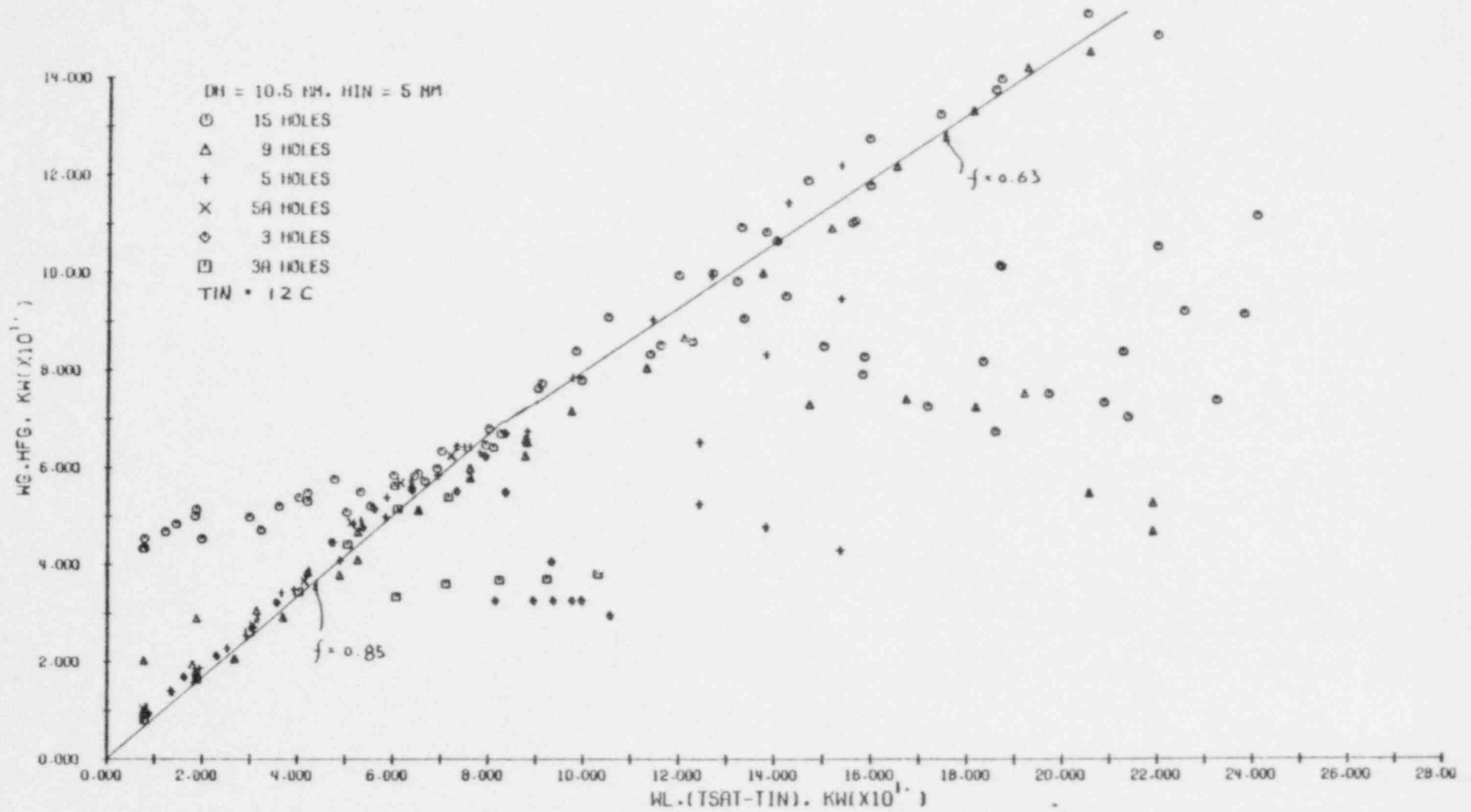


Figure 36. Weep Point Data Taken at $T_{in} = 12^{\circ}\text{C}$ and $h_{in} = 5\text{ mm}$.

region) where the weeping is continuous, the oscillatory weeping will occur once the thermodynamic boundary is reached. After passing the $R_T = 1$ line, the oscillatory weep point boundary is close to the thermodynamic boundary $R_T = 1$. The mixing efficiency(f) for 3 hole and 5 hole data is 0.85, the mixing efficiency(f) for 9 hole and 15 hole data is 0.63.

2. A stable no weeping have been observed for all the experiments with different plates.

By assuming the steam is condensed in a hemispherical steam jet with its diameter equal to the diameter of the hole, the condensation heat transfer coefficients in this stable no weeping condition can be estimated with the aid of the thermocouples reading at the vicinity of the plate:

Therefore, for 15 hole data, the steam enthalpy flux at the beginning of the stable no weeping condition is around 9.6 KW, the temperature at the vicinity of the plate is 340 K, and the heat transfer area per hole is

$$A_b = 0.5 D_h^2 = 1.73 \times 10^{-4} \text{ m}^2 \quad (66)$$

$$\begin{aligned} h' &= Q/A_b \Delta T = 96000 / (15 \times 1.73 \times 10^{-4}) (373 - 340) \\ &= 1.12 \times 10^6 \text{ W/m}^2 \text{ K} \end{aligned} \quad (67)$$

For 9 hole,

$$h' = 74000 / (9 \times 1.73 \times 10^{-4}) (373 - 337) = 1.32 \times 10^6 \text{ W/m}^2 \text{ K} \quad (68)$$

For 5 hole,

$$h' = 52000 \text{ W} / (5 \times 1.73 \times 10^{-4} \text{ m}^2) (373 - 339) = 1.76 \times 10^6 \text{ W/m}^2 \text{ K} \quad (69)$$

and for 3 hole

$$\begin{aligned} h' &= 33000 \text{ W} / (3 \times 1.73 \times 10^{-4} \text{ m}^2) (373 - 333) \\ &= 1.58 \times 10^6 \text{ W/m}^2 \text{ K} \end{aligned} \quad (70)$$

All these condensation heat transfer coefficients are of the same order of magnitude. As a result of this high rate of condensation right above the plate, the possibility of the collapse of steam in the liquid pool and the oscillatory weeping along with this collapse are totally eliminated.

Decreasing the steam enthalpy flux below the stable no weeping region will allow some cold water to penetrate through the holes of the plate. This cold water will condense some steam before it can reach the plate; as a result, more cold water will be drawn down through the plate, triggering total dumping.

5.3 Effect of Liquid Inlet Spray Position

Figure 37 and 38 are the 15 hole and 9 hole data taken at different water inlet spray position. It shows that the weep point data obtained at $h_{in} = 305$ and 710 mm (water spray above the pool) are the same. The data taken at $h_{in} = 102$ mm lie between the data of $h_{in} = 5$ mm and $h_{in} = 305$ mm.

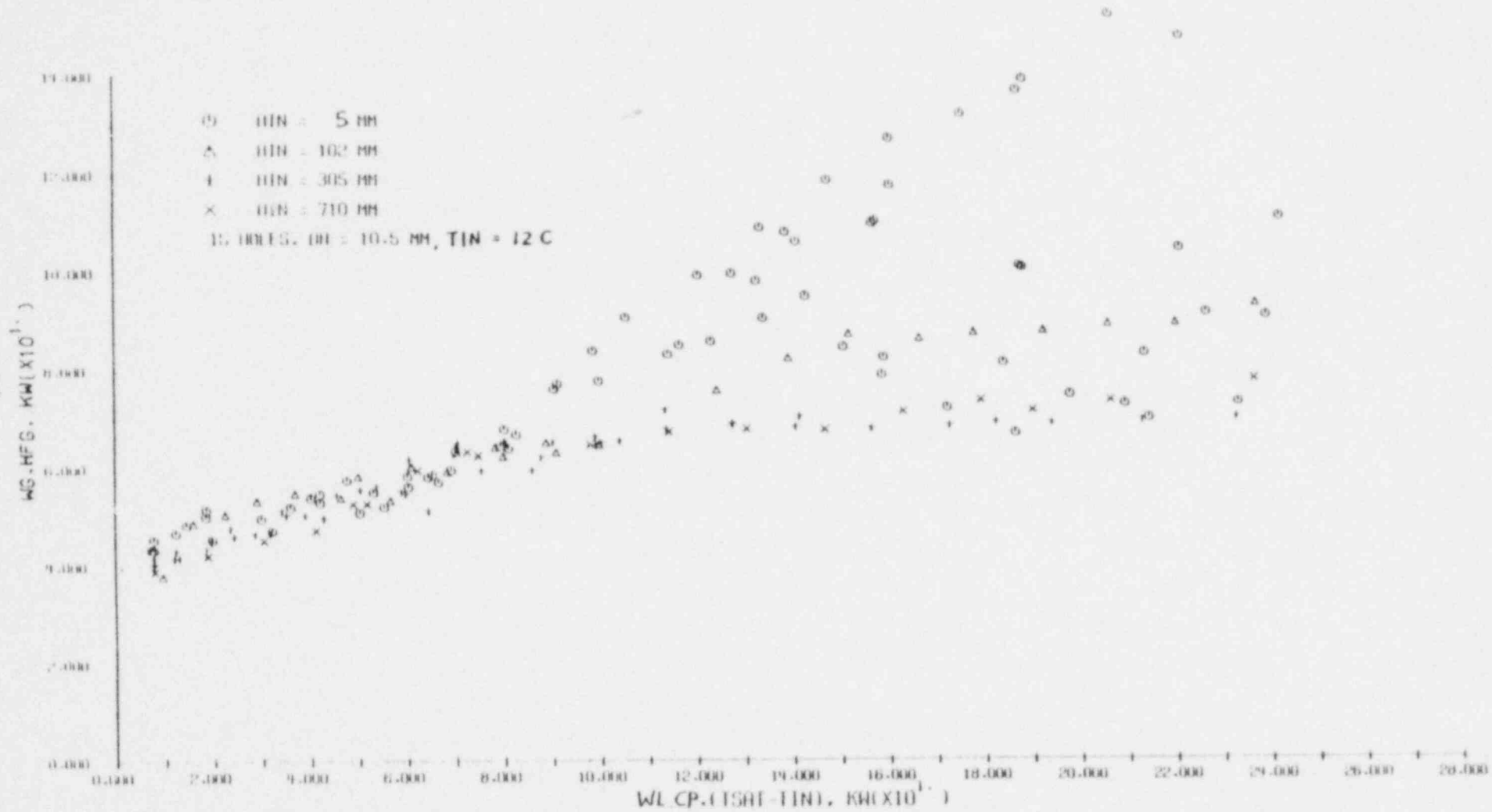


Figure 37. Effect of Liquid Inlet Spray Nozzle Position on Weep Point, 15 Holes Data.

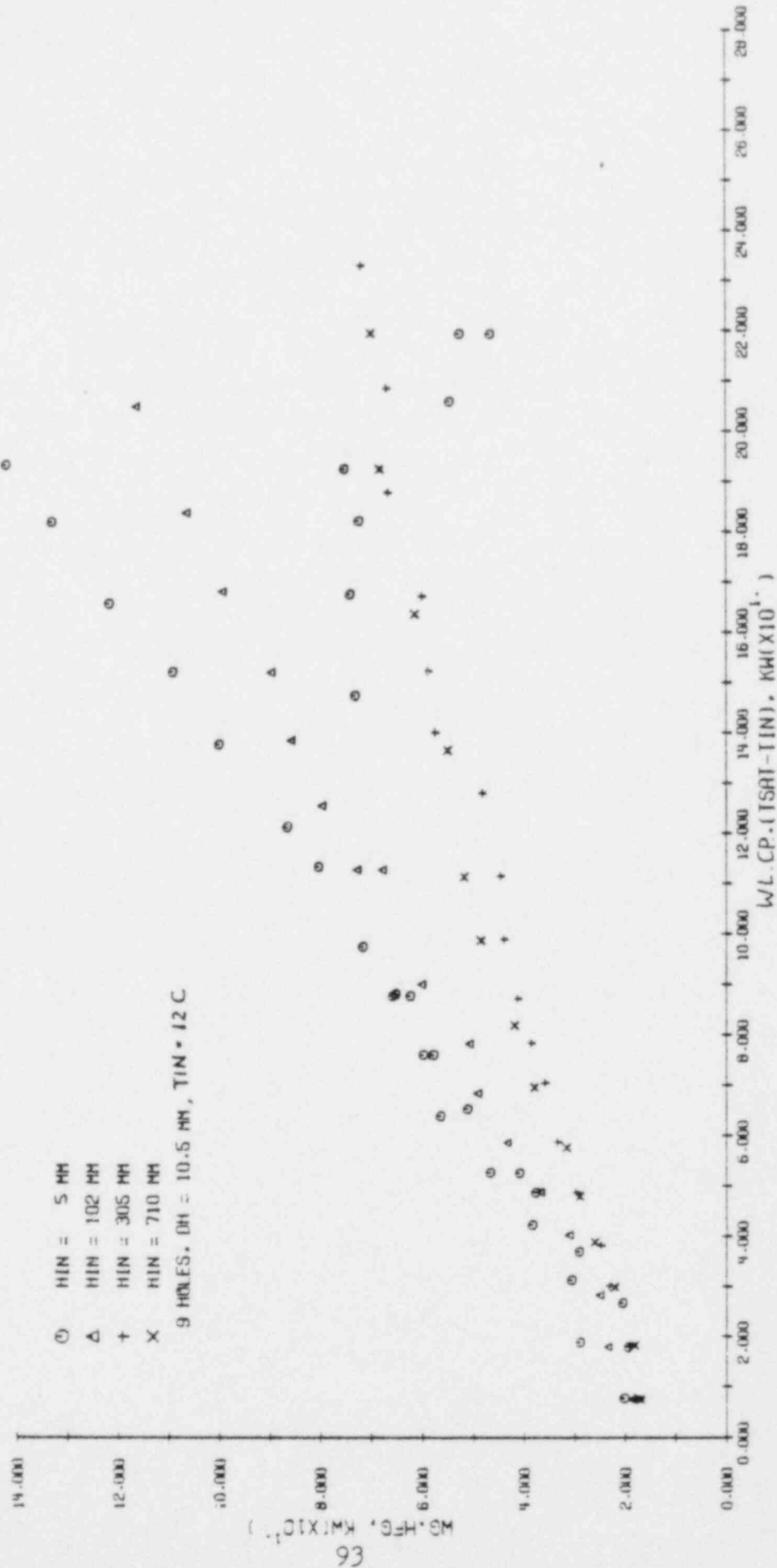


Figure 38. Effect of Liquid Inlet Spray Nozzle Position on Weep Point, 9 Holes Data.

6. Conclusions and Suggestions

Based on the information collected in the present study, the following conclusions can be made:

- a. By introducing the new dimensionless flow rate scaling H^* , which represents a smooth transition between J^* and K^* scaling, the air/water data obtained at 7 perforated plates with different numbers and diameters of holes can be correlated by a conventional flooding equation in the form of

$$H_g^{*1/2} + H_f^{*1/2} = C \quad (55)$$

$$\text{where } H_{f,g}^* = [\rho_{f,g}/g_w(\rho_f - \rho_g)]^{1/2} j_{f,g} \quad (50)$$

and w is given in equation (51) and (52), the coefficient C is given in equation (56).

- b. The liquid spray position, liquid inlet flow rate, soft volume and the head of liquid pool above the plate do not have any discernible effect on the rate of weeping in the present air/water experiment.
- c. The steam/cold water weep point data which were obtained at high liquid inlet spray position can be related to equation (55) by introducing an effective steam flow rate, which is defined by equation (63).
- d. Two types of weeping were observed when the the channel was running in high liquid spray experiment: For low water flow rate and subcooling the weeping at the weep point is smooth and continuous; As the water flow rate or subcooling becomes high, oscillatory or intermittent weeping was observed.

- e. For water inlet near the plate, a stable no weeping region was observed at high water flow and subcooling. In this region, all the steam was condensed right above the plate, leaving a clear layer of liquid above a bubbly region. Increasing the steam flow rate causes oscillatory weeping, while decreasing the steam flow below this region will result in total dumping.

Several suggestions are made for further investigations:

- a. The validity of H^* scaling, which is highly dependent on the construction of the α function, should be checked over a larger parameter range, and larger scale.
- b. The void fraction of the two-phase mixture above the plate should be checked by pressure measurement.
- c. The mixing efficiency, which could be a function of liquid spray position, method of liquid injection, perforation ratio of the plate, and channel geometry, should be further studied.

7. Reference:

- (1). Sherwood, T. K., et al., Ind. Eng. Chem. 30, pp765 (1938).
- (2). Lobo, W. E., et al., Trans. ALCHE, 41, pp693 (1945).
- (3). Bulletin HY-30, Hy-Park Packings, Norton Co., (1977).
- (4). Sherwood, T. K., et al, "Mass Transfer", pp599-603
McGraw-Hill, Inc., New York (1975).
- (5). Tien, C. L. and C. P. Liu, "Survey on Vertical Two-Phase
Countercurrent Flooding" NP-984 (1979).
- (6). Wallis, G. B., et al., "Analysis of ECC Delivery",
CREARE TN-231 (1976).
- (7). Ueda, T. and S. Suzuki, "Behaviour of Liquid Films and
Flooding in Counter-Current Two-Phase Flow. Part 2.
Flow in Annuli and Rod Bundles", Int. J. Multiphase Flow,
4, pp157-170 (1978).
- (8). Jones, D. D., "Subcooled Counter-Current Flow Limiting
Characteristics of the Upper Region of a BWR Fuel
Bundle", General Electric Company, Nuclear Systems
Products Division, BD/ECC Program, NEDG-NUREG-23549
(1977).

- (9). Mayfield, F. D., et al., "Perforated-Plate Distillation Columns", Ind. Eng. Chem., 44 9, pp2238-49, Sept. (1952).
- (10). Arnold, D. S., et al., "Performance of Perforated-Plate Distillation Columns", Chem. Eng. Prog., 48 12, pp633-42, (1952).
- (11). Zenz, F. A., "How to Calculate Capacities of Perforated-Plates", Petroleum Refiner, 33 2, pp99-102, Feb. (1954).
- (12). Hunt, C. D., et al., "Capacity Factors in the Performance of Perforated-Plate Columns", AIChE J., 1 4, pp441-51, (1955).
- (13). Jones, P. D., and ~~Mathew~~ Van Winkle, "Variables in Perforated-Plate Column Efficiency and Pressure Drop", Ind. Eng. Chem., 49 2, pp232-38, (1957).
- (14). Leibson I., et al., "Design of Perforated Plate Fractionating Towers", Chem. Eng. Prog., 53 3, pp127-33, (1957).
- (15). Block, J. A., "Condensation-Driven Fluid Motion", EPRI Workshop on Basic Two-Phase Flow Modeling, Tampa, Florida, March 1, (1979).

- (16). Biddulph, M. W., and D. J. Stephens, "Oscillating Behavior on Distillation Trays", AICHE J., 20 1, pp60-66 (1974).
- (17). Hughmark, G. A., et al., "How to Design Perforated Trays", petroleum Refiner, 37 2, pp127-33,(1957).
- (18). Huang, C. J., et al., "Design of Perforated Plate Fractionating Towers", Chem. Eng. Prog., 53 3, pp127m-132m, (1957).
- (19). Eduljee, H. E., "Design of Sieve-Type Distillation Plates", British Chem. Engineering, pp320-26, June (1959).
- (20). Davies, J. A., "What to Consider in Your Fractionator Tray Design, Part 2 Perforated Trays", Petro/Chem. Engineer, pp250-3, Nov. (1961).
- (21). Smith, B. D., W. L. Bolles and J. R. Fair, "Design of Equilibrium Stage Process", pp548, McGraw-Hill Book Company, New York (1963).
- (22). Perry, R. H. and C. H. Chilton, "Chemical Engineers' Hand book", 5th edition, pp18-7, McGraw-Hill Book Company, New York (1973).
- (23). McCann, D. J. and R. G. H. Prince, "Bubble Formation and

- Weeping At a Submerged Orifice", Chem. Eng. Science, 24, pp801-814 (1969).
- (24). Showkry E. and V. Kolar, "On the Hydrodynamics of Sieve Plates Without Downcomers", The Chem. Eng. J., 8, pp41-51 (1974).
- (25). Wallis, G. B., "One-Dimensional Two-Phase Flow", pp343-344, McGraw-Hill, Inc., New York (1969).
- (26). Pushkina, O. L. and Y. L. Sorokin, "Breakdown of Liquid Film Motion in Vertical Tubes", Heat Transfer-Soviet Research, 1 5, pp56 (1969).
- (27). Sun, K. H. and R. T. Fernandez, "Counter-Current Flow Limitation Correlation for BWR Bundles During LOCA", ANS Transaction, 27, pp605 (1977).
- (28). Sun, K. H., "Flooding Correlations for BWR Bundle Upper Tieplates and Bottom Side-Entry Orifices", Second Multi-Phase Flow and Heat Transfer Symposium-Workshop, Miami Beach, Florida, April (1979).
- (29). Bharathan, D., "Air-Water Countercurrent Annular Flow in Vertical Tubes", EPRI Report NP-786 (1978).

- (30). Shires, G. L. and A. R. Pickering, "The Flooding Phenomena in Countercurrent Two-Phase Flow", Symposium on Two Phase Flow, ppB501-B538, Exeter, (1965).
- (31). Block, J. A. and Crowley, C. J., "Effects of Steam Up-Flow and Superheated Walls on ECC Delivery in a Simulated Multiloop PWR Geometry", Creare Technical Note TN-210, May (1975).
- (32). Block, J. A. and Crowley, C. J., "Effects of Cold Leg Steam and Flow Baffles on ECC Delivery in a Simulated Multiloop PWR Geometry with Steam Upflow", Creare Technical Note TN-214, July (1975).
- (33). Crowley, C. J. and Block, J. A., "ECC Delivery Study-Experimental Results and Discussion", Creare Technical Note TN-217, October (1975).
- (34). Cudnik, R. A., et al., "Steam-Water Mixing and System Hydrodynamics Program, Task 4", NUREG/CR-0147, BMI-2003, Battelle Columbus Laboratories (1978).*
- (35). Block, J. A. and H. Rothe, "Progress on ECC By Pass Scaling", Creare TN-272, NUREG/CR-0048, R-2 (1977).*

- (36). Carbiener, W. A., et al., "Steam-Water Mixing and System Hydrodynamics Program, Task 4", NUREG/CR-0034, BMI-1993, Battelle Columbus Laboratories (1977).*
- (37). Richter, H. J. and S. L. Murphy, "Effect of Scale on Two-Phase Countercurrent Flow Flooding in Annuli, Final Report", Thayer School of Engineering, Dartmouth College, Hanover, N. H., NUREG/CR-0822 (1979).**
- (38). Wallis, G. B., "One-Dimensional Two-Phase Flow", pp288, McGraw-Hill, Inc., New York (1969).
- (39). Wallis, G. B. and S. Makkenchery, "The Hanging Film Phenomena in Vertical Annular Two-Phase Flow", ASME Journal of Fluids Engineering, pp297-298, Sept. (1974).
- (40). Collier, R. P., et al., "Steam-Water Mixing and System Hydrodynamics Program, Quarterly Progress Reprot, Jan.-Mar. 1979", NUREG/ CR-0897, BMI-2029, Battelle Columbus Laboratories (1979).**
- (41). Tobin, R., "CCFL Test Results, Phasel-TLTA 7x7 Bundle", General Electric Company, Nuclear System Products Divison, BD/ECC Program, GEAP-21304-5 (1977).

- (42). Naitoh, M., K. Chino and R. Kawabe, "Restrictive Effect of Ascending Steam on Falling Water During Top Spray Emergency Core Cooling", J. of Nuclear Science and Technology, 15 11, pp806 (1978).
- (43). Jacoby J. K., et. al., "Final Report on 3-D Experiment Project Air/Water Upper Plenum Experiments", USNRC, 3DP-TR-001, Nov. (1978).
- (44). Jones, D. D., "Test Report TLTA Components CCFL Tests", General Electric Company, NEDG-NUREG-23732 (1977).
- (45). Graham, G., "Summary of Recent Thayer School Annulus Penetration Results; Memorandum", Thayer School of Engineering, Dartmouth College, May 20 (1975).
- (46). Cudnik, R. A. and R. O. Wooton, "Penetration of Injected ECC Water through the Downcomer Annulus in the Presence of Reverse Core Steam Flow", Battelle Columbus Laboratories Report, November (1974).
- (47) Wallis, G. B., J. T. Kuo, "The Behavior of Gas-Liquid Interface in Vertical Tubes", Int. J. of Multiphase Flow, 2 521 (1976).
- (48) Cudnik, R. A. et. al., "Flooding of Counter-Current Steam-

Water Flow in An Annulus", Topics in Two-Phase Heat Transfer and Flow, pp107-113, ASME(1978).

(49). Block, J. A., "Condensation-Driven Fluid Motions", Creare Incorporated, Paper submitted to the International Journal of Multiphase Flow(1979).

(50). Duffey, R. B., et. al., "The Condensation Induced Transition from Bubbling to Liquid Downflow in a Turbulent Two-Phase Pool", Paper submitted to the 18th National Heat Transfer Conference, SanDiego, (1979).

(51). Bankoff, S. G., et. al., "Condensation Rates in Steam-Water Mixing", Annual Progress Report, Northwestern University, Evanston, Ill., Feb., (1979).

(52). Jacoby, J. K., et. al., "Quick Look Report on KUU Support Column Air-Water Experiment", EG&G Report, RDW-23-78 (1978).

*Available for purchase from the National Technical Information Service, Springfield, VA 22161.

**Available for purchase from the NRC/GPO Sales Program, U.S. Nuclear Regulatory Commission, Washington, DC 20555, and the National Technical Information Service, Springfield, VA 22161.

Appendix I. Computer Program List and the Air/Water
Reduced Data.

The input of this program includes: IP,WF,WG, and PG. where

- IP = 1, 15 hole data
2, 9 hole data
3, 5(5A) hole data
4, 3(3A) hole data
5, 40 hole data
6, 2 hole data

- WF : liquid mass flow rate, lbs/sec.
WG : air rotameter reading, SCFM.
PG : air rotameter pressure gauge reading, psig.

Depending the selection of DH(characteristic length), the program can calculate the dimensionless velocity in the form of J^* , K^* , or H^* .

The output of the program includes:

- JG, JF : superficial gas and liquid velocity through holes,
(m/s).
JGS, JFS : dimensionless velocity, either J^* , K^* , or H^* .
the data shown are in H^* .
JGS5, JFS5 : square root of the dimensionless velocity.
C : coefficient C in the flooding equation.

The data will also be plotted as JGS5 vs. JFS5.

POOR ORIGINAL

1468

03/13/79 11.10.13

FTN 4.4.40

74/4

PROGRAM JEGS

```

PROGRAM JEGS
  EQUIP TAPE 931
  READ (1) (A, B, C, D, E, F, G, H, I, J, K, L, M, N, O, P, Q, R, S, T, U, V, W, X, Y, Z)
  PRINT (A, B, C, D, E, F, G, H, I, J, K, L, M, N, O, P, Q, R, S, T, U, V, W, X, Y, Z)
  IF (A .EQ. 'A') THEN
    PRINT 'A'
  ELSE IF (A .EQ. 'B') THEN
    PRINT 'B'
  ELSE IF (A .EQ. 'C') THEN
    PRINT 'C'
  ELSE IF (A .EQ. 'D') THEN
    PRINT 'D'
  ELSE IF (A .EQ. 'E') THEN
    PRINT 'E'
  ELSE IF (A .EQ. 'F') THEN
    PRINT 'F'
  ELSE IF (A .EQ. 'G') THEN
    PRINT 'G'
  ELSE IF (A .EQ. 'H') THEN
    PRINT 'H'
  ELSE IF (A .EQ. 'I') THEN
    PRINT 'I'
  ELSE IF (A .EQ. 'J') THEN
    PRINT 'J'
  ELSE IF (A .EQ. 'K') THEN
    PRINT 'K'
  ELSE IF (A .EQ. 'L') THEN
    PRINT 'L'
  ELSE IF (A .EQ. 'M') THEN
    PRINT 'M'
  ELSE IF (A .EQ. 'N') THEN
    PRINT 'N'
  ELSE IF (A .EQ. 'O') THEN
    PRINT 'O'
  ELSE IF (A .EQ. 'P') THEN
    PRINT 'P'
  ELSE IF (A .EQ. 'Q') THEN
    PRINT 'Q'
  ELSE IF (A .EQ. 'R') THEN
    PRINT 'R'
  ELSE IF (A .EQ. 'S') THEN
    PRINT 'S'
  ELSE IF (A .EQ. 'T') THEN
    PRINT 'T'
  ELSE IF (A .EQ. 'U') THEN
    PRINT 'U'
  ELSE IF (A .EQ. 'V') THEN
    PRINT 'V'
  ELSE IF (A .EQ. 'W') THEN
    PRINT 'W'
  ELSE IF (A .EQ. 'X') THEN
    PRINT 'X'
  ELSE IF (A .EQ. 'Y') THEN
    PRINT 'Y'
  ELSE IF (A .EQ. 'Z') THEN
    PRINT 'Z'
  ELSE
    PRINT 'OTHER CHARACTER'
  END IF
  END

```


80

```

JF=JF73.08
Z=JGSA+JFSA
PRINT 20,JG,JG5,JG5A,JF,JFS,JFSA,7

```

```

20 FORMAT(112X,7F12.3,7I
19 FORMAT(122X,*JG,HZS
C JG5 * ,771 JG55 JF,HZS JFS

```

85

```

C
GO TO 2
IF 11=0.1 GO TO 71
IF 11=0.2 GO TO 72
IF 11=0.3 GO TO 73
IF 11=0.4 GO TO 74
IF 11=0.5 GO TO 75
IF 11=0.6 GO TO 76
IF 11=0.7 GO TO 77

```

90

```

71 I1=I+1
IA=I
I2=I+2
JF=JF+1
JG=JG+1
JG5=JG5+1
JF5=JF5+1
JFS=JFS+1
JFSA=JFSA+1
JGSA=JGSA+1
JG5A=JG5A+1
GO TO 1

```

95

```

JF=JF+1
JG=JG+1
JG5=JG5+1
JF5=JF5+1
JFS=JFS+1
JFSA=JFSA+1
JGSA=JGSA+1
JG5A=JG5A+1
GO TO 1

```

100

```

72 I1=I+1
I2=I+2
JF=JF+1
JG=JG+1
JG5=JG5+1
JF5=JF5+1
JFS=JFS+1
JFSA=JFSA+1
JGSA=JGSA+1
JG5A=JG5A+1
GO TO 1

```

105

```

73 I1=I+1
I2=I+2
JF=JF+1
JG=JG+1
JG5=JG5+1
JF5=JF5+1
JFS=JFS+1
JFSA=JFSA+1
JGSA=JGSA+1
JG5A=JG5A+1
GO TO 1

```

110

```

74 I1=I+1
I2=I+2
JF=JF+1
JG=JG+1
JG5=JG5+1
JF5=JF5+1
JFS=JFS+1
JFSA=JFSA+1
JGSA=JGSA+1
JG5A=JG5A+1
GO TO 1

```

115

```

75 I1=I+1
I2=I+2
JF=JF+1
JG=JG+1
JG5=JG5+1
JF5=JF5+1
JFS=JFS+1
JFSA=JFSA+1
JGSA=JGSA+1
JG5A=JG5A+1
GO TO 1

```

120

```

76 I1=I+1
I2=I+2
JF=JF+1
JG=JG+1
JG5=JG5+1
JF5=JF5+1
JFS=JFS+1
JFSA=JFSA+1
JGSA=JGSA+1
JG5A=JG5A+1
GO TO 1

```

125

```

77 I1=I+1
I2=I+2
JF=JF+1
JG=JG+1
JG5=JG5+1
JF5=JF5+1
JFS=JFS+1
JFSA=JFSA+1
JGSA=JGSA+1
JG5A=JG5A+1
GO TO 1

```

130

```

78 I1=I+1
I2=I+2
JF=JF+1
JG=JG+1
JG5=JG5+1
JF5=JF5+1
JFS=JFS+1
JFSA=JFSA+1
JGSA=JGSA+1
JG5A=JG5A+1
GO TO 1

```

135

```

79 I1=I+1
I2=I+2
JF=JF+1
JG=JG+1
JG5=JG5+1
JF5=JF5+1
JFS=JFS+1
JFSA=JFSA+1
JGSA=JGSA+1
JG5A=JG5A+1
GO TO 1

```

140

```

80 I1=I+1
I2=I+2
JF=JF+1
JG=JG+1
JG5=JG5+1
JF5=JF5+1
JFS=JFS+1
JFSA=JFSA+1
JGSA=JGSA+1
JG5A=JG5A+1
GO TO 1

```

145

150

155

106

POOR ORIGINAL

BLOCK	ADDRESS	LENGTH	FILE	DATE	PROCESSOR	VER	LEVEL	MAP IMAGE	COMMENTS
SKELETON	29373	51	SYSDI0	01/10/78	FTM	4.6	433	4464	OPT-2
CHLDR	29364	101	SYSDI0	01/10/78	FTM	4.6	433	4464	OPT-2
MARCO	29355	110	SYSDI0	01/10/78	FTM	4.6	433	4464	OPT-2
MEOSU	29346	110	SYSDI0	01/10/78	FTM	4.6	433	4464	OPT-2
7500	29337	105	SYSDI0	01/10/78	FTM	4.6	433	4464	OPT-2
APPELL	29328	105	SYSDI0	01/10/78	FTM	4.6	433	4464	OPT-2
AXIS	29319	105	SYSDI0	01/10/78	FTM	4.6	433	4464	OPT-2
LINPLM	29310	105	SYSDI0	01/10/78	FTM	4.6	433	4464	OPT-2
MELT	29301	105	SYSDI0	01/10/78	FTM	4.6	433	4464	OPT-2
MUSG	29292	105	SYSDI0	01/10/78	FTM	4.6	433	4464	OPT-2
PLTSG	29283	105	SYSDI0	01/10/78	FTM	4.6	433	4464	OPT-2
PLT37	29274	105	SYSDI0	01/10/78	FTM	4.6	433	4464	OPT-2
SYMBOL	29265	105	SYSDI0	01/10/78	FTM	4.6	433	4464	OPT-2
CPRESS	29256	105	SYSDI0	01/10/78	FTM	4.6	433	4464	OPT-2
CPUSYS	29247	105	SYSDI0	01/10/78	FTM	4.6	433	4464	OPT-2
ENCODE	29238	105	SYSDI0	01/10/78	FTM	4.6	433	4464	OPT-2
GOTERK	29229	105	SYSDI0	01/10/78	FTM	4.6	433	4464	OPT-2
RENKX	29220	105	SYSDI0	01/10/78	FTM	4.6	433	4464	OPT-2
RENKX	29211	105	SYSDI0	01/10/78	FTM	4.6	433	4464	OPT-2
SYSDI	29202	105	SYSDI0	01/10/78	FTM	4.6	433	4464	OPT-2
XTOM	29193	105	SYSDI0	01/10/78	FTM	4.6	433	4464	OPT-2
EXPMSG	29184	105	SYSDI0	01/10/78	FTM	4.6	433	4464	OPT-2
SYSDI	29175	105	SYSDI0	01/10/78	FTM	4.6	433	4464	OPT-2
FLM(1)	29166	105	SYSDI0	01/10/78	FTM	4.6	433	4464	OPT-2

.734 CP SECONDS 526000 CH STORAGE USED 7 TABLE MOVES

JG.M/S	JG	JGSS	JF.M/S	JFS	JFSS	C
0.000	0.000	0.000	.609	3.720	.993	.993
0.000	0.000	0.000	.127	.774	.456	.456
5.004	1.057	.533	.127	.774	.456	.456
6.348	1.456	.627	.051	.554	.385	1.213
9.760	2.061	.744	.052	.310	.231	1.015
16.711	3.534	.974	0.003	0.000	0.000	.974
0.000	0.000	0.000	.109	1.161	.558	.958
7.775	1.642	.664	.093	.319	.373	1.037
5.095	1.074	.537	.141	.876	.495	1.822
6.445	1.372	.607	.127	.744	.467	1.054
5.655	1.194	.566	.109	.317	.494	1.362
11.372	2.402	.803	.074	.145	.198	1.001
0.000	0.000	0.000	.364	2.233	.774	.774
1.270	.631	.431	.215	1.314	.532	1.022
4.341	.927	.499	.192	1.114	.547	1.048
5.004	1.017	.533	.103	.473	.211	1.044
5.445	1.243	.674	.112	.463	.212	1.049

15 hole

POOR ORIGINAL

POOR ORIGINAL

OPT-2 SEND MONEY MESSAGE
 9672/272 PROCEEDS SYSTEM GROUP ST.
 FORMATED. MOVE INTO CORP
 COMPUTED GO TO LEADERS
 ISSUE MESSAGE TO THE OFFICER
 PIGNOMEATIC LINE OF COSTS OF M. OPT-ALL.
 USED CALLABLE ERROR PROCEDURE
 DEAL TO INTERCEPT IDENTIFICATION.
 COMMON ERROR MESSAGE FOR IDENTIFICATION.
 AUXILIARY MATH LIBRARY LINK FOR ERRORS.

601

0.000	0.000	0.000	.183	1.154	.557	.557
1.184	.250	.259	.183	1.154	.557	.116
2.248	.475	.357	.183	1.154	.557	.314
3.325	.808	.466	.170	1.039	.529	.334
4.325	.914	.495	.159	.972	.511	1.005
5.538	.781	.458	.174	1.061	.514	.332
6.015	.848	.477	.159	1.032	.526	1.004
6.421	.934	.501	.158	.964	.509	1.010
5.326	1.125	.550	.141	.861	.481	1.030
6.304	1.331	.598	.136	.833	.473	1.071
7.202	1.608	.665	.128	.553	.420	1.085
8.469	1.789	.693	.080	.490	.363	1.056
9.264	1.944	.722	.064	.392	.324	1.047
10.024	2.117	.754	.051	.324	.293	1.049
10.384	2.193	.767	.045	.295	.267	1.049
11.162	2.358	.796	.033	.232	.250	1.045
12.899	2.724	.855	.023	.133	.193	1.048
17.633	3.724	1.000	0.000	0.000	0.000	1.000
JG, M/S	JGS	JGSS	JF, M/S	JFS	JFSS	C
9 hole						
2.919	.621	.468	.103	.662	.475	.335
3.451	.729	.490	.103	.614	.457	.956
11.751	2.432	.919	0.000	0.000	0.000	.919
4.011	.847	.537	.084	.515	.413	.356
0.000	0.000	0.000	.551	3.370	1.071	1.071
1.743	.368	.354	.207	1.263	.636	1.010
1.3-7	.284	.311	.227	1.386	.847	.398
2.440	.515	.419	.137	.818	.534	.723
2.205	.466	.338	.147	.838	.533	.951
6.371	1.348	.677	.045	.272	.192	.383
10.382	2.193	.864	.016	.023	.184	1.018
8.353	1.764	.775	.017	.102	.187	.367
3.090	0.000	0.000	.314	2.111	.671	.311

POOR ORIGINAL

POOR ORIGINAL

	JG	JG,M/S	JG5	JG55	JF,M/S	JF5	JF55	C
1.610	.340	.340	.340	.340	.216	1.333	.474	1.014
2.634	.569	.440	.440	.440	.132	.811	.575	.863
2.145	.453	.333	.333	.333	.179	.946	.568	.360
1.004	.635	.465	.465	.465	.106	.651	.471	.456
3.611	.753	.510	.510	.510	.093	.571	.461	.351
4.559	.963	.573	.573	.573	.071	.433	.385	.357
6.177	1.305	.667	.667	.667	.035	.214	.270	.937
6.734	1.422	.696	.696	.696	.030	.161	.243	.944
10.535	2.225	.871	.871	.871	0.000	0.000	0.000	.671
5 hole								
0.000	0.000	0.000	0.000	0.000	.734	4.469	1.316	1.316
3.007	.635	.495	.495	.495	.151	.925	.597	1.032
2.312	.488	.434	.434	.434	.191	1.170	.672	1.195
2.892	.611	.485	.485	.485	.155	.951	.605	1.091
3.765	.799	.555	.555	.555	.115	.706	.522	1.077
8.688	1.835	.841	.841	.841	0.000	0.000	0.000	.841
0.000	0.000	0.000	0.000	0.000	1.206	7.375	1.645	1.686
5.170	1.032	.649	.649	.649	.074	.453	.418	1.067
2.920	.617	.488	.488	.488	.158	.965	.610	1.097
2.287	.483	.432	.432	.432	.191	1.170	.672	1.103
6.444	1.361	.724	.724	.724	.033	.216	.249	1.013
8.943	1.899	.856	.856	.856	0.000	0.000	0.000	.856
3.000	0.000	0.000	0.000	0.000	.572	3.502	1.162	1.162
2.312	.488	.434	.434	.434	.196	1.193	.688	1.114
2.934	.613	.486	.486	.486	.151	.925	.597	1.084
3.878	.815	.562	.562	.562	.092	.561	.455	1.027
4.754	1.004	.622	.622	.622	.073	.361	.374	.386
12.063	2.548	.991	.991	.991	0.000	0.000	0.000	.991
3.000	3.300	0.000	0.000	0.000	.232	1.417	.733	.734
.347	.062	.177	.177	.177	.232	1.417	.733	.816
1.021	.216	.288	.288	.288	.282	1.417	.733	1.027
1.074	.225	.244	.244	.244	.294	1.334	.733	1.034
1.253	.334	.354	.354	.354	.233	1.273	.733	1.115

4.105	.909	.592	.101	.620	.483	1.081
3.738	.802	.556	.121	.739	.534	1.030
2.310	.503	.440	.161	.983	.615	1.026
3.225	.681	.512	.134	.813	.561	1.074

JG, H/S	JGS	JGSS	JF, H/S	JFS	JFSS	C
5A hole						
0.000	0.000	0.000	.333	2.071	.894	.894
.567	.120	.215	.301	1.841	.842	1.057
.721	.152	.242	.231	1.783	.823	1.071
1.073	.227	.296	.213	1.302	.704	1.004
1.343	.284	.331	.167	1.020	.627	.958
1.702	.359	.372	.125	.763	.542	.915
1.945	.411	.398	.117	.718	.526	.924
2.246	.474	.428	.101	.616	.487	.915
2.588	.547	.459	.084	.513	.445	.904
2.962	.626	.491	.073	.449	.415	.907
4.076	.861	.576	.041	.250	.311	.887
.565	.119	.214	.265	1.623	.791	1.005
.716	.156	.245	.239	1.462	.751	.995
1.304	.275	.326	.169	1.033	.631	.957
1.936	.409	.397	.100	.609	.485	.882
1.325	.240	.328	.164	1.000	.621	.943
1.711	.361	.373	.128	.782	.543	.922
2.213	.467	.425	.102	.622	.493	.914
2.500	.528	.451	.082	.500	.433	.890
1.463	.309	.345	.140	.804	.576	.921
.946	.200	.278	.201	1.231	.683	.956

JG, H/S	JGS	JGSS	JF, H/S	JFS	JFSS	C
3 hole						
0.000	0.000	0.000	1.122	6.802	1.671	1.671
.732	.135	.251	.271	1.659	.822	1.073
.391	.083	.183	.257	1.571	.803	.933
1.317	.278	.337	.221	1.403	.703	1.032
1.317	.409	.404	.147	.311	.273	1.012

POOR ORIGINAL COPY

POOR ORIGINAL

JG, M/S	JG5	JG55	JF, M/S	JFS	JF55	C
7.112	1.312	.658	.672	.440	.353	1.313
7.906	1.670	.691	.063	.386	.332	1.073
9.863	1.873	.732	.951	.323	.304	1.034
14.547	3.063	.939	0.000	0.000	0.000	.359
JG, M/S	JG5	JG55	JF, M/S	JFS	JF55	C
2 hok						
0.000	0.000	0.000	.212	1.293	.843	.840
.353	.074	.201	.212	1.293	.840	1.042
.595	.126	.261	.202	1.238	.523	1.042
.921	.135	.325	.148	.903	.701	1.026
1.251	.264	.379	.112	.686	.611	.990
1.005	.229	.353	.163	.996	.735	1.009
1.705	.360	.443	.111	.682	.603	1.051
2.311	.488	.515	.064	.394	.453	.376
2.965	.626	.584	.047	.265	.394	.378
3.592	.759	.642	.034	.229	.351	.395
4.873	1.029	.748	.025	.156	.291	1.039
0.000	0.000	0.000	.260	1.593	.931	.311
.205	.043	.153	.250	1.528	.512	1.005
.306	.065	.187	.243	1.465	.893	1.086
.460	.037	.230	.213	1.340	.654	1.083
.757	.160	.295	.162	.991	.734	1.029
1.069	.276	.350	.122	.743	.533	.583
1.504	.318	.416	.090	.548	.346	.451
1.714	.256	.373	.177	1.062	.707	1.140
2.149	.454	.457	.064	.390	.460	.357
2.629	.555	.549	.053	.364	.443	.934
3.730	.788	.654	.030	.184	.315	.971
0.000	0.000	0.000	.168	1.026	.747	.747
.039	.203	.332	.150	.920	.707	1.039
1.221	.258	.376	.119	.843	.673	1.934
1.726	.355	.445	.094	.576	.561	1.006
3.000	.650	.543	.035	.277	.334	.333
.148	.471	.640	.079	.17	.104	.113

POOR ORIGINAL

	J6	J65	J655	JF,M/S	JFS	JF55	0.000	1.000
15 hole								
h _{in} = 445 mm								
	J6,M/S	J65	J655	JF,M/S	JFS	JF55	0.000	1.000
	0.000	0.000	0.000	.127	.777	.557	.557	.557
	2.362	.699	.366	.127	.777	.537	.537	.823
	8.609	1.776	.691	.076	.564	.353	.353	1.043
	0.854	1.546	.623	.110	.671	.625	.625	1.047
	9.128	1.928	.719	.058	.357	.310	.310	1.029
	9.937	2.099	.751	.048	.293	.240	.240	1.031
	11.656	2.562	.813	.020	.122	.181	.181	.954
	3.235	.603	.528	.181	1.105	.545	.545	.973
	3.554	.751	.549	.168	1.030	.526	.526	.975
	4.977	1.051	.531	.153	.877	.585	.585	1.015
	6.066	1.281	.586	.125	.763	.553	.553	1.039
	6.712	1.518	.617	.101	.618	.407	.407	1.024
	0.000	0.000	0.000	.283	1.734	.687	.687	.682
	1.626	.343	.304	.233	1.426	.619	.619	.922
	1.882	.397	.327	.210	1.336	.599	.599	.926
	2.437	.515	.372	.205	1.257	.581	.581	.953
	4.055	.856	.479	.152	.930	.500	.500	.979
	5.464	1.154	.557	.127	.774	.456	.456	1.012
	6.666	1.512	.616	.113	.693	.431	.431	1.047
	8.412	1.777	.691	.065	.395	.326	.326	1.016
	9.506	2.008	.734	.050	.306	.286	.286	1.021
	11.519	2.516	.805	.022	.189	.189	.189	.994
	J6,M/S	J65	J655	JF,M/S	JFS	JF55		

Appendix II. Computer Program List and the Steam/Water
Reduced Data.

The input of this program includes:

VTS steam venturi temperature reading(mV).
 VPS steam venturi pressure reading(V).
 VWS steam venturi pressure drop reading(V).
 VTG steam temperature at the channel inlet(mV).
 VPG steam pressure at the channel inlet(V).
 WL reading of water rotameter 1(lbs/min).
 VTL water inlet temperature reading(mV).
 IP perforated plate no. defined in Appendix I.
 RUN run no. in the form of XXXX.ZZ, where XXXX shows the
 test run no., and ZZ is the height of water inlet
 spray in inches.
 VTLO water overflow temperature(mV).
 VTP temperature reading 2 mm above the plate(mV).
 WLL reading of water rotameter 2(lbs/sec.).

The output of the program includes:

RUN run no.
 PER perforation ratio.
 WS, WL steam and water mass flow rate(kg/s).
 VGH j_g (m/s).
 VLH j_f (m/s).
 EHG $W_s h_{fg}$ (KW).
 EHL $W_f C_p (T_{sat} - T_{f,in})$ (KW).
 EHLO $W_f C_p (T_{out} - T_{f,in})$ (KW).
 REH EHL/EHG
 JGS H_g^*/C^2
 JLS H_f^*/C^2
 TSC, TLC, TLOC, TLPC temperature of steam inlet, water inlet
 water outlet, and two-phase mixture at 2
 mm above the plate ($^{\circ}C$).

807.24	.254	.27E-01	.54E+00	63.85	.72	88.26	192.09	74.06	2.81	1.77	142.5	141.6	14.8	97.0	98.4
808.24	.254	.27E-01	.62E+00	64.89	.82	69.93	219.02	71.76	3.13	1.79	1.31	141.6	14.8	92.7	98.7
27.00	.141	.46E-02	.21E-01	19.72	.05	10.74	8.15	7.98	.76	1.05	.35	141.6	9.1	98.7	98.9
28.00	.141	.58E-02	.35E-01	24.98	.09	13.72	13.50	12.48	.98	1.18	.43	141.6	8.8	93.1	98.7
29.00	.141	.79E-02	.51E-01	34.19	.12	18.67	19.49	18.66	1.04	1.38	.54	141.6	8.1	96.3	97.7
30.00	.141	.12E-01	.82E-01	52.49	.20	28.79	31.62	29.52	1.19	1.73	.78	141.6	7.4	93.8	96.3
31.00	.141	.16E-01	.11E+00	78.77	.26	38.78	42.65	39.96	1.09	1.99	.79	141.6	7.4	94.6	98.7
32.00	.141	.21E-01	.14E+00	89.06	.33	48.88	54.21	49.55	1.09	2.23	.88	141.6	7.1	93.6	97.5
33.00	.141	.27E-01	.19E+00	117.01	.46	64.17	74.69	63.99	1.15	2.55	1.04	141.6	6.9	94.1	98.2
34.00	.141	.24E-01	.16E+00	104.75	.40	57.61	64.02	58.80	1.11	2.42	.97	141.6	6.9	92.4	98.2
59.00	.141	.59E-02	.35E-01	25.53	.09	13.91	13.32	12.94	.96	1.19	.45	141.6	10.1	97.5	96.3
60.00	.141	.96E-02	.66E-01	41.46	.16	22.77	25.12	23.28	1.10	1.52	.61	141.6	9.3	93.4	92.8
61.00	.141	.15E-01	.96E-01	62.93	.23	34.20	36.55	34.66	1.07	1.87	.74	141.6	8.8	95.3	97.9
62.00	.141	.19E-01	.12E+00	81.98	.30	44.66	47.54	44.97	1.06	2.13	.84	141.6	8.6	95.0	98.1
63.00	.141	.23E-01	.15E+00	97.90	.37	53.73	58.64	54.54	1.03	2.34	.93	141.6	8.6	93.6	93.7
64.00	.141	.27E-01	.20E+00	115.80	.48	64.18	76.02	66.12	1.18	2.54	1.06	141.6	8.4	88.1	84.0
830.00	.141	.36E-02	.21E-01	15.30	.05	8.32	7.55	7.47	.91	.92	.35	141.6	15.8	99.1	98.9
831.00	.141	.67E-02	.51E-01	28.84	.12	15.83	17.84	16.48	1.13	1.27	.64	141.6	15.5	93.4	98.2
832.00	.141	.11E-01	.83E-01	46.06	.20	25.32	29.26	26.79	1.16	1.60	.69	141.6	15.5	92.9	98.7
833.00	.141	.15E-01	.11E+00	63.09	.27	34.76	39.22	35.25	1.33	1.88	.79	141.6	15.3	91.4	98.9
834.00	.141	.17E-01	.14E+00	73.57	.33	40.69	48.68	42.53	1.20	2.03	.88	141.6	15.0	89.3	98.2
835.00	.141	.21E-01	.16E+00	83.99	.40	49.79	58.42	50.97	1.12	2.24	.97	141.6	13.0	89.0	98.7

POOR ORIGINAL

POOR ORIGINAL

836.00	.141	.242-01	.194+00	105.01	.47	58.25	69.13	59.02	1.19	2.42	1.05	141.6	15.0	87.4	98.2
837.00	.141	.262-01	.222+00	113.07	.53	62.90	77.03	64.95	1.24	2.51	1.12	141.6	15.0	85.3	98.4
838.00	.141	.272-01	.252+00	116.24	.59	65.84	87.86	72.03	1.31	2.57	1.18	141.6	14.8	85.4	98.4
839.00	.141	.282-01	.252+00	121.02	.59	67.38	87.86	72.03	1.30	2.58	1.18	141.6	14.8	85.4	98.4
840.00	.141	.332-01	.272+00	141.18	.65	78.36	97.64	81.13	1.25	2.41	1.25	141.6	14.8	87.3	98.2
841.00	.141	.342-01	.322+00	162.48	.77	80.35	116.43	95.81	1.27	3.01	1.35	141.6	14.8	86.1	98.2
842.00	.141	.412-01	.362+00	178.10	.85	99.29	126.57	103.82	1.27	3.15	1.42	141.6	14.8	84.7	97.7
843.00	.141	.482-01	.402+00	205.14	.95	114.31	142.44	117.28	1.25	3.18	1.51	141.6	14.8	84.9	96.3
844.00	.141	.512-01	.432+00	218.05	1.04	122.87	153.54	121.61	1.26	3.49	1.55	141.6	14.8	82.3	96.0
845.00	.141	.302-01	.432+00	185.63	1.04	96.78	153.54	98.59	1.52	3.04	1.56	141.6	14.8	69.5	93.4
846.00	.141	.172-01	.432+00	71.45	1.04	62.88	153.54	55.74	3.58	2.00	1.56	141.6	14.8	48.7	49.4
847.00	.141	.192-01	.392+00	80.00	.93	47.71	138.10	48.45	2.89	2.11	1.43	141.6	14.8	46.7	46.1
848.00	.141	.342-01	.392+00	145.08	.97	83.15	138.10	87.11	1.65	2.84	1.48	141.6	14.8	68.5	88.8
849.00	.141	.262-01	.352+00	113.06	.84	65.27	124.18	71.65	1.00	2.51	1.41	141.6	14.8	64.0	82.5
850.00	.141	.212-01	.352+00	88.96	.85	72.45	124.18	53.39	2.37	2.23	1.41	141.6	14.8	51.4	66.1
851.04	.141	.392-02	.212-01	12.72	.85	6.91	7.57	7.43	1.10	.84	.85	141.6	15.5	99.3	98.7
852.04	.141	.762-02	.512-01	32.65	.12	18.07	17.88	15.31	.93	1.15	.54	141.6	15.5	95.7	97.5
853.04	.141	.102-01	.622-01	44.00	.20	24.25	28.92	25.52	1.19	1.87	.61	141.6	15.3	91.2	98.4
854.04	.141	.132-01	.112+00	54.38	.27	30.29	39.31	32.47	1.30	1.74	.79	141.6	15.0	85.2	97.2
855.04	.141	.172-01	.142+00	71.47	.33	39.71	48.68	42.67	1.23	2.00	.88	141.6	15.0	89.5	98.4
856.00	.141	.192-01	.162+00	80.78	.40	45.24	58.42	46.05	1.23	2.12	.97	141.6	15.0	82.0	98.4
857.04	.141	.202-01	.192+00	88.17	.47	49.53	69.13	53.16	1.40	2.22	1.12	141.6	15.0	80.3	98.4

POOR ORIGINAL

858.04	.141	.24E-01	.22E+00	101.58	.53	58.16	77.83	60.09	1.15	2.40	1.12	141.5	15.0	80.6	68.4
859.04	.141	.26E-01	.25E+00	111.37	.59	63.26	87.62	60.65	1.33	2.40	1.14	141.6	15.0	71.8	86.9
860.04	.141	.28E-01	.28E+00	121.20	.67	68.14	99.31	75.77	1.66	2.60	1.26	141.5	15.0	79.9	98.9
861.04	.141	.30E-01	.28E+00	127.94	.67	71.93	99.31	75.77	1.18	2.67	1.26	141.6	15.0	79.9	98.9
862.04	.141	.32E-01	.31E+00	138.05	.75	78.09	110.81	79.83	1.67	2.77	1.33	141.5	15.0	76.2	89.3
863.04	.141	.34E-01	.35E+00	144.86	.84	82.11	124.26	87.76	1.51	2.86	1.41	141.6	15.0	75.8	95.8
864.04	.141	.39E-01	.39E+00	169.17	.93	95.62	137.78	99.90	1.64	3.07	1.48	141.6	15.0	76.7	98.2
865.04	.141	.42E-01	.44E+00	174.72	1.05	101.72	155.50	105.56	1.53	3.16	1.57	141.6	16.8	72.6	89.0
1130.12	.141	.88E-02	.11E+00	37.91	.26	21.95	35.97	19.35	1.64	1.55	.78	141.5	19.0	62.5	89.1
1131.12	.141	.12E-01	.16E+00	51.12	.40	23.57	56.21	30.75	1.30	1.69	.97	141.6	18.2	61.0	97.9
1132.12	.141	.17E-01	.22E+00	71.80	.53	42.61	75.60	42.58	1.77	2.03	1.12	141.6	17.7	66.2	78.5
1133.12	.141	.21E-01	.28E+00	95.82	.67	52.76	96.13	51.67	1.82	2.25	1.26	140.4	17.7	61.8	95.1
1134.12	.141	.54E-02	.31E-01	23.65	.12	13.30	17.61	12.08	1.31	1.14	.54	141.6	17.7	76.8	97.0
1135.12	.141	.11E-01	.16E+00	46.91	.33	27.27	46.38	25.69	1.72	1.67	.88	133.3	18.0	61.8	91.7
1136.12	.141	.15E-01	.19E+00	59.32	.46	34.21	65.77	38.62	1.92	1.82	1.00	141.2	18.0	65.4	87.1
1137.12	.141	.24E-01	.34E+00	102.98	.82	59.84	116.51	60.33	1.35	2.46	1.33	141.6	17.7	60.1	81.1
1138.12	.141	.29E-01	.43E+00	104.85	1.04	62.12	148.58	55.79	2.39	2.42	1.57	141.5	17.7	68.6	95.8
1139.12	.141	.24E-01	.51E+00	104.85	1.23	61.01	174.12	67.68	2.75	2.42	1.71	141.6	17.7	60.7	86.6
1140.12	.141	.25E-01	.59E+00	108.03	1.41	64.11	201.21	71.13	3.16	2.45	1.82	141.5	17.7	67.6	75.8
1141.12	.141	.27E-01	.66E+00	114.23	1.58	69.22	228.26	68.11	3.27	2.52	1.91	141.6	17.5	55.0	74.6
35.12	.141	.63E-02	.23E-01	18.36	.05	10.09	6.83	8.16	.67	1.01	.16	141.5	5.1	92.6	33.8
36.12	.141	.53E-02	.15E-01	27.74	.09	12.67	11.54	11.41	1.17	1.13	.16	141.6	8.6	84.1	94.1

37.12	.141	.66E-02	.51E-01	28.43	.12	16.09	19.07	19.97	1.79	1.76	.58 141.6	8.1	77.8	86.3
38.12	.141	.82E-02	.82E-01	35.35	.20	20.19	31.28	19.23	1.53	1.40	.64 141.6	8.4	64.7	88.1
39.12	.141	.12E-01	.11E+00	50.79	.26	29.31	42.00	23.70	1.43	1.68	.79 141.6	8.4	64.6	91.0
40.12	.141	.18E-01	.16E+00	79.54	.40	47.59	63.03	23.61	1.32	2.11	.37 141.6	8.4	47.7	72.6
41.12	.141	.20E-01	.19E+00	87.44	.46	52.31	73.50	27.53	1.41	2.21	1.04 141.6	8.4	42.7	72.4
42.12	.141	.23E-01	.22E+00	98.76	.53	59.09	84.00	31.48	1.42	2.35	1.12 141.6	8.4	42.7	72.4
43.12	.141	.25E-01	.25E+00	105.86	.59	63.33	94.50	35.42	1.49	2.43	1.18 141.6	8.4	42.7	72.4
44.12	.141	.27E-01	.27E+00	114.11	.66	68.27	105.00	39.35	1.54	2.52	1.25 141.6	8.4	42.7	72.4
65.12	.141	.53E-02	.35E-01	22.86	.09	12.76	13.28	10.91	1.04	1.13	.45 141.6	10.3	86.0	95.0
66.12	.141	.76E-02	.67E-01	32.74	.16	18.55	25.36	18.44	1.17	1.35	.62 141.6	9.3	75.3	86.7
67.12	.141	.11E-01	.96E-01	45.48	.23	25.85	36.55	25.87	1.41	1.59	.74 141.6	8.8	73.4	95.0
68.12	.141	.14E-01	.12E+00	58.18	.30	32.90	47.12	35.00	1.43	1.80	.84 141.6	8.6	76.5	86.0
69.12	.141	.18E-01	.16E+00	79.05	.40	44.70	62.83	46.67	1.41	2.10	.97 141.6	8.6	76.5	96.0
70.12	.141	.23E-01	.22E+00	98.29	.54	56.31	85.05	56.07	1.51	2.34	1.12 141.6	8.4	68.8	65.2
90.00	.141	.44E-02	.21E-01	19.07	.05	10.37	7.62	7.50	.73	1.03	.35 141.6	15.0	98.7	97.7
91.00	.141	.69E-02	.51E-01	29.73	.12	16.31	18.61	17.16	1.14	1.29	.54 141.6	12.1	93.1	91.0
92.00	.141	.12E-01	.82E-01	50.66	.20	27.76	36.58	28.71	1.10	1.68	.58 141.6	11.1	94.6	89.0
93.00	.141	.15E-01	.11E+00	66.64	.27	36.63	41.39	37.87	1.13	1.93	.76 141.6	10.6	92.4	92.9
94.00	.141	.21E-01	.14E+00	88.79	.33	48.65	51.23	46.12	1.05	2.23	.88 141.6	10.6	94.6	91.9
95.00	.141	.24E-01	.16E+00	103.33	.40	56.81	61.47	56.41	1.08	2.40	.97 141.6	10.6	92.6	92.9
96.00	.141	.26E-01	.19E+00	112.33	.46	62.40	71.92	61.57	1.15	2.50	1.04 141.6	10.3	87.1	62.2
97.12	.141	.44E-02	.21E-01	19.08	.05	10.4	7.75	7.61	.75	1.13	.35 141.6	13.5	98.7	97.9

POOD ORIGINAL

POOR ORIGINAL

JAN 1971

98.12	.141	.58E-02	.51E-01	24.97	.12	14.01	18.56	14.55	1.32	1.18	.56	141.6	12.1	81.1	55.6
99.12	.141	.83E-02	.82E-01	35.68	.20	20.33	30.36	20.77	1.53	1.41	.68	141.6	11.1	71.9	98.7
100.12	.141	.11E-01	.11E+00	45.60	.26	26.20	40.87	25.73	1.56	1.53	.75	141.6	10.8	67.1	99.6
101.12	.141	.14E-01	.14E+00	58.12	.33	33.27	51.04	31.47	1.54	1.80	.88	141.6	10.8	60.1	98.2
102.12	.141	.16E-01	.16E+00	69.57	.40	39.68	61.33	41.66	1.55	1.37	.97	141.6	10.8	71.4	97.9
103.12	.141	.18E-01	.18E+00	76.31	.46	44.96	72.12	46.11	1.58	2.09	1.04	141.6	10.1	67.6	98.9
104.12	.141	.21E-01	.22E+00	89.95	.53	52.00	82.19	48.71	1.58	2.24	1.12	141.6	10.3	63.5	98.7
105.12	.141	.24E-01	.25E+00	101.73	.59	58.14	92.47	61.76	1.59	2.38	1.14	141.6	10.3	70.2	98.6
106.12	.141	.25E-01	.27E+00	105.59	.66	60.35	102.74	68.62	1.70	2.43	1.25	141.6	10.3	70.2	98.6
119.00	.085	.38E-02	.31E-01	27.15	.09	8.95	7.62	7.17	.85	1.25	.46	141.6	15.0	35.0	93.4
120.00	.085	.74E-02	.51E-01	52.91	.20	17.53	18.51	17.00	1.06	1.77	.71	141.6	12.6	92.9	82.5
121.00	.085	.11E-01	.82E-01	81.91	.33	27.16	30.44	27.85	1.12	2.20	.90	141.6	10.8	32.4	92.6
122.00	.085	.16E-01	.11E+00	114.42	.44	37.79	41.78	39.22	1.10	2.60	1.05	141.6	9.8	34.6	83.2
123.00	.085	.20E-01	.14E+00	145.05	.55	48.07	51.94	47.72	1.08	2.92	1.17	141.6	9.3	32.6	86.1
124.00	.085	.23E-01	.17E+00	165.63	.68	55.13	63.87	56.93	1.16	3.12	1.30	141.6	10.1	90.2	90.5
125.00	.085	.23E-01	.19E+00	165.30	.78	55.04	73.15	65.00	1.33	3.12	1.39	141.6	10.1	30.0	77.
126.00	.085	.27E-01	.19E+00	193.02	.78	64.27	73.15	65.00	1.14	3.37	1.39	141.6	10.1	90.0	77.2
127.00	.085	.22E-01	.22E+00	159.98	.88	54.63	83.32	60.23	1.52	3.02	1.48	141.6	9.1	74.8	73.6
128.00	.085	.27E-01	.22E+00	195.94	.88	66.98	83.32	60.23	1.24	3.40	1.48	141.6	9.1	74.8	73.6
129.00	.085	.16E-01	.25E+00	113.78	.99	40.54	93.23	41.73	2.30	2.59	1.52	141.6	9.2	50.1	26.4
130.00	.085	.11E-01	.28E+00	81.40	1.12	29.66	105.66	31.19	1.56	2.15	1.57	141.6	9.6	36.3	24.4
163.00	.085	.40E-02	.24E-01	24.26	.10	9.41	8.64	7.65	.92	1.25	.40	141.6	13.8	89.7	91.9

120

POOR ORIGINAL

104.00	.007	.11E-04	.44E-01	20.34	.410	10.00	1E+02	1E+03	.471	1.11E	1.11E-01	1E+01	1E+02	1E+03	1E+04	1E+05
165.00	.085	.90E-02	.63E-01	63.92	.25	21.12	22.94	21.50	1.03	1.94	.73	161.6	17.1	36.1	78.6	
166.00	.085	.14E-01	.96E-01	97.10	.38	37.11	35.66	33.19	1.11	2.39	.08	141.6	11.1	91.8	52.9	
167.00	.085	.19E-01	.13E+00	134.61	.50	44.52	47.00	41.76	1.06	2.87	1.17	141.6	10.8	11.8	86.7	
168.00	.085	.20E-01	.15E+00	142.36	.58	47.56	53.95	46.30	1.13	2.90	1.20	141.6	11.8	88.1	81.7	
169.00	.085	.22E-01	.15E+00	154.55	.60	51.35	55.91	50.91	1.09	3.02	1.23	141.6	11.6	91.2	74.8	
170.00	.085	.24E-01	.17E+00	170.88	.69	57.07	63.81	55.39	1.12	3.17	1.31	141.6	11.6	88.3	74.6	
171.00	.085	.26E-01	.21E+00	181.60	.85	62.22	70.25	61.26	1.27	3.29	1.46	141.6	11.3	79.3	75.1	
172.00	.085	.13E-01	.24E+00	89.91	.96	32.56	89.41	79.15	2.75	2.30	1.55	141.6	11.3	60.2	23.2	
173.00	.085	.13E-01	.25E+00	89.91	1.01	32.56	91.48	80.47	2.87	2.30	1.53	141.6	11.3	60.2	23.2	
174.00	.085	.13E-01	.26E+00	89.91	1.05	32.56	97.54	81.80	3.00	2.30	1.52	141.6	11.3	60.2	23.2	
175.00	.085	.13E-01	.27E+00	89.91	1.07	32.56	99.57	82.46	3.06	2.30	1.56	141.6	11.3	60.2	23.2	
176.00	.085	.13E-01	.22E+00	89.91	.88	32.56	81.29	26.50	2.59	2.30	1.48	141.6	11.3	60.2	23.2	
1115.12	.085	.93E-02	.11E+00	66.14	.45	22.76	38.14	26.53	1.68	1.97	1.06	141.6	18.7	70.9	92.2	
1116.12	.085	.11E-01	.17E+00	76.21	.67	26.53	56.96	32.01	2.15	2.12	1.29	141.6	18.2	66.2	90.0	
1117.12	.085	.16E-01	.22E+00	116.10	.88	40.63	75.17	46.36	1.85	2.52	1.48	141.6	18.0	62.0	91.1	
1118.12	.085	.19E-01	.27E+00	135.16	1.10	47.83	91.96	43.55	1.96	2.82	1.65	135.9	18.0	56.0	81.3	
1119.12	.085	.93E-02	.13E+00	66.51	.54	23.37	46.04	23.17	1.97	1.98	1.16	140.7	18.0	53.6	80.2	
1120.12	.085	.15E-01	.19E+00	106.77	.77	37.10	65.77	37.83	1.77	2.51	1.38	141.6	18.0	55.2	88.1	
1121.12	.085	.54E-02	.51E-01	38.86	.20	13.24	17.35	12.43	1.31	1.61	.71	141.5	18.0	75.7	92.3	
1122.12	.085	.17E-01	.36E+00	124.74	1.36	54.40	118.40	47.43	2.67	2.71	1.45	141.6	17.7	50.7	87.1	
1123.12	.085	.19E-01	.43E+00	141.31	1.72	48.02	148.20	60.80	2.83	2.80	1.67	141.2	17.7	43.3	80.2	

1124.12	.085	.19E-01	.52E+00	133.44	2.08	47.80	178.72	61.35	3.74	2.40	2.27	141.6	17.7	46.9	13.1
1125.12	.085	.19E-01	.58E+00	137.33	2.31	49.87	198.31	50.06	3.39	2.84	2.40	141.6	17.7	38.5	82.0
1126.12	.085	.19E-01	.47E+00	133.39	1.87	48.20	161.68	46.97	3.15	2.80	2.16	141.6	17.7	41.5	79.6
1127.12	.085	.18E-01	.39E+00	129.89	1.56	44.95	156.64	44.78	3.00	2.71	1.97	141.6	17.5	44.4	85.6
1128.12	.085	.19E-01	.65E+00	136.22	2.59	49.96	223.07	53.44	4.50	2.81	2.54	141.6	17.5	37.1	84.4
131.12	.085	.29E-02	.21E-01	28.99	.09	6.33	7.79	7.54	1.11	1.11	.46	141.6	13.0	97.7	97.7
132.12	.085	.51E-02	.49E-01	36.37	.20	12.48	18.31	12.66	1.47	1.46	.70	141.6	11.3	72.6	94.1
133.12	.085	.85E-02	.83E-01	58.44	.33	20.88	31.24	21.14	1.56	1.89	.91	141.6	10.3	70.9	14.6
134.12	.085	.11E-01	.11E+00	76.61	.44	26.48	41.21	27.56	1.56	2.17	1.04	141.6	10.1	70.2	92.7
135.12	.085	.14E-01	.14E+00	94.43	.55	34.34	51.65	33.76	1.50	2.42	1.17	141.6	9.8	68.8	93.6
136.12	.085	.15E-01	.17E+00	109.98	.67	37.34	63.02	47.93	1.59	2.54	1.29	141.6	9.8	78.4	77.0
137.12	.085	.16E-01	.19E+00	118.96	.77	40.62	72.51	43.25	1.78	2.62	1.38	141.6	9.6	62.3	81.4
138.12	.085	.18E-01	.22E+00	130.19	.88	45.91	83.29	42.97	1.81	2.77	1.48	141.6	9.6	56.2	86.4
139.12	.085	.20E-01	.25E+00	140.15	.99	49.10	93.44	52.45	1.90	2.47	1.57	141.6	5.6	60.1	91.4
140.12	.085	.21E-01	.27E+00	146.71	1.10	51.48	103.53	58.15	2.02	2.94	1.65	141.6	9.6	29.3	53.6
141.12	.085	.24E-02	.14E-02	17.83	.01	5.75	1.28	1.84	.22	1.00	.18	141.6	11.1	84.4	94.7
177.24	.085	.38E-02	.21E-01	26.94	.09	9.01	7.57	6.46	.84	1.76	.46	141.6	15.5	87.6	96.5
178.24	.085	.38E-02	.34E-02	26.95	.01	8.84	1.13	1.17	.13	1.24	.18	141.6	15.8	95.3	59.8
179.24	.085	.55E-02	.51E-01	33.00	.20	13.48	18.44	12.46	1.18	1.52	.71	141.6	12.8	71.7	94.1
180.24	.085	.71E-02	.83E-01	51.85	.33	17.72	30.75	18.36	1.74	1.73	.31	141.6	11.8	65.9	95.0
181.24	.085	.96E-02	.11E+00	68.62	.44	23.66	40.53	26.65	1.71	2.01	1.34	141.6	11.6	69.7	55.0
182.24	.085	.13E-01	.14E+00	83.70	.55	31.11	50.68	31.21	1.53	2.38	1.17	141.6	11.3	65.4	96.2

183.24	.085	.16E-01	.16E+00	115.17	.66	39.71	61.11	40.17	1.34	2.50	1.28	141.6	11.1	74.2	95.9
184.24	.085	.18E-01	.19E+00	110.20	.77	44.91	71.32	51.11	1.60	2.77	1.38	141.6	11.1	74.8	95.9
185.24	.085	.19E-01	.22E+00	118.22	.88	47.94	81.96	51.11	1.71	2.85	1.45	141.6	10.6	66.4	97.0
186.24	.085	.21E-01	.24E+00	143.11	.98	51.78	91.44	58.12	1.77	2.97	1.56	141.6	10.1	67.1	87.1
187.24	.085	.23E-01	.27E+00	165.56	1.10	57.77	101.83	59.21	1.76	3.12	1.65	141.6	11.1	62.7	35.1
188.00	.085	.34E-02	.21E-01	24.12	.09	8.02	7.81	5.96	.97	1.19	.66	141.6	12.8	60.5	97.9
189.00	.085	.70E-02	.51E-01	49.64	.20	16.41	18.82	17.57	1.15	1.71	.71	141.6	11.1	94.1	84.7
190.00	.085	.11E-01	.82E-01	79.06	.33	26.17	29.64	27.42	1.13	2.16	.93	141.6	12.0	93.4	86.9
191.00	.085	.14E-01	.11E+00	103.28	.44	34.30	40.19	36.26	1.17	2.47	1.04	141.6	12.3	91.4	88.8
192.00	.085	.19E-01	.14E+00	132.89	.55	44.21	50.38	44.92	1.14	2.80	1.17	141.6	12.1	86.9	70.6
193.00	.085	.13E-01	.16E+00	95.87	.66	33.45	60.62	34.85	1.81	2.34	1.28	141.6	11.8	62.5	35.1
194.00	.085	.21E-01	.18E+00	153.17	.66	51.44	60.79	50.43	1.18	3.00	1.28	141.6	11.6	86.9	71.4
195.00	.085	.14E-01	.19E+00	102.23	.77	35.99	70.93	36.80	1.97	2.45	1.38	141.6	11.6	57.4	31.1
196.00	.085	.22E-01	.19E+00	158.51	.77	53.74	71.32	54.98	1.31	3.06	1.38	141.6	11.1	79.6	69.4
197.00	.085	.14E-01	.22E+00	103.43	.88	36.76	82.13	37.88	2.24	2.47	1.48	141.6	10.3	51.7	29.4
198.00	.085	.15E-01	.25E+00	103.63	.99	37.05	92.21	38.98	2.43	2.47	1.57	141.6	10.6	48.4	29.8
199.00	.085	.15E-01	.27E+00	103.65	1.10	37.92	103.02	27.18	2.72	2.47	1.65	141.6	10.1	33.8	29.1
200.12	.085	.21E-02	.34E-02	14.88	.01	5.07	1.25	.92	.25	.94	.18	141.6	11.3	76.2	99.4
201.12	.085	.32E-02	.21E-01	22.70	.09	7.70	7.73	5.94	1.01	1.16	.66	141.6	11.0	79.4	95.0
202.12	.085	.58E-02	.51E-01	41.19	.20	14.07	18.61	13.38	1.32	1.56	.71	141.6	12.1	75.1	87.1
203.12	.085	.84E-02	.83E-01	60.16	.33	20.74	30.71	20.32	1.44	1.88	.91	141.6	11.3	70.0	81.7
204.12	.085	.10E-01	.11E+00	71.82	.43	26.00	39.32	33.43	1.49	2.04	1.04	141.6	11.1	64.7	88.1

POOR ORIGINAL

205.12	.085	.12E-01	.13E+00	81.59	.56	29.27	69.93	28.06	1.71	2.77	1.16	161.6	11.3	51.1	75.6
206.12	.085	.13E-01	.14E+00	31.18	.66	32.64	60.96	35.70	1.87	2.36	1.28	161.6	11.3	50.3	81.7
207.12	.085	.14E-01	.15E+00	97.96	.77	36.50	71.72	37.60	2.08	2.60	1.38	161.6	10.6	57.2	81.3
208.12	.085	.15E-01	.16E+00	101.88	.88	39.72	81.51	64.72	2.28	2.85	1.48	161.6	11.1	59.3	86.6
209.12	.085	.15E-01	.17E+00	107.81	.99	38.38	91.70	40.86	2.39	2.52	1.57	161.6	11.1	50.7	80.1
210.12	.085	.15E-01	.17E+00	107.81	1.10	38.38	101.69	45.68	2.66	2.52	1.65	161.6	11.1	50.7	80.1
211.24	.085	.17E-02	.16E-02	19.20	.81	6.56	1.19	.84	.18	1.06	.18	161.6	15.0	75.0	98.4
212.24	.085	.13E-02	.21E-01	23.37	.89	7.31	7.62	5.55	.94	1.17	.46	161.6	17.2	79.1	93.4
213.24	.085	.12E-02	.16E-01	37.39	.20	12.78	17.43	12.36	1.37	1.68	.70	161.6	15.3	75.0	93.4
214.24	.085	.17E-02	.16E-01	55.63	.33	28.18	29.77	8.64	1.68	1.81	.91	161.6	15.0	39.0	50.1
215.24	.085	.18E-02	.11E+00	70.27	.43	26.47	39.25	23.03	1.60	2.03	1.06	161.6	12.0	66.0	37.2
216.24	.085	.12E-01	.14E+00	85.64	.55	29.81	50.52	29.16	1.79	2.24	1.17	161.6	11.8	72.7	96.3
217.24	.085	.13E-01	.16E+00	31.19	.66	32.86	60.62	30.87	1.85	2.36	1.28	161.6	11.8	56.7	87.9
218.24	.085	.15E-01	.19E+00	104.91	.77	37.00	71.32	36.23	1.93	2.69	1.38	161.6	11.1	66.3	87.9
219.24	.085	.16E-01	.22E+00	111.69	.88	39.46	81.86	60.06	2.05	2.56	1.48	161.6	11.6	55.3	87.5
220.24	.085	.16E-01	.25E+00	115.51	.99	41.16	91.65	68.11	2.22	2.61	1.57	161.6	11.1	50.3	85.0

Subroutine PHIS2

- a) General Description: To estimate the specific volume, enthalpy, and entropy of saturated and/or superheated steam.
- b) Computational Procedure : The equations and constants used in this subroutine are described in ASME Steam Tables, 3rd edition.

c) Usage

1) Calling Sequence : CALL PHIS2(T,P,ID,V,S,H)

2) Arguments	:	ID = 1 (SI Unit)	2 (English Unit)
		T	K
			°F
		P	kPa
			psi
		V	m ³ /kg
			ft ³ /lb _m
		S	kJ/kg.K
			Btu/lb _m °R
		H	kJ/kg
			Btu/lbm

d) Required Subroutines & Storage & Tapes : None

POOR ORIGINAL

PROGRAM MEE? 7674 OPT-I TRACE 1970377 39-61-67

```

1 PROGRAM MEE? INPUT, OUTPUT, TAPE 991
2 DIMENSION A(4), B(2), C(10)
3 DATA A(1), A(2), B(1), B(2), C(1), C(2), C(3), C(4), C(5), C(6), C(7), C(8), C(9), C(10)
4 DATA 1.0, 2.0, 3.0, 4.0, 5.0, 6.0, 7.0, 8.0, 9.0, 10.0, 11.0, 12.0, 13.0, 14.0, 15.0
5
6
7
8
9
10
11
12
13
14
15
16
17
18
19
20
21
22
23
24
25
26
27
28
29
30
31
32
33
34
35
36
37
38
39
40
41
42
43
44
45
46
47
48
49
50
51
52
53
54
55
56
57
58
59
60
61
62
63
64
65
66
67
68
69
70
71
72
73
74
75

```


223.00	.423	.35E-01	.34E+00	50.73	.27	86.02	122.53	86.02	1.03	1.00	.67	145.1	12.6	74.6	37
224.00	.423	.37E-01	.37E+00	53.48	.23	90.86	133.40	90.92	1.07	1.06	.63	145.1	12.6	77.1	37.6
225.00	.423	.39E-01	.39E+00	55.85	.31	95.35	142.11	92.15	1.43	1.47	.72	145.1	12.6	69.3	51.0
226.00	.423	.34E-01	.41E+00	48.94	.33	84.43	150.01	82.18	1.77	1.38	.79	146.1	12.6	60.6	45.1
227.00	.423	.33E-01	.43E+00	47.44	.35	87.76	158.31	79.53	1.91	1.75	.76	145.1	12.6	55.5	75.8
228.00	.423	.33E-01	.50E+00	47.10	.40	81.72	183.22	94.60	2.25	1.75	.81	145.1	12.6	59.6	75.0
229.00	.423	.29E-01	.54E+00	42.36	.43	75.23	197.06	72.19	2.62	1.78	.86	145.1	12.6	64.7	56.7
231.00	.423	.33E-01	.58E+00	47.14	.47	83.70	212.50	80.33	2.56	1.35	.87	145.1	12.3	65.7	43.1
232.00	.423	.36E-01	.62E+00	51.80	.49	92.08	225.37	83.82	2.45	1.62	.90	145.1	12.3	64.0	57.9
233.00	.423	.36E-01	.65E+00	51.50	.52	91.44	237.90	88.98	2.60	1.41	.93	145.1	12.8	65.4	56.4
601.00	.423	.19E-01	.21E+01	27.89	.02	45.45	7.77	7.72	.17	1.04	.17	141.6	13.3	93.6	99.1
602.00	.423	.21E-01	.40E+01	29.67	.03	46.32	14.39	16.29	.30	1.07	.21	141.3	13.6	93.4	99.1
608.00	.423	.35E-01	.27E+00	50.48	.22	84.04	98.13	83.97	1.17	1.00	.60	141.6	12.6	87.3	95.1
609.00	.423	.32E-01	.25E+00	45.88	.20	76.29	90.17	77.86	1.19	1.33	.57	141.6	12.6	88.1	94.6
610.00	.423	.25E-01	.19E+00	36.03	.15	59.75	68.93	62.18	1.15	1.18	.50	130.7	12.6	91.4	92.9
611.00	.423	.22E-01	.14E+00	31.26	.11	50.86	50.10	43.47	.93	1.10	.43	141.6	12.3	98.4	57.5
612.00	.423	.21E-01	.62E+01	30.58	.07	49.69	29.87	23.48	.60	1.09	.33	143.3	12.6	98.3	98.7
613.00	.423	.22E-01	.22E+00	38.76	.17	64.99	76.15	67.25	1.23	1.23	.58	141.6	12.6	88.3	94.1
614.00	.423	.22E-01	.15E+00	31.80	.12	52.07	55.11	51.05	1.06	1.11	.45	141.6	12.6	96.7	95.4
615.00	.423	.24E-01	.16E+00	34.41	.13	56.17	60.11	56.88	1.07	1.17	.47	145.1	12.6	95.1	96.6
616.00	.423	.23E-01	.11E+00	33.20	.09	53.87	40.08	39.69	.74	1.13	.38	144.6	12.6	90.1	98.9
617.00	.423	.22E-01	.51E+01	31.67	.04	51.67	15.51	18.34	.30	1.11	.27	144.6	12.6	93.1	92.1

POOR ORIGINAL

644.00	.423	.52E-01	.44E+00	75.28	.35	127.60	159.57	117.39	1.25	1.71	.76	141.6	12.6	77.0	97.7
645.00	.423	.55E-01	.48E+00	78.33	.38	132.65	174.21	129.7	1.31	1.74	.79	141.6	12.6	77.5	98.7
646.00	.423	.60E-01	.51E+00	81.78	.41	141.33	187.06	146.57	1.45	1.90	.82	141.6	12.6	86.7	117.8
651.00	.423	.62E-01	.60E+00	89.70	.68	185.34	216.73	181.90	2.03	1.92	.84	141.6	12.6	83.1	85.6
652.00	.423	.64E-01	.66E+00	93.05	.93	111.79	240.58	183.33	2.15	1.96	.83	141.6	12.6	80.1	89.1
648.00	.423	.58E-01	.51E+00	82.58	.41	139.85	187.06	138.81	1.36	1.75	.82	141.6	12.6	77.5	96.8
650.00	.423	.63E-01	.56E+00	90.40	.45	153.10	204.93	152.14	1.34	1.87	.86	141.6	12.6	77.5	96.3
651.00	.423	.63E-01	.60E+00	98.49	.68	148.77	219.73	205.47	1.68	1.87	.84	141.6	12.6	94.3	73.6
690.00	.423	.33E-01	.27E+00	46.73	.22	77.93	93.36	83.73	1.27	1.35	.60	141.6	13.3	86.4	95.3
691.00	.423	.42E-01	.35E+00	59.65	.28	99.92	126.78	102.98	1.27	1.52	.68	141.6	13.3	83.7	97.3
692.00	.423	.44E-01	.39E+00	63.11	.31	105.93	140.11	106.69	1.32	1.57	.77	141.6	13.5	79.4	95.8
693.00	.423	.45E-01	.43E+00	64.11	.35	110.25	155.85	98.85	1.41	1.58	.75	141.6	13.3	68.3	86.1
694.00	.423	.41E-01	.52E+00	58.49	.41	101.60	186.48	105.61	1.84	1.51	.82	141.6	13.5	62.5	74.6
695.00	.423	.29E-01	.84E+00	41.50	.52	73.71	232.15	95.54	1.15	1.27	.92	141.6	13.5	43.1	56.5
696.00	.423	.29E-01	.58E+00	41.01	.46	73.42	208.52	73.89	2.84	1.26	.87	141.6	13.5	44.2	57.0
697.00	.423	.29E-01	.47E+00	41.01	.38	72.61	171.53	74.19	2.36	1.27	.79	141.6	13.5	50.9	61.1
698.00	.423	.45E-01	.43E+00	65.27	.35	110.85	156.39	112.55	1.41	1.59	.76	141.6	13.5	75.8	93.8
699.00	.423	.45E-01	.38E+00	64.65	.31	108.44	137.43	110.77	1.27	1.58	.74	141.6	13.5	83.9	95.5
256.04	.423	.25E-01	.14E+00	35.87	.11	58.49	45.81	48.77	.85	1.18	.44	142.6	13.0	48.2	98.9
257.04	.423	.26E-01	.17E+00	37.00	.13	60.43	60.77	58.83	1.01	1.20	.47	142.6	13.0	47.2	98.9
258.04	.423	.27E-01	.19E+00	38.37	.15	63.21	70.14	64.20	1.11	1.27	.50	142.6	13.0	92.6	98.3
259.04	.423	.26E-01	.22E+00	37.77	.18	62.61	79.73	71.41	1.27	1.21	.4	140.6	13.0	91.0	98.3

260.04	.423	.26E-01	.25E+00	37.79	.20	63.49	90.66	72.93	1.43	1.21	.27	141.6	14.8	99.1	99.7
901.04	.423	.16E-01	.27E-01	23.28	.07	37.95	9.56	9.47	.25	.35	.19	141.6	14.8	99.1	99.9
902.04	.423	.21E-01	.44E-01	23.90	.06	44.74	15.84	15.68	.37	1.08	.24	141.6	14.8	99.1	98.9
403.04	.423	.22E-01	.63E-01	31.06	.05	50.61	22.41	22.27	.44	1.19	.29	141.6	15.0	99.4	99.4
404.04	.423	.23E-01	.82E-01	32.76	.07	53.38	29.01	28.88	.54	1.13	.33	141.6	15.0	99.4	99.6
405.04	.423	.23E-01	.10E+00	33.59	.08	54.84	34.84	34.26	.67	1.14	.37	141.6	15.0	98.4	99.1
906.04	.423	.25E-01	.19E+00	35.62	.15	59.38	48.15	57.41	1.15	1.18	.50	141.6	15.0	86.6	98.9
907.04	.423	.27E-01	.28E+00	39.06	.20	65.41	64.60	71.87	1.35	1.23	.57	141.6	15.0	84.8	98.9
908.04	.423	.23E-01	.13E+00	33.07	.10	51.96	46.34	45.62	.86	1.13	.41	141.6	15.0	94.7	98.7
910.04	.423	.27E-01	.22E+00	38.79	.18	64.47	74.08	67.33	1.21	1.23	.54	141.6	15.0	84.3	98.6
911.04	.423	.23E-01	.16E+00	32.62	.13	53.44	56.47	54.14	1.06	1.13	.46	141.6	15.0	96.5	99.1
912.04	.423	.27E-01	.24E+00	38.67	.22	65.03	99.60	77.19	1.53	1.22	.61	141.6	14.8	80.8	98.3
913.04	.423	.31E-01	.35E+00	44.71	.28	76.12	123.87	86.54	1.83	1.32	.66	141.6	14.8	74.3	98.9
914.04	.423	.34E-01	.39E+00	48.34	.31	82.86	138.68	92.81	1.64	1.37	.72	141.6	15.0	71.9	98.4
915.04	.423	.36E-01	.43E+00	51.62	.34	87.69	151.15	95.61	1.72	1.41	.75	141.6	15.0	69.8	98.7
916.04	.423	.35E-01	.47E+00	49.97	.37	86.71	165.74	93.55	1.91	1.39	.78	141.6	15.0	63.0	98.7
917.04	.423	.35E-01	.88E+00	50.50	.40	88.00	177.07	94.93	2.01	1.40	.81	141.6	15.0	60.6	98.4
918.04	.423	.33E-01	.84E+00	50.40	.43	88.44	191.43	93.42	2.12	1.40	.84	141.6	15.0	56.6	98.7
919.04	.423	.36E-01	.58E+00	51.05	.46	89.76	204.34	97.08	2.28	1.41	.87	141.6	15.0	55.1	98.9
920.04	.423	.36E-01	.62E+00	51.08	.49	89.98	219.07	100.38	2.43	1.41	.90	141.6	14.8	54.1	98.9
921.04	.423	.37E-01	.66E+00	51.10	.53	94.07	235.71	99.62	2.61	1.44	.94	141.6	15.0	50.9	98.9
7.12	.423	.34E-01	.22E+00	34.98	.18	64.71	85.34	60.77	1.43	1.17	.54	141.6	6.8	72.3	60.3

POOR ORIGINAL

8.12	.423	.21E-01	.16E+00	30.62	.13	51.27	64.12	53.17	1.25	1.09	.97	141.6	5.6	89.0	99.1
9.12	.423	.21E-01	.11E+00	30.53	.09	49.78	42.68	42.29	.86	1.09	.18	141.6	6.9	99.1	99.4
10.12	.423	.20E-01	.82E-01	28.68	.07	46.77	31.71	31.33	.64	1.06	.33	141.6	7.1	98.9	99.1
11.12	.423	.19E-01	.51E-01	27.61	.06	45.54	19.85	19.32	.43	1.04	.56	141.6	7.6	98.5	118.4
73.12	.423	.17E-01	.34E-02	24.37	.00	39.71	1.23	1.71	.81	.97	.07	141.6	13.3	99.1	.2
74.12	.423	.18E-01	.21E-01	25.53	.02	41.62	7.77	7.69	.13	1.00	.17	141.6	13.3	99.1	.2
75.12	.423	.18E-01	.33E-01	25.51	.03	41.61	12.02	11.87	.29	1.00	.21	141.6	11.6	98.9	.2
77.12	.423	.22E-01	.93E-01	30.92	.07	50.47	35.83	34.41	.63	1.16	.35	141.6	10.1	98.4	.2
76.12	.423	.20E-01	.63E-01	29.22	.05	47.68	23.48	23.12	.49	1.07	.29	141.6	11.1	98.7	.2
78.12	.423	.23E-01	.12E+00	33.45	.10	54.62	45.45	44.54	.83	1.14	.40	141.6	9.8	98.2	.2
79.12	.423	.23E-01	.16E+00	33.70	.13	55.27	58.68	55.93	1.06	1.14	.45	141.6	9.8	95.8	.2
80.12	.423	.25E-01	.20E+00	35.48	.16	59.59	75.28	68.58	1.25	1.17	.51	141.6	9.3	87.1	.2
81.12	.423	.26E-01	.23E+00	36.67	.18	62.30	87.49	63.93	1.50	1.19	.55	141.6	9.1	75.5	.2
82.12	.423	.27E-01	.27E+00	38.54	.22	65.73	101.74	73.33	1.58	1.22	.60	141.6	9.1	73.4	.2
249.12	.423	.17E-01	.21E-01	24.70	.02	40.26	7.77	7.67	.19	.98	.17	142.6	13.3	98.9	99.4
250.12	.423	.18E-01	.34E-01	25.58	.03	43.18	12.25	12.89	.28	1.01	.21	144.1	13.0	98.9	99.1
259.12	.423	.27E-01	.19E+00	38.36	.15	64.35	69.94	54.17	1.09	1.22	.58	144.1	12.8	80.3	98.9
260.12	.423	.27E-01	.22E+00	39.36	.18	65.62	79.93	64.78	1.25	1.23	.54	144.4	12.8	83.5	99.1
261.12	.423	.27E-01	.25E+00	38.58	.20	65.44	89.92	62.69	1.37	1.22	.57	144.6	12.4	73.6	99.1
262.12	.423	.26E-01	.27E+00	38.21	.22	65.46	99.41	62.75	1.51	1.22	.60	144.4	12.8	67.5	99.1
263.12	.423	.27E-01	.27E+00	38.91	.22	66.58	98.51	63.46	1.48	1.23	.60	144.1	13.0	69.0	99.1
264.12	.423	.27E-01	.31E+00	39.24	.25	68.11	111.11	60.89	1.56	1.23	.64	144.1	13.0	53.1	98.9

POOR ORIGINAL

265.12	.423	.28E-01	.35E+00	39.80	.28	69.37	127.13	64.21	1.83	1.24	.64	145.1	13.6	57.0	98.9
266.12	.423	.28E-01	.39E+00	40.19	.31	70.71	140.91	61.01	1.93	1.25	.77	145.1	13.0	50.7	98.9
680.12	.423	.26E-01	.27E+00	37.68	.22	64.87	96.78	58.85	1.57	1.21	.60	141.2	13.8	65.2	99.1
681.12	.423	.28E-01	.35E+00	39.87	.28	69.17	126.97	70.14	1.84	1.24	.68	145.6	13.5	61.1	98.9
682.12	.423	.27E-01	.48E+00	38.95	.38	68.94	172.05	70.12	2.50	1.23	.79	145.1	13.3	48.6	99.1
683.12	.423	.27E-01	.64E+00	39.08	.52	70.57	211.75	60.94	3.28	1.23	.92	145.1	13.5	38.3	99.1
684.12	.423	.27E-01	.59E+00	38.91	.47	70.00	212.09	62.25	3.03	1.23	.88	143.1	13.3	38.7	99.1
685.12	.423	.27E-01	.54E+00	38.72	.43	69.49	193.31	59.11	2.78	1.22	.84	144.1	13.5	40.0	99.1
686.12	.423	.27E-01	.50E+00	38.88	.40	69.63	181.67	59.54	2.61	1.23	.81	141.8	13.3	41.7	98.9
687.12	.423	.27E-01	.43E+00	38.56	.35	68.16	195.87	61.47	2.28	1.22	.75	141.1	13.5	47.6	98.9
688.12	.423	.27E-01	.39E+00	39.07	.31	68.50	140.11	64.50	2.04	1.23	.72	145.1	13.5	51.1	99.1
689.12	.423	.29E-01	.31E+00	41.59	.25	72.10	113.05	65.80	1.57	1.27	.66	145.4	13.3	61.0	99.1
675.12	.423	.23E-01	.16E+00	32.90	.13	54.68	59.44	50.40	1.09	1.13	.47	141.1	13.5	86.9	99.1
674.12	.423	.24E-01	.15E+00	34.33	.12	56.34	53.43	43.09	.95	1.15	.44	144.1	13.5	92.9	99.1
673.12	.423	.27E-01	.22E+00	38.85	.18	65.01	80.24	65.80	1.23	1.23	.54	141.6	13.5	84.4	99.1
672.12	.423	.21E-01	.11E+00	30.84	.09	50.41	38.92	37.34	.77	1.04	.38	142.3	13.3	96.5	99.1
660.12	.423	.17E-01	.21E-01	24.80	.02	40.48	7.84	7.70	.19	.38	.17	141.6	12.6	98.4	98.7
661.12	.423	.23E-01	.11E+00	33.31	.09	54.45	46.98	39.02	.74	1.14	.38	141.6	12.6	97.7	99.1
662.12	.423	.19E-01	.51E-01	26.79	.04	43.73	18.51	18.17	.43	1.02	.25	141.6	12.6	98.4	98.7
663.12	.423	.18E-01	.35E-01	25.57	.03	41.71	12.93	12.83	.31	1.00	.22	141.5	12.3	98.9	99.1
664.12	.423	.20E-01	.66E-01	28.24	.05	46.14	24.30	23.41	.51	1.05	.30	141.6	12.3	98.7	99.1
665.12	.423	.22E-01	.93E-01	31.38	.07	51.29	34.14	33.27	.77	1.10	.40	141.5	12.3	97.7	98.9

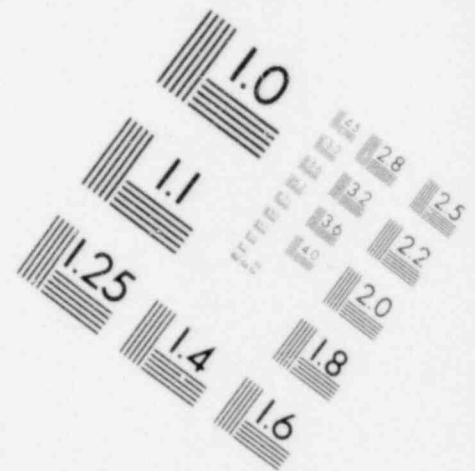
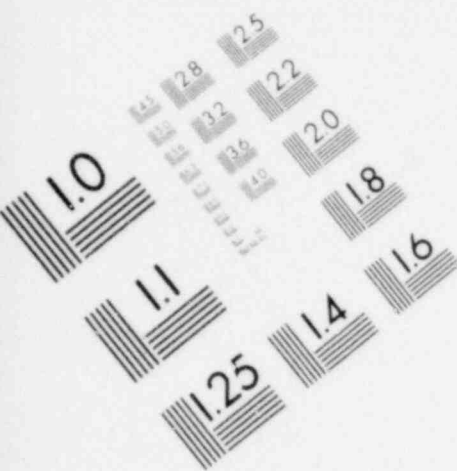
666.12	.423	.28E-01	.19E+00	39.49	.15	67.20	70.33	73.46	1.00	1.00	.37	141.6	12.3	96.3	98.9
667.12	.423	.20E-01	.78E-01	28.43	.06	46.60	28.61	27.38	.61	1.05	.37	141.6	12.3	96.3	98.9
668.12	.423	.24E-01	.14E+00	33.81	.11	55.47	50.24	47.54	.91	1.15	.43	141.6	12.3	95.3	98.9
669.12	.423	.26E-01	.16E+00	37.67	.13	61.81	60.24	57.05	.97	1.21	.47	141.6	12.3	95.3	98.3
767.12	.423	.18E-01	.21E-01	25.64	.02	41.92	6.57	6.52	.16	1.00	.17	137.7	26.6	97.4	99.6
768.12	.423	.21E-01	.51E-01	30.43	.04	49.71	14.74	14.61	.30	1.04	.26	141.6	30.3	94.8	93.4
769.12	.423	.22E-01	.82E-01	30.88	.07	50.41	23.95	23.41	.47	1.10	.33	141.6	29.8	98.4	99.6
770.12	.423	.22E-01	.11E+00	31.27	.09	51.00	31.27	30.78	.61	1.10	.37	141.6	29.8	98.9	99.4
771.12	.423	.22E-01	.14E+00	31.94	.11	52.27	40.19	38.46	.77	1.11	.43	141.6	29.8	97.8	99.4
772.12	.423	.22E-01	.16E+00	31.56	.13	52.20	48.39	42.17	.93	1.11	.47	141.6	29.6	91.8	98.7
773.12	.423	.23E-01	.19E+00	33.24	.15	54.68	55.74	51.83	1.02	1.14	.50	141.6	30.1	94.1	99.1
774.12	.423	.24E-01	.22E+00	34.97	.18	57.00	64.30	58.56	1.11	1.17	.54	141.6	29.8	90.5	98.3
775.12	.423	.25E-01	.25E+00	35.49	.20	59.63	73.08	54.42	1.23	1.17	.57	141.6	29.6	82.0	98.1
776.12	.423	.27E-01	.28E+00	38.53	.22	64.69	81.30	61.11	1.26	1.22	.60	141.6	29.6	83.5	99.1
777.12	.423	.28E-01	.35E+00	39.88	.28	67.85	103.75	66.61	1.51	1.24	.68	141.6	29.6	74.8	98.9
779.12	.423	.27E-01	.41E+00	39.84	.33	67.16	120.19	65.83	1.73	1.23	.73	141.6	29.6	68.3	98.9
780.12	.423	.28E-01	.48E+00	39.80	.38	69.12	140.45	65.13	2.03	1.24	.79	141.6	29.6	62.7	99.1
781.12	.423	.28E-01	.55E+00	40.29	.44	70.25	160.13	63.62	2.24	1.25	.85	141.6	29.8	60.3	99.1
782.12	.423	.28E-01	.62E+00	40.74	.50	71.54	182.77	68.53	2.53	1.26	.91	141.6	29.6	56.0	99.1
784.12	.423	.24E-01	.28E+00	34.74	.22	57.84	61.21	46.61	1.05	1.18	.50	141.6	46.3	82.1	98.3
785.12	.423	.22E-01	.24E+00	31.81	.20	52.68	53.90	45.41	1.02	1.11	.57	140.2	47.1	91.7	98.9
786.12	.423	.22E-01	.22E+00	32.24	.18	52.64	47.77	44.55	.91	1.12	.54	141.6	47.5	96.0	98.9

787.12	.423	.22E-01	.19E+00	31.63	.16	51.82	42.61	37.67	.82	1.11	.60	144.1	47.1	91.1	99.4
788.12	.423	.23E-01	.16E+00	32.70	.13	53.19	34.24	33.05	.64	1.13	.45	144.1	47.4	98.2	99.5
789.12	.423	.21E-01	.12E+00	30.78	.10	50.08	27.13	26.07	.54	1.09	.60	144.1	47.1	37.3	99.6
790.12	.423	.21E-01	.85E-01	29.77	.07	48.35	19.05	18.66	.39	1.07	.11	144.1	46.2	94.3	99.1
791.12	.423	.18E-01	.41E-01	26.02	.03	42.29	8.93	8.73	.21	1.00	.23	144.4	47.6	94.1	99.4
792.12	.423	.25E-01	.35E+00	36.34	.28	60.66	75.52	95.07	1.25	1.19	.58	141.6	47.5	85.1	99.1
793.12	.423	.25E-01	.42E+00	35.84	.34	60.75	94.72	54.02	1.56	1.18	.75	141.5	46.6	77.0	93.6
794.12	.423	.27E-01	.51E+00	38.13	.41	64.92	113.63	54.43	1.75	1.22	.82	141.5	47.1	74.1	99.1
795.12	.423	.26E-01	.56E+00	38.00	.45	65.09	124.64	55.46	1.91	1.21	.86	141.6	47.1	70.7	99.1
796.12	.423	.25E-01	.44E+00	35.76	.35	58.97	73.26	51.21	1.34	1.17	.76	141.6	46.7	84.7	99.1
797.12	.423	.25E-01	.36E+00	35.18	.29	58.04	64.20	52.80	1.11	1.17	.69	141.6	47.2	92.4	98.7
798.12	.423	.24E-01	.32E+00	34.26	.26	56.56	57.94	47.41	1.03	1.15	.65	141.6	47.0	92.7	98.7
799.12	.423	.21E-01	.26E+00	30.59	.21	50.51	46.91	38.76	.93	1.09	.58	141.6	46.2	91.9	98.9
670.12	.423	.21E-01	.22E+00	29.57	.18	48.57	39.67	35.13	.82	1.07	.54	141.5	46.7	95.3	99.4
671.12	.423	.20E-01	.17E+00	29.07	.14	47.48	30.79	29.51	.65	1.06	.47	141.6	46.2	98.2	99.4
672.12	.423	.20E-01	.11E+00	28.28	.09	46.11	19.83	19.33	.43	1.05	.38	141.5	46.7	98.3	99.4
673.12	.423	.20E-01	.51E-01	28.54	.04	46.56	9.01	8.72	.19	1.05	.26	141.5	47.4	98.7	99.4
674.12	.423	.19E-01	.63E-01	27.18	.05	44.19	7.54	7.38	.17	1.03	.22	141.6	71.4	93.4	93.4
675.12	.423	.20E-01	.11E+00	28.27	.09	46.11	12.65	12.15	.27	1.05	.18	141.6	72.4	98.3	99.4
676.12	.423	.19E-01	.16E+00	27.40	.13	44.71	17.82	16.74	.40	1.03	.27	141.5	74.1	98.4	99.4
677.12	.423	.20E-01	.22E+00	28.43	.18	46.43	24.81	23.10	.51	1.05	.34	141.5	73.6	98.3	99.4
678.12	.423	.20E-01	.28E+00	28.44	.22	46.55	30.54	27.04	.64	1.05	.41	141.5	73.8	97.0	99.4

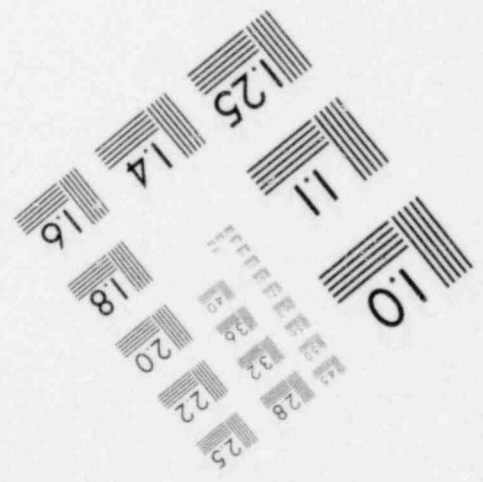
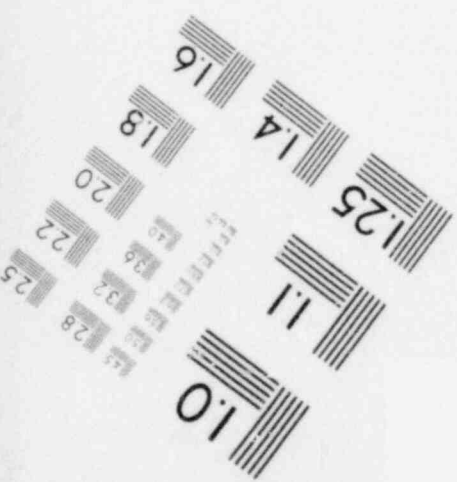
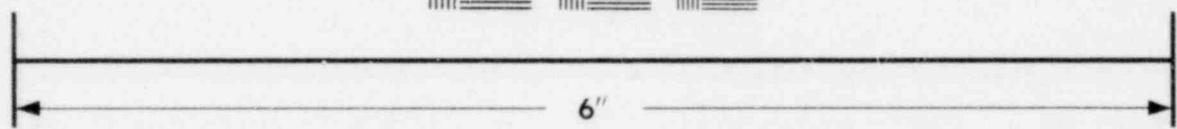
POOR ORIGINAL

879.12	.423	.19E-01	.31E+00	27.47	.25	45.09	35.06	28.32	.74	1.31	.64	141.5	73.1	95.1	99.1
83.24	.423	.17E-01	.21E+01	23.83	.02	36.90	7.95	7.81	.29	.96	.17	141.5	11.1	98.4	.2
84.24	.423	.18E-01	.51E+01	25.85	.04	42.17	18.82	18.99	.45	1.00	.26	141.5	11.1	98.9	.2
85.24	.423	.19E-01	.82E+01	27.75	.07	45.24	30.52	30.07	.67	1.04	.35	141.5	10.6	98.7	.2
86.24	.423	.20E-01	.11E+00	28.97	.09	47.29	41.21	40.59	.87	1.06	.34	141.5	10.1	98.4	.2
87.24	.423	.22E-01	.14E+00	32.24	.11	52.65	51.65	50.61	.94	1.12	.43	141.5	9.8	98.2	.2
88.24	.423	.25E-01	.16E+00	36.50	.13	59.61	61.98	60.73	1.04	1.19	.47	141.5	9.8	98.2	.2
89.24	.423	.27E-01	.19E+00	38.62	.15	63.43	72.31	68.34	1.14	1.22	.50	141.5	9.8	95.0	.3
922.24	.423	.26E-01	.27E+00	37.88	.22	65.00	97.64	62.97	1.50	1.21	.60	141.5	14.8	69.7	98.7
923.24	.423	.27E-01	.32E+00	38.94	.26	67.51	113.83	65.36	1.63	1.23	.65	141.5	14.8	63.7	98.9
924.24	.423	.27E-01	.37E+00	38.96	.29	68.16	130.01	66.19	1.91	1.23	.69	141.5	14.8	58.2	98.9
925.24	.423	.27E-01	.41E+00	38.63	.33	68.84	146.20	67.40	2.15	1.22	.74	141.5	14.8	50.1	98.9
926.24	.423	.28E-01	.46E+00	40.72	.37	71.73	162.38	74.87	2.26	1.26	.78	141.5	14.8	54.1	98.9
927.24	.423	.29E-01	.50E+00	41.86	.40	74.03	178.56	77.28	2.41	1.28	.81	141.5	14.8	51.7	98.9
928.24	.423	.28E-01	.53E+00	40.37	.43	72.02	189.35	70.27	2.63	1.25	.84	141.5	14.8	46.4	98.7
929.24	.423	.29E-01	.58E+00	41.49	.46	74.04	205.64	75.68	2.78	1.27	.87	141.5	14.8	46.9	98.7
930.24	.423	.30E-01	.66E+00	43.71	.53	78.32	235.44	79.87	3.01	1.30	.93	141.5	14.8	43.7	98.9
931.24	.423	.26E-01	.21E+00	37.54	.17	62.67	74.60	62.67	1.19	1.21	.53	141.5	14.8	86.4	98.7
932.24	.423	.22E-01	.14E+00	32.17	.11	52.66	48.82	47.09	.93	1.12	.43	141.5	14.8	97.0	98.7
930.00	.254	.83E-02	.51E-01	19.88	.07	19.47	17.83	17.76	.32	.39	.14	141.5	15.2	99.1	98.9
931.00	.254	.86E-02	.76E-01	20.46	.10	20.54	26.77	22.01	1.10	1.20	.46	141.5	15.3	84.9	94.6
932.00	.254	.16E-01	.14E+00	37.37	.18	37.63	48.68	36.53	1.23	1.32	.62	141.5	15.0	82.3	97.0

POOR ORIGINAL



**IMAGE EVALUATION
TEST TARGET (MT-3)**



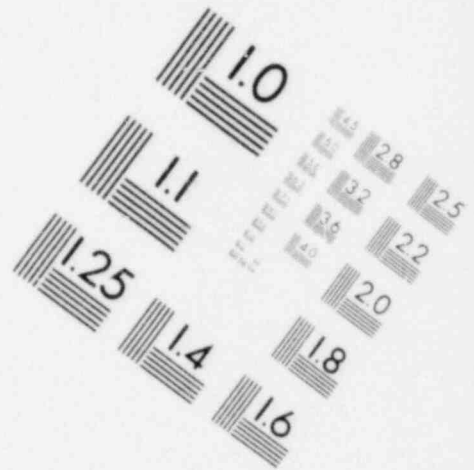
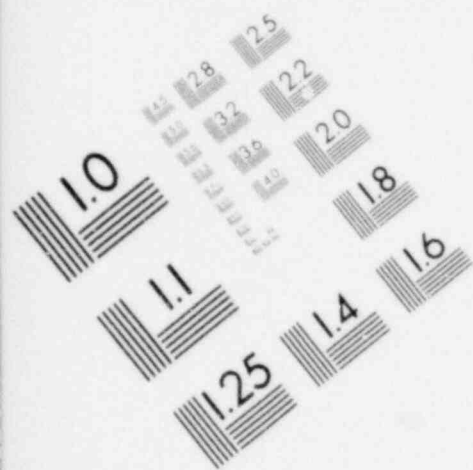
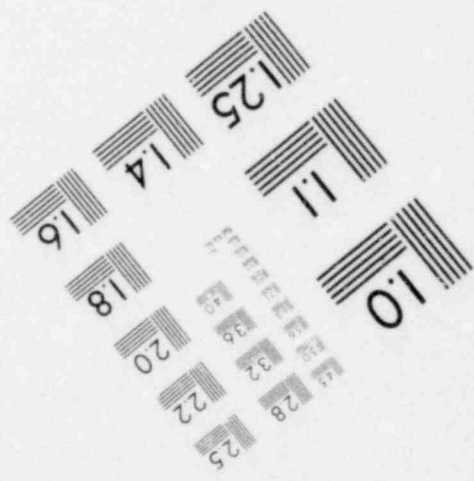
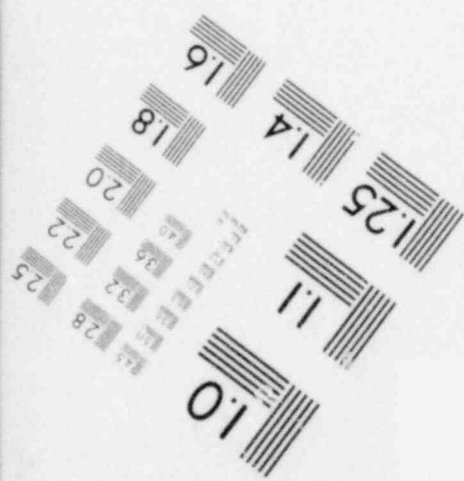
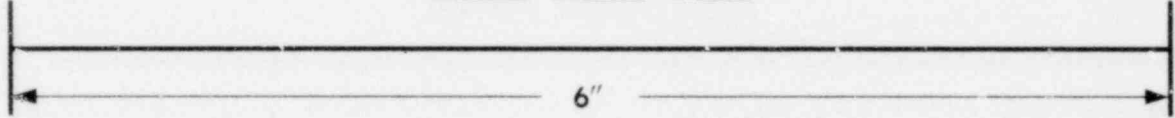
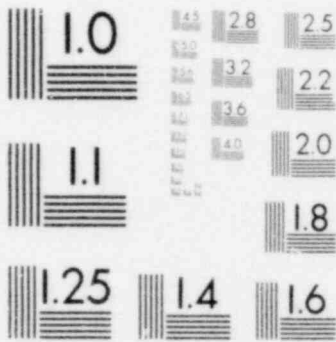


**IMAGE EVALUATION
TEST TARGET (MT-3)**



POOR ORIGINAL

933.00	.254	.14E-01	.19E+00	20.50	.14	29.00	30.00	30.25	1.20	1.00	151.6	15.0	96.3	97.7
934.00	.254	.17E-01	.15E+00	40.54	.20	40.90	52.67	61.66	1.23	1.81	161.6	15.0	87.0	95.5
935.00	.254	.21E-01	.18E+00	50.83	.25	51.17	65.21	82.55	1.24	1.58	141.6	15.0	11.5	97.7
936.00	.254	.25E-01	.21E+00	59.68	.29	59.73	75.96	92.25	1.27	1.71	161.6	15.0	86.7	98.2
937.00	.254	.27E-01	.25E+00	66.70	.33	65.13	88.01	70.15	1.35	1.79	161.6	15.0	82.8	98.2
938.00	.254	.35E-02	.21E-01	28.63	.03	28.19	7.73	7.65	.14	1.01	141.6	13.8	93.1	99.1
939.00	.254	.12E-01	.21E-01	29.59	.07	28.95	18.87	18.74	.65	1.71	161.6	10.8	93.5	99.6
940.00	.254	.13E-01	.27E-01	31.83	.11	30.64	31.28	29.43	1.07	1.76	161.6	8.6	96.6	98.6
941.00	.254	.16E-01	.11E+00	38.80	.15	38.33	67.23	39.52	1.10	1.88	161.6	7.9	96.1	98.9
942.00	.254	.20E-01	.14E+00	45.99	.18	46.71	59.65	47.18	1.13	1.52	161.6	8.1	98.3	96.3
943.00	.254	.24E-01	.16E+00	57.02	.22	56.60	63.85	53.29	1.13	1.68	161.6	7.1	91.4	98.7
944.00	.254	.24E-01	.21E+00	57.19	.29	57.75	75.94	59.88	1.32	1.68	161.6	15.0	82.3	97.2
945.00	.254	.26E-01	.25E+00	61.35	.33	62.31	87.62	65.87	1.41	1.76	160.9	15.0	78.9	97.0
946.00	.254	.27E-01	.25E+00	66.86	.33	65.87	87.62	65.87	1.33	1.79	160.9	15.0	78.9	97.0
947.00	.254	.29E-01	.27E+00	70.36	.37	71.55	97.35	71.53	1.36	1.85	161.6	15.0	77.5	95.8
948.00	.254	.33E-01	.32E+00	78.93	.43	80.32	113.13	83.11	1.41	1.97	161.6	15.0	77.5	95.0
949.00	.254	.36E-01	.34E+00	85.14	.46	86.56	120.95	89.21	1.40	2.05	161.6	15.0	77.7	94.3
950.00	.254	.41E-01	.39E+00	98.68	.52	100.87	137.29	100.97	1.47	2.20	161.6	16.8	77.5	95.3
951.00	.254	.29E-01	.41E+00	69.29	.55	72.93	147.14	71.58	2.02	1.85	161.6	16.8	56.2	82.7
952.00	.254	.29E-01	.47E+00	69.70	.63	76.00	172.23	75.21	2.25	1.85	160.6	16.8	51.1	81.6
953.00	.254	.28E-01	.51E+00	67.71	.68	72.30	181.40	72.74	2.51	1.83	161.6	16.8	50.9	86.2
954.00	.254	.39E-01	.54E+00	76.71	.72	75.13	193.95	83.62	2.52	1.87	161.6	16.8	51.1	86.0

POOR ORIGINAL

951.00	.254	.21E-01	.58E+00	49.96	.77	54.60	205.54	45.83	3.76	1.57	1.77	161.6	16.8	51.8	47.1
952.00	.254	.20E-01	.62E+00	48.09	.82	52.66	219.02	46.36	6.15	1.56	1.51	161.6	16.8	47.8	47.4
953.00	.254	.18E-01	.62E+00	47.67	.82	46.72	219.02	56.36	4.63	1.45	1.31	161.6	16.8	47.8	47.4
954.00	.254	.65E-01	.48E+00	107.22	.57	109.08	151.53	111.05	1.33	2.30	1.03	161.6	16.8	77.2	65.3
955.00	.254	.50E-01	.46E+00	120.08	.62	121.76	185.08	124.67	1.36	2.63	1.16	161.6	16.8	79.1	95.5
956.00	.254	.55E-01	.51E+00	131.44	.68	133.11	181.26	136.43	1.36	2.54	1.13	161.6	16.8	73.3	96.5
957.00	.254	.59E-01	.54E+00	140.15	.72	142.02	192.49	145.92	1.36	2.63	1.23	161.6	16.8	79.4	97.2
958.00	.254	.60E-01	.58E+00	142.72	.77	145.37	202.54	148.83	1.61	2.65	1.27	161.6	16.8	76.5	91.1
959.00	.254	.83E-02	.61E-01	19.88	.87	19.47	17.88	17.70	.92	.99	.18	161.6	15.5	99.1	98.9
960.00	.254	.86E-02	.76E-01	28.46	.18	20.54	26.77	22.01	1.10	1.00	.56	161.6	15.3	84.3	64.6
961.00	.254	.16E-01	.18E+00	37.37	.18	37.59	48.08	38.53	1.29	1.16	.62	161.6	15.0	82.3	97.0
962.00	.254	.12E-01	.10E+00	28.98	.14	29.09	36.88	30.86	1.27	1.20	.54	161.6	15.0	86.3	96.7
963.00	.254	.17E-01	.18E+00	40.54	.20	40.20	52.57	41.66	1.29	1.61	.16	161.6	15.0	82.0	95.5
964.00	.254	.21E-01	.18E+00	50.83	.25	51.14	65.23	52.55	1.28	1.58	.72	161.6	15.0	81.5	97.5
965.00	.254	.25E-01	.21E+00	59.48	.29	59.73	75.36	62.25	1.27	1.71	.77	161.6	15.0	86.7	98.2
966.00	.254	.27E-01	.25E+00	56.70	.33	65.19	88.01	70.15	1.35	1.79	.83	161.6	15.0	87.8	98.2
20.00	.254	.66E-02	.21E-01	20.63	.83	20.19	7.73	7.65	.38	1.01	.24	161.6	13.8	93.1	93.1
21.00	.254	.12E-01	.51E-01	29.59	.87	28.96	18.87	18.74	.65	1.21	.38	161.6	10.8	93.4	56.4
22.00	.254	.13E-01	.82E-01	31.03	.11	30.63	31.28	29.43	1.02	1.24	.68	161.6	8.4	94.6	98.4
23.00	.254	.16E-01	.11E+00	38.80	.15	38.11	42.23	39.32	1.10	1.18	.56	161.6	7.9	94.1	97.9
24.00	.254	.20E-01	.14E+00	46.99	.18	46.71	52.64	47.18	1.13	1.22	.62	161.6	8.1	90.4	66.3
25.00	.254	.24E-01	.16E+00	57.02	.22	56.69	63.85	53.23	1.13	1.68	.50	161.6	7.1	93.4	68.7

POOR ORIGINAL

940.00	.254	.294-01	.210+00	57.19	.29	57.75	75.94	59.00	1.37	1.10	.77	141.7	15.0	47.0	97.2
941.00	.254	.265-01	.250+00	61.35	.33	62.31	87.62	65.07	1.51	1.74	.83	140.3	15.0	78.3	97.6
942.00	.254	.276-01	.250+00	64.85	.33	65.87	87.62	65.07	1.33	1.79	.83	140.7	15.0	78.9	97.0
943.00	.254	.237-01	.272+00	70.36	.37	71.55	97.36	71.53	1.36	1.66	.82	141.6	15.0	77.5	95.8
944.00	.254	.338-01	.370+00	78.99	.43	80.37	113.11	83.11	1.61	1.97	.35	141.6	15.0	77.5	95.0
945.00	.254	.360-01	.340+00	85.14	.46	86.54	120.95	89.21	1.60	2.05	.97	141.6	15.0	77.7	95.3
946.00	.254	.610-01	.390+00	98.40	.52	100.07	137.23	100.97	1.37	2.20	1.04	141.6	16.8	77.5	95.3
947.00	.254	.200-01	.610+00	53.25	.55	72.39	147.16	71.58	2.02	1.45	1.07	141.6	14.8	56.7	53.7
948.00	.254	.290-01	.675+00	69.70	.63	74.00	167.23	75.21	2.26	1.65	1.14	140.6	16.8	53.1	41.5
949.00	.254	.240-01	.510+00	67.71	.68	72.30	181.89	72.74	2.51	1.83	1.10	141.2	14.8	48.9	44.2
950.00	.254	.380-01	.580+00	70.71	.72	75.13	192.05	82.57	2.56	1.87	1.23	141.6	16.8	51.4	44.0
951.00	.254	.210-01	.580+00	59.45	.77	54.60	205.54	55.89	1.76	1.57	1.27	141.6	14.8	33.8	47.1
952.00	.254	.280-01	.650+00	48.09	.82	52.86	219.07	46.36	4.16	1.54	1.31	141.6	16.8	32.8	47.4
953.00	.254	.180-01	.670+00	42.67	.82	46.72	219.07	46.36	4.53	1.45	1.31	141.6	14.8	32.8	47.4
954.00	.254	.650-01	.630+00	107.27	.97	109.08	151.53	111.05	1.33	2.30	1.09	141.6	16.8	77.2	95.3
955.00	.254	.500-01	.660+00	120.88	.62	121.76	165.04	124.67	1.36	2.43	1.14	141.6	16.8	75.3	95.5
956.00	.254	.550-01	.510+00	131.44	.68	133.11	181.26	138.83	1.36	2.54	1.19	141.6	16.8	79.0	94.5
957.00	.254	.590-01	.540+00	140.15	.72	142.08	192.69	145.92	1.36	2.63	1.23	141.6	16.8	79.4	97.2
958.00	.254	.600-01	.560+00	142.72	.77	145.17	205.54	148.43	1.46	2.65	1.27	141.6	16.8	76.5	93.1
959.04	.254	.600-02	.710-01	19.11	.03	18.74	7.62	7.57	.01	.92	.24	141.6	15.0	98.0	96.7
960.04	.254	.100-01	.510-01	23.97	.07	23.48	17.04	17.75	.77	1.03	.34	141.6	15.0	98.3	98.4
961.04	.254	.110-01	.600-01	23.46	.11	25.11	20.37	20.21	1.14	1.17	.27	141.6	15.0	93.0	97.3

962.04	.254	.13E+01	.11E+00	.15	31.26	40.23	32.89	1.29	1.24	.56	141.6	14.8	86.4	98.4
963.04	.254	.15E+01	.14E+00	.18	36.76	48.82	35.35	1.33	1.33	.67	141.6	14.8	76.5	98.6
964.04	.254	.18E+01	.16E+00	.22	43.67	58.53	44.74	1.35	1.42	.68	141.6	14.8	70.3	98.7
965.04	.254	.20E+01	.19E+00	.26	49.27	68.35	53.69	1.33	1.56	.73	141.6	14.8	71.7	98.7
966.04	.254	.22E+01	.22E+00	.29	50.85	78.11	58.80	1.54	1.57	.78	141.6	14.8	74.6	98.7
967.04	.254	.25E+01	.25E+00	.34	60.18	86.83	62.25	1.53	1.70	.84	141.6	14.8	73.4	98.6
968.04	.254	.28E+01	.32E+00	.42	67.91	112.50	73.19	1.66	1.80	.94	141.6	14.8	70.2	98.4
969.04	.254	.30E+01	.32E+00	.42	72.78	112.50	73.19	1.53	1.67	.94	141.6	14.8	70.2	97.9
970.04	.254	.32E+01	.35E+00	.47	79.68	125.22	79.69	1.57	1.35	.99	141.6	14.8	59.0	98.4
971.04	.254	.35E+01	.39E+00	.52	85.90	138.10	86.33	1.51	2.02	1.04	141.6	14.8	58.1	98.7
972.04	.254	.36E+01	.43E+00	.57	89.78	151.59	83.19	1.63	2.06	1.09	141.6	14.8	64.9	98.7
973.04	.254	.40E+01	.47E+00	.63	99.42	167.82	104.02	1.63	2.18	1.14	141.6	14.8	67.6	98.4
974.04	.254	.43E+01	.51E+00	.69	106.57	183.20	110.89	1.72	2.25	1.20	141.6	14.8	66.4	97.9
975.04	.254	.47E+01	.57E+00	.77	116.50	204.19	116.67	1.75	2.35	1.26	141.6	14.8	63.5	97.9
976.12	.254	.73E+02	.21E+01	.83	16.99	7.64	7.58	.45	.92	.74	141.6	14.8	98.4	98.9
977.12	.254	.81E+02	.51E+01	.87	19.84	18.84	17.19	.95	.98	.38	141.6	14.8	36.8	98.7
978.12	.254	.96E+02	.85E+01	.88	23.13	30.13	24.22	1.30	1.86	.49	141.6	14.8	83.7	98.7
979.12	.254	.10E+03	.11E+02	.84	24.77	38.11	26.14	1.54	1.80	.55	141.6	14.8	73.1	98.7
980.12	.254	.12E+03	.14E+02	.88	29.70	48.77	31.35	1.64	1.80	.67	141.6	14.8	59.5	97.7
981.12	.254	.14E+03	.16E+02	.82	33.36	58.76	36.63	1.75	1.74	.68	141.6	14.8	67.4	98.7
982.12	.254	.14E+03	.20E+02	.76	35.80	70.51	39.74	1.97	1.80	.74	141.6	14.8	67.7	98.2
983.12	.254	.15E+03	.22E+02	.79	48.35	74.34	43.23	2.33	1.34	.73	141.6	14.8	56.3	98.6

NO 1000 5/27 98.4

984.12	.254	.16E-01	.24E+00	33.17	.33	41.22	87.15	43.51	2.11	1.39		
985.12	.254	.17E-01	.20E+00	41.26	.37	43.89	98.91	41.85	2.23	1.43	.00	1-1.6 16.5 50.7 98.4
986.12	.254	.18E-01	.31E+00	42.10	.42	46.59	111.45	54.39	2.50	1.44	.03	1-1.6 16.5 56.2 98.2
987.12	.254	.19E-01	.36E+00	46.93	.48	48.16	127.92	47.33	2.66	1.63	1.00	1-1.6 16.5 66.2 98.2
988.12	.254	.22E-01	.39E+00	53.75	.52	57.35	139.87	56.21	2.64	1.53	1.05	1-1.6 16.5 68.3 97.3
989.12	.254	.23E-01	.43E+00	54.84	.57	58.63	152.03	57.58	2.59	1.54	1.03	1-1.6 16.5 66.3 98.2
990.12	.254	.24E-01	.47E+00	56.15	.63	60.00	165.91	65.14	2.78	1.56	1.16	1-1.6 16.5 67.9 98.4
991.12	.254	.26E-01	.52E+00	61.41	.70	66.63	187.43	52.56	2.81	1.76	1.21	1-1.6 16.5 76.5 98.4
992.12	.254	.26E-01	.58E+00	61.75	.78	66.97	208.03	58.96	3.11	1.74	1.27	1-1.6 16.5 78.7 98.7
993.12	.254	.28E-01	.65E+00	66.25	.87	71.89	233.44	65.18	3.23	1.81	1.35	1-1.6 16.5 78.5 97.7
994.24	.254	.23E-02	.21E-01	17.33	.03	16.93	7.57	7.63	.65	.92	.26	1-1.6 15.5 98.4 98.9
995.24	.254	.27E-02	.32E-01	18.50	.07	18.13	18.32	17.98	1.01	.95	.38	1-1.6 15.5 98.4 98.7
996.24	.254	.32E-02	.45E-01	22.08	.11	22.04	29.89	25.66	1.36	1.04	.49	1-1.6 15.5 88.1 5.7
997.24	.254	.33E-01	.41E+00	25.53	.15	26.00	38.83	28.86	1.43	1.12	.55	1-1.6 15.3 76.8 98.7
998.24	.254	.32E-01	.46E+00	28.24	.18	29.01	47.96	31.92	1.65	1.18	.61	1-1.6 15.3 71.7 98.4
999.24	.254	.33E-01	.47E+00	30.43	.22	31.66	57.61	33.50	1.62	1.23	.68	1-1.6 16.8 65.2 98.7
801.24	.254	.35E-01	.28E+00	36.59	.26	37.98	69.52	41.21	1.83	1.34	.74	1-1.6 15.0 65.4 98.4
802.24	.254	.33E-01	.23E+00	40.14	.31	41.87	81.78	45.70	1.95	1.41	.80	1-1.6 15.0 67.5 98.4
803.24	.254	.33E-01	.28E+00	46.03	.37	48.54	98.62	47.70	2.03	1.41	.88	1-1.6 16.8 56.8 98.7
804.24	.254	.26E-01	.31E+00	46.97	.42	51.76	111.13	51.87	2.15	1.54	.93	1-1.6 16.8 56.6 98.7
805.24	.254	.23E-01	.36E+00	51.44	.51	54.93	136.33	53.75	2.44	1.52	.93	1-1.6 16.8 68.4 98.7
806.24	.254	.24E-01	.44E+00	56.86	.61	61.40	163.73	61.13	2.66	1.62	1.13	1-1.6 16.3 61.8 98.4

POOR ORIGINAL

618.00	.423	.25E-01	.16E+00	35.57	.14	58.25	64.12	59.25	1.10	1.17	.48	145.1	12.6	93.4	97.0
619.00	.423	.35E-01	.37E+00	50.86	.26	85.25	116.03	94.43	1.36	1.41	.65	141.6	12.6	83.7	93.1
620.00	.423	.40E-01	.36E+00	58.10	.29	98.37	131.88	97.87	1.34	1.50	.49	141.6	12.6	77.5	91.7
621.00	.423	.48E-01	.44E+00	69.58	.45	117.98	159.55	117.89	1.45	1.54	.76	141.6	12.6	76.7	91.2
623.00	.423	.31E-01	.43E+00	55.08	.35	79.26	157.97	78.28	1.09	* 1.32	.75	141.2	12.3	55.8	63.5
625.00	.423	.26E-01	.51E+00	37.65	.41	67.47	185.75	48.56	3.26	1.21	.82	141.5	12.3	44.7	64.4
626.00	.423	.54E-01	.51E+00	76.85	.61	137.49	185.75	68.56	1.45	1.73	.82	141.5	12.3	44.7	64.4
624.00	.423	.27E-01	.58E+00	39.14	.47	70.33	213.51	73.33	3.01	1.23	.88	140.7	12.3	42.5	44.4
630.00	.423	.19E-01	.21E+01	26.63	.02	43.40	7.79	7.79	.18	1.07	.17	141.5	13.0	97.4	99.1
631.00	.423	.20E-01	.34E+01	28.59	.03	46.68	12.24	12.16	.26	1.05	.24	140.4	13.0	39.4	94.1
632.00	.423	.21E-01	.51E+01	30.22	.06	49.99	18.40	18.27	.37	1.09	.26	142.6	13.0	90.4	93.1
633.00	.423	.22E-01	.99E+01	31.85	.08	52.83	35.37	35.71	.63	1.11	.36	140.2	12.8	93.4	93.1
636.00	.423	.23E-01	.12E+00	33.66	.09	54.75	41.96	41.44	.77	1.14	.39	143.0	12.8	98.3	98.9
635.00	.423	.24E-01	.15E+00	33.75	.12	55.00	52.35	52.58	.95	1.14	.44	141.5	12.8	93.4	97.7
636.00	.423	.25E-01	.16E+00	35.58	.13	58.34	59.94	55.71	1.03	1.17	.47	143.8	12.8	93.8	94.6
637.00	.423	.26E-01	.19E+00	38.09	.15	63.35	69.34	53.59	1.10	1.22	.50	142.4	12.8	87.1	97.3
638.00	.423	.29E-01	.22E+00	48.89	.18	67.99	79.33	68.38	1.14	1.26	.54	141.5	12.8	88.1	98.2
639.00	.423	.32E-01	.25E+00	46.63	.20	77.12	90.92	79.97	1.18	1.35	.57	141.6	12.8	89.5	98.2
640.00	.423	.38E-01	.29E+00	54.70	.23	90.93	105.01	98.38	1.15	1.44	.52	141.5	12.6	87.4	97.2
641.00	.423	.41E-01	.33E+00	59.49	.26	99.50	119.05	98.06	1.20	1.52	.60	141.6	12.6	84.2	98.2
642.00	.423	.45E-01	.36E+00	65.86	.29	109.40	132.63	104.63	1.21	1.59	.64	141.6	12.6	81.5	97.7
643.00	.423	.49E-01	.40E+00	70.96	.32	119.03	147.53	113.36	1.24	1.64	.73	141.5	12.6	83.3	98.3


```

1  FUNCTION TEMF
   FC24 = 2.8221E0 TO 1
   FC24 = 5.9285E-19772
5  FC24 = 1.573951E0 TO 2
   FC24 = 6.81371E0 TO 3
10 FC24 = 8.02845E-47449
   FC24 = 1.779E-57787
   RELOC
   END

```

SYMBOLIC REFERENCE MAP (R=1)

ENTRY POINTS

4 TEMF
 VARIABLES 5N
 2 FC REAL
 0 V REAL

STATEMENT LABELS

10 5

STATEMENTS

LENGTH 530

PROGRAM 43

530

43

51 TEMF

20 2

25 1

REAL

POOR ORIGINAL

```

1 SUBROUTINE PHISZ (P, I, O, V, S, M)
2 DIMENSION N(100), M(100), S(100), M(100)
3 DO 10 I=1,100
4   N(I)=0
5   M(I)=0
6   S(I)=0
7   M(I)=0
8   S(I)=0
9   M(I)=0
10  S(I)=0
11  M(I)=0
12  S(I)=0
13  M(I)=0
14  S(I)=0
15  M(I)=0
16  S(I)=0
17  M(I)=0
18  S(I)=0
19  M(I)=0
20  S(I)=0
21  M(I)=0
22  S(I)=0
23  M(I)=0
24  S(I)=0
25  M(I)=0
26  S(I)=0
27  M(I)=0
28  S(I)=0
29  M(I)=0
30  S(I)=0
31  M(I)=0
32  S(I)=0
33  M(I)=0
34  S(I)=0
35  M(I)=0
36  S(I)=0
37  M(I)=0
38  S(I)=0
39  M(I)=0
40  S(I)=0
41  M(I)=0
42  S(I)=0
43  M(I)=0
44  S(I)=0
45  M(I)=0
46  S(I)=0
47  M(I)=0
48  S(I)=0
49  M(I)=0
50  S(I)=0
51  M(I)=0
52  S(I)=0
53  M(I)=0
54  S(I)=0
55  M(I)=0
56  S(I)=0
57  M(I)=0
58  S(I)=0
59  M(I)=0
60  S(I)=0
61  M(I)=0
62  S(I)=0
63  M(I)=0
64  S(I)=0
65  M(I)=0
66  S(I)=0
67  M(I)=0
68  S(I)=0
69  M(I)=0
70  S(I)=0
71  M(I)=0
72  S(I)=0
73  M(I)=0
74  S(I)=0
75  M(I)=0
76  S(I)=0
77  M(I)=0
78  S(I)=0
79  M(I)=0
80  S(I)=0
81  M(I)=0
82  S(I)=0
83  M(I)=0
84  S(I)=0
85  M(I)=0
86  S(I)=0
87  M(I)=0
88  S(I)=0
89  M(I)=0
90  S(I)=0
91  M(I)=0
92  S(I)=0
93  M(I)=0
94  S(I)=0
95  M(I)=0
96  S(I)=0
97  M(I)=0
98  S(I)=0
99  M(I)=0
100 S(I)=0

```

POOR ORIGINAL

```

80 10=05 MU=6,8
81 20=10 MU=6,8
82 30=15 MU=6,8
83 40=20 MU=6,8
84 50=25 MU=6,8
85 60=30 MU=6,8
86 70=35 MU=6,8
87 80=40 MU=6,8
88 90=45 MU=6,8
89 100=50 MU=6,8
90 110=55 MU=6,8
91 120=60 MU=6,8
92 130=65 MU=6,8
93 140=70 MU=6,8
94 150=75 MU=6,8
95 160=80 MU=6,8
96 170=85 MU=6,8
97 180=90 MU=6,8
98 190=95 MU=6,8
99 200=100 MU=6,8
100 210=105 MU=6,8
101 220=110 MU=6,8
102 230=115 MU=6,8
103 240=120 MU=6,8
104 250=125 MU=6,8
105 260=130 MU=6,8
106 270=135 MU=6,8
107 280=140 MU=6,8
108 290=145 MU=6,8
109 300=150 MU=6,8
110 310=155 MU=6,8
111 320=160 MU=6,8
112 330=165 MU=6,8
113 340=170 MU=6,8
114 350=175 MU=6,8
115 360=180 MU=6,8
116 370=185 MU=6,8
117 380=190 MU=6,8
118 390=195 MU=6,8
119 400=200 MU=6,8
120 410=205 MU=6,8
121 420=210 MU=6,8
122 430=215 MU=6,8
123 440=220 MU=6,8
124 450=225 MU=6,8
125 460=230 MU=6,8
126 470=235 MU=6,8
127 480=240 MU=6,8
128 490=245 MU=6,8
129 500=250 MU=6,8
130 510=255 MU=6,8
131 520=260 MU=6,8
132 530=265 MU=6,8
133 540=270 MU=6,8
134 550=275 MU=6,8
135 560=280 MU=6,8
136 570=285 MU=6,8
137 580=290 MU=6,8
138 590=295 MU=6,8
139 600=300 MU=6,8
140 610=305 MU=6,8
141 620=310 MU=6,8
142 630=315 MU=6,8
143 640=320 MU=6,8
144 650=325 MU=6,8
145 660=330 MU=6,8
146 670=335 MU=6,8
147 680=340 MU=6,8
148 690=345 MU=6,8
149 700=350 MU=6,8
150 710=355 MU=6,8
151 720=360 MU=6,8
152 730=365 MU=6,8
153 740=370 MU=6,8
154 750=375 MU=6,8
155 760=380 MU=6,8
156 770=385 MU=6,8
157 780=390 MU=6,8
158 790=395 MU=6,8
159 800=400 MU=6,8
160 810=405 MU=6,8
161 820=410 MU=6,8
162 830=415 MU=6,8
163 840=420 MU=6,8
164 850=425 MU=6,8
165 860=430 MU=6,8
166 870=435 MU=6,8
167 880=440 MU=6,8
168 890=445 MU=6,8
169 900=450 MU=6,8
170 910=455 MU=6,8
171 920=460 MU=6,8
172 930=465 MU=6,8
173 940=470 MU=6,8
174 950=475 MU=6,8
175 960=480 MU=6,8
176 970=485 MU=6,8
177 980=490 MU=6,8
178 990=495 MU=6,8
179 1000=500 MU=6,8
180 1010=505 MU=6,8
181 1020=510 MU=6,8
182 1030=515 MU=6,8
183 1040=520 MU=6,8
184 1050=525 MU=6,8
185 1060=530 MU=6,8
186 1070=535 MU=6,8
187 1080=540 MU=6,8
188 1090=545 MU=6,8
189 1100=550 MU=6,8
190 1110=555 MU=6,8
191 1120=560 MU=6,8
192 1130=565 MU=6,8
193 1140=570 MU=6,8
194 1150=575 MU=6,8
195 1160=580 MU=6,8
196 1170=585 MU=6,8
197 1180=590 MU=6,8
198 1190=595 MU=6,8
199 1200=600 MU=6,8
200 1210=605 MU=6,8
201 1220=610 MU=6,8
202 1230=615 MU=6,8
203 1240=620 MU=6,8
204 1250=625 MU=6,8
205 1260=630 MU=6,8
206 1270=635 MU=6,8
207 1280=640 MU=6,8
208 1290=645 MU=6,8
209 1300=650 MU=6,8
210 1310=655 MU=6,8
211 1320=660 MU=6,8
212 1330=665 MU=6,8
213 1340=670 MU=6,8
214 1350=675 MU=6,8
215 1360=680 MU=6,8
216 1370=685 MU=6,8
217 1380=690 MU=6,8
218 1390=695 MU=6,8
219 1400=700 MU=6,8
220 1410=705 MU=6,8
221 1420=710 MU=6,8
222 1430=715 MU=6,8
223 1440=720 MU=6,8
224 1450=725 MU=6,8
225 1460=730 MU=6,8
226 1470=735 MU=6,8
227 1480=740 MU=6,8
228 1490=745 MU=6,8
229 1500=750 MU=6,8
230 1510=755 MU=6,8
231 1520=760 MU=6,8
232 1530=765 MU=6,8
233 1540=770 MU=6,8
234 1550=775 MU=6,8
235 1560=780 MU=6,8
236 1570=785 MU=6,8
237 1580=790 MU=6,8
238 1590=795 MU=6,8
239 1600=800 MU=6,8
240 1610=805 MU=6,8
241 1620=810 MU=6,8
242 1630=815 MU=6,8
243 1640=820 MU=6,8
244 1650=825 MU=6,8
245 1660=830 MU=6,8
246 1670=835 MU=6,8
247 1680=840 MU=6,8
248 1690=845 MU=6,8
249 1700=850 MU=6,8
250 1710=855 MU=6,8
251 1720=860 MU=6,8
252 1730=865 MU=6,8
253 1740=870 MU=6,8
254 1750=875 MU=6,8
255 1760=880 MU=6,8
256 1770=885 MU=6,8
257 1780=890 MU=6,8
258 1790=895 MU=6,8
259 1800=900 MU=6,8
260 1810=905 MU=6,8
261 1820=910 MU=6,8
262 1830=915 MU=6,8
263 1840=920 MU=6,8
264 1850=925 MU=6,8
265 1860=930 MU=6,8
266 1870=935 MU=6,8
267 1880=940 MU=6,8
268 1890=945 MU=6,8
269 1900=950 MU=6,8
270 1910=955 MU=6,8
271 1920=960 MU=6,8
272 1930=965 MU=6,8
273 1940=970 MU=6,8
274 1950=975 MU=6,8
275 1960=980 MU=6,8
276 1970=985 MU=6,8
277 1980=990 MU=6,8
278 1990=995 MU=6,8
279 2000=1000 MU=6,8
280 2010=1005 MU=6,8
281 2020=1010 MU=6,8
282 2030=1015 MU=6,8
283 2040=1020 MU=6,8
284 2050=1025 MU=6,8
285 2060=1030 MU=6,8
286 2070=1035 MU=6,8
287 2080=1040 MU=6,8
288 2090=1045 MU=6,8
289 2100=1050 MU=6,8
290 2110=1055 MU=6,8
291 2120=1060 MU=6,8
292 2130=1065 MU=6,8
293 2140=1070 MU=6,8
294 2150=1075 MU=6,8
295 2160=1080 MU=6,8
296 2170=1085 MU=6,8
297 2180=1090 MU=6,8
298 2190=1095 MU=6,8
299 2200=1100 MU=6,8
300 2210=1105 MU=6,8
301 2220=1110 MU=6,8
302 2230=1115 MU=6,8
303 2240=1120 MU=6,8
304 2250=1125 MU=6,8
305 2260=1130 MU=6,8
306 2270=1135 MU=6,8
307 2280=1140 MU=6,8
308 2290=1145 MU=6,8
309 2300=1150 MU=6,8
310 2310=1155 MU=6,8
311 2320=1160 MU=6,8
312 2330=1165 MU=6,8
313 2340=1170 MU=6,8
314 2350=1175 MU=6,8
315 2360=1180 MU=6,8
316 2370=1185 MU=6,8
317 2380=1190 MU=6,8
318 2390=1195 MU=6,8
319 2400=1200 MU=6,8
320 2410=1205 MU=6,8
321 2420=1210 MU=6,8
322 2430=1215 MU=6,8
323 2440=1220 MU=6,8
324 2450=1225 MU=6,8
325 2460=1230 MU=6,8
326 2470=1235 MU=6,8
327 2480=1240 MU=6,8
328 2490=1245 MU=6,8
329 2500=1250 MU=6,8
330 2510=1255 MU=6,8
331 2520=1260 MU=6,8
332 2530=1265 MU=6,8
333 2540=1270 MU=6,8
334 2550=1275 MU=6,8
335 2560=1280 MU=6,8
336 2570=1285 MU=6,8
337 2580=1290 MU=6,8
338 2590=1295 MU=6,8
339 2600=1300 MU=6,8
340 2610=1305 MU=6,8
341 2620=1310 MU=6,8
342 2630=1315 MU=6,8
343 2640=1320 MU=6,8
344 2650=1325 MU=6,8
345 2660=1330 MU=6,8
346 2670=1335 MU=6,8
347 2680=1340 MU=6,8
348 2690=1345 MU=6,8
349 2700=1350 MU=6,8
350 2710=1355 MU=6,8
351 2720=1360 MU=6,8
352 2730=1365 MU=6,8
353 2740=1370 MU=6,8
354 2750=1375 MU=6,8
355 2760=1380 MU=6,8
356 2770=1385 MU=6,8
357 2780=1390 MU=6,8
358 2790=1395 MU=6,8
359 2800=1400 MU=6,8
360 2810=1405 MU=6,8
361 2820=1410 MU=6,8
362 2830=1415 MU=6,8
363 2840=1420 MU=6,8
364 2850=1425 MU=6,8
365 2860=1430 MU=6,8
366 2870=1435 MU=6,8
367 2880=1440 MU=6,8
368 2890=1445 MU=6,8
369 2900=1450 MU=6,8
370 2910=1455 MU=6,8
371 2920=1460 MU=6,8
372 2930=1465 MU=6,8
373 2940=1470 MU=6,8
374 2950=1475 MU=6,8
375 2960=1480 MU=6,8
376 2970=1485 MU=6,8
377 2980=1490 MU=6,8
378 2990=1495 MU=6,8
379 3000=1500 MU=6,8
380 3010=1505 MU=6,8
381 3020=1510 MU=6,8
382 3030=1515 MU=6,8
383 3040=1520 MU=6,8
384 3050=1525 MU=6,8
385 3060=1530 MU=6,8
386 3070=1535 MU=6,8
387 3080=1540 MU=6,8
388 3090=1545 MU=6,8
389 3100=1550 MU=6,8
390 3110=1555 MU=6,8
391 3120=1560 MU=6,8
392 3130=1565 MU=6,8
393 3140=1570 MU=6,8
394 3150=1575 MU=6,8
395 3160=1580 MU=6,8
396 3170=1585 MU=6,8
397 3180=1590 MU=6,8
398 3190=1595 MU=6,8
399 3200=1600 MU=6,8
400 3210=1605 MU=6,8
401 3220=1610 MU=6,8
402 3230=1615 MU=6,8
403 3240=1620 MU=6,8
404 3250=1625 MU=6,8
405 3260=1630 MU=6,8
406 3270=1635 MU=6,8
407 3280=1640 MU=6,8
408 3290=1645 MU=6,8
409 3300=1650 MU=6,8
410 3310=1655 MU=6,8
411 3320=1660 MU=6,8
412 3330=1665 MU=6,8
413 3340=1670 MU=6,8
414 3350=1675 MU=6,8
415 3360=1680 MU=6,8
416 3370=1685 MU=6,8
417 3380=1690 MU=6,8
418 3390=1695 MU=6,8
419 3400=1700 MU=6,8
420 3410=1705 MU=6,8
421 3420=1710 MU=6,8
422 3430=1715 MU=6,8
423 3440=1720 MU=6,8
424 3450=1725 MU=6,8
425 3460=1730 MU=6,8
426 3470=1735 MU=6,8
427 3480=1740 MU=6,8
428 3490=1745 MU=6,8
429 3500=1750 MU=6,8
430 3510=1755 MU=6,8
431 3520=1760 MU=6,8
432 3530=1765 MU=6,8
433 3540=1770 MU=6,8
434 3550=1775 MU=6,8
435 3560=1780 MU=6,8
436 3570=1785 MU=6,8
437 3580=1790 MU=6,8
438 3590=1795 MU=6,8
439 3600=1800 MU=6,8
440 3610=1805 MU=6,8
441 3620=1810 MU=6,8
442 3630=1815 MU=6,8
443 3640=1820 MU=6,8
444 3650=1825 MU=6,8
445 3660=1830 MU=6,8
446 3670=1835 MU=6,8
447 3680=1840 MU=6,8
448 3690=1845 MU=6,8
449 3700=1850 MU=6,8
450 3710=1855 MU=6,8
451 3720=1860 MU=6,8
452 3730=1865 MU=6,8
453 3740=1870 MU=6,8
454 3750=1875 MU=6,8
455 3760=1880 MU=6,8
456 3770=1885 MU=6,8
457 3780=1890 MU=6,8
458 3790=1895 MU=6,8
459 3800=1900 MU=6,8
460 3810=1905 MU=6,8
461 3820=1910 MU=6,8
462 3830=1915 MU=6,8
463 3840=1920 MU=6,8
464 3850=1925 MU=6,8
465 3860=1930 MU=6,8
466 3870=1935 MU=6,8
467 3880=1940 MU=6,8
468 3890=1945 MU=6,8
469 3900=1950 MU=6,8
470 3910=1955 MU=6,8
471 3920=1960 MU=6,8
472 3930=1965 MU=6,8
473 3940=1970 MU=6,8
474 3950=1975 MU=6,8
475 3960=1980 MU=6,8
476 3970=1985 MU=6,8
477 3980=1990 MU=6,8
478 3990=1995 MU=6,8
479 4000=2000 MU=6,8
480 4010=2005 MU=6,8
481 4020=2010 MU=6,8
482 4030=2015 MU=6,8
483 4040=2020 MU=6,8
484 4050=2025 MU=6,8
485 4060=2030 MU=6,8
486 4070=2035 MU=6,8
487 4080=2040 MU=6,8
488 4090=2045 MU=6,8
489 4100=2050 MU=6,8
490 4110=2055 MU=6,8
491 4120=2060 MU=6,8
492 4130=2065 MU=6,8
493 4140=2070 MU=6,8
494 4150=2075 MU=6,8
495 4160=2080 MU=6,8
496 4170=2085 MU=6,8
497 4180=2090 MU=6,8
498 4190=2095 MU=6,8
499 4200=2100 MU=6,8
500 4210=2105 MU=6,8
501 4220=2110 MU=6,8
502 4230=2115 MU=6,8
503 4240=2120 MU=6,8
504 4250=2125 MU=6,8
505 4260=2130 MU=6,8
506 4270=2135 MU=6,8
507 4280=2140 MU=6,8
508 4290=2145 MU=6,8
509 4300=2150 MU=6,8
510 4310=2155 MU=6,8
511 4320=2160 MU=6,8
512 4330=2165 MU=6,8
513 4340=2170 MU=6,8
514 4350=2175 MU=6,8
515 4360=2180 MU=6,8
516 4370=2185 MU=6,8
517 4380=2190 MU=6,8
518 4390=2195 MU=6,8
519 4400=2200 MU=6,8
520 4410=2205 MU=6,8
521 4420=2210 MU=6,8
522 4430=2215 MU=6,8
523 4440=2220 MU=6,8
524 4450=2225 MU=6,8
525 4460=2230 MU=6,8
526 4470=2235 MU=6,8
527 4480=2240 MU=6,8
528 4490=2245 MU=6,8
529 4500=2250 MU=6,8
530 4510=2255 MU=6,8
531 4520=2260 MU=6,8
532 4530=2265 MU=6,8
533 4540=2270 MU=6,8
534 4550=2275 MU=6,8
535 4560=2280 MU=6,8
536 4570=2285 MU=6,8
537 4580=2290 MU=6,8
538 4590=2295 MU=6,8
539 4600=2300 MU=6,8
540 4610=2305 MU=6,8
541 4620=2310 MU=6,8
542 4630=2315 MU=6,8
543 4640=2320 MU=6,8
544 4650=2325 MU=6,8
545 4660=2330 MU=6,8
546 4670=2335 MU=6,8
547 4680=2340 MU=6,8
548 4690=2345 MU=6,8
549 4700=2350 MU=6,8
550 4710=2355 MU=6,8
551 4720=2360 MU=6,8
552 4730=2365 MU=6,8
553 4740=2370 MU=6,8
554 4750=2375 MU=6,8
555 4760=2380 MU=6,8
556 4770=2385 MU=6,8
557 4780=2390 MU=6,8
558 4790=2395 MU=6,8
559 4800=2400 MU=6,8
560 4810=2405 MU=6,8
561 4820=2410 MU=6,8
562 4830=2415 MU=6,8
563 4840=2420 MU=6,8
564 4850=2425 MU=6,8
565 4860=2430 MU=6,8
566 4870=2435 MU=6,8
567 4880=2440 MU=6,8
568 4890=2445 MU=6,8
569 4900=2450 MU=6,8
570 4910=2455 MU=6,8
571 4920=2460 MU=6,8
572 4930=2465 MU=6,8
573 4940=2470 MU=6,8
574 4950=2475 MU=6,8
575 4960=2480 MU=6,8
576 4970=2485 MU=6,8
577 4980=2490 MU=6,8
578 4990=2495 MU=6,8
579 5000=2500 MU=6,8
580 5010=2505 MU=6,8
581 5020=2510 MU=6,8
582 5030=2515 MU=6,8
583 5040=2520 MU=6,8
584 5050=2525 MU=6,8
585 5060=2530 MU=6,8
586 5070=2535 MU=6,8
587 5080=2540 MU=6,8
588 5090=2545 MU=6,8
589 5100=2550 MU=6,8
590 5110=2555 MU=6,8
591 5120=2560 MU=6,8
592 5130=2565 MU=6,8
593 5140=2570 MU=6,8
594 5150=2575 MU=6,8
595 5160=2580 MU=6,8
596 5170=2585 MU=6,8
597 5180=2590 MU=6,8
598 5190=2595 MU=6,8
599 5200=2600 MU=6,8
600 5210=2605 MU=6,8
601 5220=2610 MU=6,8
602 5230=2615 MU=6,8
603 5240=2620 MU=6,8
604 5250=2625 MU=6,8
605 5260=2630 MU=6,8
606 5270=2635 MU=6,8
607 5280=2640 MU=6,8
608 5290=2645 MU=6,8
609 5300=2650 MU=6,8
610 5310=2655 MU=6,8
611 5320=2660 MU=6,8
612 5330=2665 MU=6,8
613 5340=2670 MU=6,8
614 5350=2675 MU=6,8
615 5360=2680 MU=6,8
616 5370=2685 MU=6,8
617 5380=2690 MU=6,8
618 5390=2695 MU=6,8
619 5400=2700 MU=6,8
620 5410=2705 MU=6,8
621 5420=2710 MU=6,8
622 5430=2715 MU=6,8
623 5440=2720 MU=6,8
624 5450=2725 MU=6,8
625 5460=2730 MU=6,8
626 5470=2735 MU=6,8
627 5480=2740 MU=6,8
628 5490=2745 MU=6,8
629 5500=2750 MU=6,8
630 5510=2755 MU=6,8
631 5520=2760 MU=6,8
632 5530=2765 MU=6,8
633 5540=2770 MU=6,8
634 5550=2775 MU=6,8
635 5560=2780 MU=6,8
636 5570=2785 MU=6,8
637 5580=2790 MU=6,8
638 5590=2795 MU=6,8
639 5600=2800 MU=6,8
640 5610=2805 MU=6,8
641 5620=2810 MU=6,8
642 5630=2815 MU=6,8
643 5640=2820 MU=6,8
644 5650=2825 MU=6,8
645 5660=2830 MU=6,8
646 5670=2835 MU=6,8
647 5680=2840 MU=6,8
648 5690=2845 MU=6,8
649 5700=2850 MU=6,8
650 5710=2855 MU=6,8
651 5720=2860 MU=6,8
652 5730=2865 MU=6,8
653 5740=2870 MU=6,8
654 5750=2875 MU=6,8
655 5760=2880 MU=6,8
656 5770=2885 MU=6,8
657 5780=2890 MU=6,8
658 5790=2895 MU=6,8
659 5800=2900 MU=6,8
660 5810=2905 MU=6,8
661 5820=2910 MU=6,8
662 5830=2915 MU=6,8
663 5840=2920 MU=6,8
664 5850=2925 MU=6,8
665 5860=2930 MU=6,8
666 5870=2935 MU=6,8
667 5880=2940 MU=6,8
668 5890=2945 MU=6,8
669 5900=2950 MU=6,8
670 5910=2955 MU=6,8
671 5920=2960 MU=6,8
672 5930=2965 MU=6,8
673 5940=2970 MU=6,8
674 5950=2975 MU=6,8
675 5960=2980 MU=6,8
676 5970=2985 MU=6,8
677 5980=2990 MU=6,8
678 5990=2995 MU=6,8
679 6000=3000 MU=6,8
680 6010=3005 MU=6,8
681 6020=3010 MU=6,8
682 6030=3015 MU=6,8
683 6040=3020 MU=6,8
684 6050=3025 MU=6,8
685 6060=3030 MU=6,8
686 6070=3035 MU=6,8
687 6080=3040 MU=6,8
688 6090=3045 MU=6,8
689 6100=3050 MU=6,8
690 6110=3055 MU=6,8
691 6120=3060 MU=6,8
692 6130=3065 MU=6,8
693 6140=3070 MU=6,8
694 6150=3075 MU=6,8
695 6160=3080 MU=6,8
696 6170=3085 MU=6,8
697 6180=3090 MU=6,8
698 6190=3095 MU=6,8
699 6200=3100 MU=6,8
700 6210=3105 MU=6,8
701 6220=3110 MU=6,8
702 6230=3115 MU=6,8
703 6240=3120 MU=6,8
704 6250=3125 MU=6,8
705 6260=3130 MU=6,8
706 6270=3135 MU=6,8
707 6280=3140 MU=6,8
708 6290=3145 MU=6,8
709 6300=3150 MU=6,8
710 6310=3155 MU=6,8
711 6320=3160 MU=6,8
712 6330=3165 MU=6,8
713 6340=3170 MU=6,8
714 6350=3175 MU=6,8
715 6360=3180 MU=6,8
716 6370=3185 MU=6,8
717 6380=3190 MU=6,8
718 6390=3195 MU=6,8
719 6400=3200 MU=6,8
720 6410=3205 MU=6,8
721 6420=3210 MU=6,8
722 6430=3215 MU=6,8
723 6440=3220 MU=6,8
724 6450=3225 MU=6,8
725 6460=3230 MU=6,8
726 6470=3235 MU=6,8
727 6480=3240 MU=6,8
728 6490=3245 MU=6,8
729 6500=3250 MU=6,8
730 6510=3255 MU=6,8
731 6520=3260 MU=6,8
732 6530=3265 MU=6,8
733 6540=3270 MU=6,8
734 6550=3275 MU=6,8
735 6560=3280 MU=6,8
736 6570=3285 MU
```


NRC FORM 335 (7-77) *		U.S. NUCLEAR REGULATORY COMMISSION BIBLIOGRAPHIC DATA SHEET		1. REPORT NUMBER (Assigned by DDC) NUREG/CR-1808	
4. TITLE AND SUBTITLE (Add Volume No., if appropriate) Countercurrent Air/Water and Steam/Water Flow above a Perforated Plate				2. (Leave blank)	
7. AUTHOR(S) Chang-Li Hsieh, S. G. Bankoff, R. S. Tankin, M. C. Yuen				3. RECIPIENT'S ACCESSION NO.	
9. PERFORMING ORGANIZATION NAME AND MAILING ADDRESS (Include Zip Code) Department of Chemical Engineering Northwestern University Evanston, Illinois 60201				5. DATE REPORT COMPLETED MONTH: October YEAR: 1979	
12. SPONSORING ORGANIZATION NAME AND MAILING ADDRESS (Include Zip Code) U.S. Nuclear Regulatory Commission Office of Nuclear Regulatory Research Washington, D. C. 20555				DATE REPORT ISSUED MONTH: November YEAR: 1980	
				6. (Leave blank)	
				8. (Leave blank)	
				10. PROJECT/TASK/WORK UNIT NO.	
				11. CONTRACT NO. FIN No. B6188	
13. TYPE OF REPORT Topical			PERIOD COVERED (Inclusive dates) October 1978-October 1979		
15. SUPPLEMENTARY NOTES				14. (Leave blank)	
16. ABSTRACT (200 words or less) <p>The perforated plate weeping phenomena have been studied in both air/water and steam/cold water systems. The air/water experiment is designed to investigate the effect of geometric factors of the perforated plate on the rate of weeping. A new dimensionless flow rate in the form of H^* is suggested. The data obtained are successfully correlated by this H^* scaling in the conventional flooding equation.</p> <p>The steam/cold water experiment is concentrated on locating the boundary between weeping and no weeping. The effects of water subcooling, water inlet flow rate, and position of water spray are investigated. Depending on the combination of these factors, several types of weeping were observed. The data obtained at high water spray position can be related to the air/water flooding correlation by replacing the steam flow rate to an effective steam flow rate, which is determined by the mixing efficiency above the plate.</p>					
17. KEY WORDS AND DOCUMENT ANALYSIS Perforated Plate Weeping Phenomena Flooding Phenomena Hydrodynamics			17a. DESCRIPTORS		
17b. IDENTIFIERS/OPEN-ENDED TERMS					
18. AVAILABILITY STATEMENT Unlimited			19. SECURITY CLASS (This report) Unclassified		21. NO. OF PAGES
			20. SECURITY CLASS (This page) Unclassified		22. PRICE \$